MODELING AND SIMULATION OF MASS TRANSFER IN AIRLIFT FERMENTORS

by

CHESTER SHOU-TIE HO

B.S.,Chung-Yuan College of Science and Engineering, 1972

A MASTER'S THESIS

submitted in partial fulfillment of the
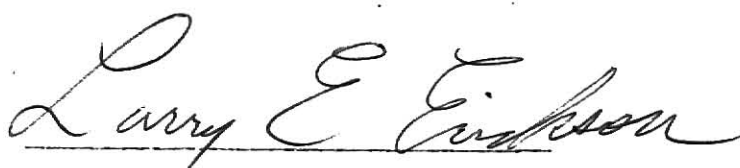
requirements for the degree

MASTER OF SCIENCE

Department of Chemical Engineering

KANSAS STATE UNIVERSITY

Manhattan, Kansas

1977

Approved by:

Major Professor

TABLE OF CONTENTS

CHAPTER I

INTRODUCTION

This work is primarily concerned with oxygen transfer and hydrocarbon substrate distribution and transport in airlift tower fermentors. The work is divided into chapters with each chapter being self contained. References, nomenclature, tables, and figures are located at the end of each chapter.

Chapter II provides a comprehensive review of the recent research which is important to oxygen transfer in tower fermentors with two liquid phases.

In Chapter III, a literature survey on hydrocarbon transfer in tower fermentors with two liquid phases is presented. The possibility of the hydrocarbon phase spreading at the cell surface and the gas-liquid inter-face is discussed.

In Chapter IV, a mathematical model for simulation of oxygen transfer in airlift fermentors is presented. The airlift fermentor is represented by a number of interconnected compartments, each of which is assumed to be well mixed. In the annular region, the model includes both upflow and downflow for the gas phase. The effect of hydrostatic pressure is also included in the model. The model is simple enough to be used in design studies and it can be easily adapted to other airlift system configurations.

Chapter V deals with the distribution of the dispersed oil phase in an airlift fermentor with two liquid phases. Since recent experimental results show that the spreading coefficient frequently becomes positive when Candida lipolytica is cultivated on n-hexadecane, the effects of oil spreading at the surface of air bubbles in an airlift fermentor are exa-mined using a mathematical model. The distribution of the oil phase with position and among the phases is determined using computer simulation.

In Chapter VI, some conclusions and recommendations are presented.

CHAPTER II

OXYGEN TRANSFER IN TOWER FERMENTORS WITH TWO LIQUID PHASES

INTRODUCTION

In cultivating yeasts on hydrocarbons, two liquid phases are present. In addition, a gas phase to provide oxygen and the microbial cells (solid phase) are present and necessary for the fermentation. Normally, providing a fermentation environment such that the microbial cells are able to grow rapidly with good product quality and quantity is considered to be difficult because of the complexity in treating a four phases system.

Transport of oxygen, carbon substrate, and inorganic nutrients to growing cells is important in fermentations with two liquid phases. Since the cells are distributed throughout the aqueous phase, at the liquid-liquid interface, and at gas-liquid interfaces, a number of transport pathways are involved. Oxygen, for example, can be transported from the gas phase directly to cells at the gas-liquid interface, to the dispersed liquid phase, or to the continuous aqueous phase. Oxygen also is distributed between the two liquid phases, to cells at the liquid-liquid interface, or to cells in the aqueous phase.

A number of parameters such as the size distribution of the dispersed oil droplets, the liquid-liquid interfacial area, the frequency of coalescence and dispersion of oil droplets, the cell adsorption and desorption at the surface of the oil droplets, the mass transfer rate, and the growth kinetics all affect the growth process. The four phases system of hydrocarbon fermentations is pictorially shown in Figure 1.

Oxygen transfer and carbon substrate transfer are both significant factors in hydrocarbon fermentations. Topics related to the interaction

of the three dispersed phases (cells, oil drops, and air bubbles) including mixing, growth kinetics, and hydrocarbon uptake by cells, must also be carefully considered. A number of excellent review papers on the general subject of mass transfer in hydrocarbon fermentations are available[2-15,125]. Literature relevant to oxygen transfer in tower fermentors with two liquid phases will be reviewed.

OXYGEN TRANSFER IN MULTIPHASE SYSTEMS

No other aspect of the fermentation process has received so much attention from chemical engineers as the oxygen transfer in broth cultivations. Oxygen from air bubbles submerged in a fermentation system must first dissolve in the culture medium and then be transported to the site of respiratory enzymes within the cell. Also, because of its sparingly low solubility in aqueous broths, oxygen has to be supplied continuously. Even a brief interruption of the supply of air may startlingly damage the respiring cells of highly aerobic organisms like Acetobacter[16]. Furthermore, it has been well recognized that the yield of fermentation products usually declines when the oxygen transfer capability of the equipment is inadequate[7].

There is increasing evidence that the biochemical activities of some microorganisms can be directed into different paths by simply changing the concentration of dissolved oxygen.[7] Control of the aeration and agitation in such fermentations may therefore be as important as control of the pH, temperature, or any other variable in the environment. This aspect is not yet very thoroughly understood, and this topic merits further research.

Many individual resistances to oxygen transfer from the sparged air bubbles to respiring cells have been proposed. Hixon and Gaden[17] in analyzing the overall oxygen transfer mechanism listed three individual rate processes as follows: (1) diffusional transfer from the gas to the liquid medium; (2) diffusional transfer through the liquid to the cell; (3) chemical reaction with oxidizable substrates through the respiratory enzymes in the cell. Bartholomew et al.[18] further divided the first rate

process listed above into two diffusional processes through the gas film and through the liquid film at the air-liquid interface. But, in hydrocarbon fermentations, four phases are present: the gas phase (air), hydrocarbon phase, aqueous phase (cultivation broth), and solid phase (microorganisms). Oxygen may be transported from the gas directly into any of the other phases, and may also be distributed between the liquid phases or between cells and either liquid. The presence of a second liquid phase in the hydrocarbon fermentation system doubles the number of interfaces across which oxygen may be transferred. Therefore, modelling the oxygen transfer in a four phase system is considerably more complex than in a three phase system.

In view of the recent controversy[19,20] concerning the correct form of the macroscopic transport equations for multiphase systems, it seems desirable to present the exact transport equation for oxygen transfer in hydrocarbon fermentations. Whitaker[19] has recently derived macroscopic equations of change for multiphase systems, which can be applied to mass transfer processes in tower systems. The mass balance for a multiphase system which was later modified by Gray[20] is

$$\frac{\partial C}{\partial t} + v \cdot \nabla C = \nabla \cdot (D \cdot \nabla C) - \sum_i K_{L,i} a_i (C - C_i^{\,o}) + R \tag{1}$$

where C = concentration, v = velocity, D = dispersion coefficient, $K_{L,i}$ = mass transfer coefficient for transport to or out of i-phase, $C_i^{\,o}$ = concentration that is in equilibrium with i-phase concentration, and R = rate of production of a chemical species. The values of C, v, D, $K_L a$, and R are all time-averaged values of the volume averaged instantaneous quantities. The following assumptions have been made in the derivation of eqn. (1): (1) no phase change occurs; (2) the fluid is incompressible;

(3) the, time-averaged value of volume fraction of the phase is independent of time. These assumptions are generally valid for fermentation systems where oxygen is the transport species except for the gas phase in tall columns where compression is not to be neglected.

In a fermentation system, the oxygen uptake rate by microorganisms may be limited by the rate of biological reaction or the oxygen transfer rate across the cell membrane or to the cell surface. In hydrocarbon fermentation, the oxygen uptake rate by microorganisms is not limited by the oxygen transfer rate to cell surfaces for oxygen concentrations ranging from 7% to 17% of the air saturated value[21,22]. It is generally desirable to operate a fermentor with the dissolved oxygen concentration at the minimum value which allows the maximum rate of biological reaction to be achieved. While the oxygen transfer resistance to the cell is negligible, the cell is treated as a reacting species. The production term, R, is then replaced by the negative value of the volumetric oxygen consumption rate by the cells[1]. Equation (1) becomes

$$\frac{\partial C}{\partial t} + v \cdot \nabla C = \nabla \cdot (D \cdot \nabla C) - \sum_i K_{L,i} a_i (C - C_i^*) - rX \qquad (2)$$

where r = specific oxygen uptake rate by cells, and X = cell concentration per unit volume of liquid dispersions. For a well mixed fermentor, the concentration gradients are zero which leads to

$$\frac{\partial C}{\partial t} = \sum_i K_{L,i} a_i (C_i^* - C) - rX \qquad (3)$$

Most researchers have regarded systems with two liquid phases as if there was only one liquid phase by assuming oxygen equilibrium between the liquids or by neglecting mass transfer to the dispersed phase. Mimura et al.[23] have found that when the volume fraction of hydrocarbons in the

liquid dispersion is 2% or less, the liquid mixture can be treated as one phase. However, the literature indicates that the dispersed liquid phase can influence oxygen transfer by absorbing oxygen or distributing it to other phases, or by influencing the fluid mechanics of the continuous phase, thereby influencing the oxygen transfer coefficients, $K_L a$, of the dispersion.

Often the oxygen transfer coefficient provides valuable information for the evaluation of fermentation equipment and is considered as one of the most important criteria for fermentor scale-up. Therefore, it may be desirable at this stage to review the methods for determining oxygen transfer coefficients, $K_L a$. Among the most commonly used methods for $K_L a$ determination, the sulfite oxidation method, the gassing-out method, and the dynamic method will be discussed here.

Sulfite Oxidation Method. The sulfite oxidation method was proposed by Cooper et al.[24] in 1944. This well-known method for measuring an oxygen transfer coefficient is still popular because the determination is very simple. The method depends on the oxidation of sulfite to sulfate by oxygen in the presence of cupric or cobalt ions as a catalyst. Cooper et al.[24] have correlated their data on the value of $K_L a$ with the power input per unit volume (P/V) and superficial gas velocity (v_s). It was reported that $K_L a$ was proportional to $(P/V)^{0.95}$ at constant v_s and to $(v_s)^{0.67}$ at constant (P/V).

Maxon and Johnson[25] have claimed that the absorption of oxygen by copper catalyzed sulphite solution must be gas film limiting. No other evidence was offered except that the sulphite oxidation reaction was extremely rapid and was independent of sulphite concentration. Finn[7,32] has criticized the gas-film limiting hypothesis and stated that the

diffusivity of oxygen through water is less than that through air by a factor of 10^4.

In an attempt to clarify the controversy on the gas-film limiting hypothesis Schultz and Gaden[26] conducted studies on oxygen transfer using an unsparged cylinder where oxygen could enter into the liquid only through a horizontal air-liquid interface. Agitation of the gas phase did not increase the transfer rate; therefore, they concluded that the gas-film was not the controlling factor.

Friedman and Lightfoot[27] reported their data on the effect of aeration and agitation on mass transfer with flat bladed impellers. They found that the air rate had little effect on power input and mass transfer in a fully baffled tank except at very low impeller speed or for very small impellers.

As for the effect of different catalysts on the sulfite-oxygen reaction, cupric and cobalt ions were generally found to be suitable to catalyze the reaction. However, Robinson and Engel[31] have found that the copper-catalyzed reaction rate was slower than the non-catalyzed reaction. They recommended the use of a cobalt catalyst instead. Finn[32] has mentioned the advantage of Co^{2+} over Cu^{2+} as the catalyst in sulphite oxidation reaction. Pirt et al.[33] have compared the rates of oxygen absorption by sodium sulphite solution using the two different catalysts. The results showed that the oxygen absorption rates were 2 to 5 times higher when Co^{2+} was used rather than Cu^{2+}.

Greenhalgh et al.[34] have compared the rate of oxygen transfer into aqueous sodium sulphite solutions with copper ions as catalyst and into a biological system of E. Coli in a mineral medium. Results showed that, in the bubble column, the mass transfer coefficients for the biological system were initially lower than those for the sulphite solution, but

increased with E. Coli concentration and finally exceeded the sulfite solution value.

In summary, even though the sulphite oxidation method is normally regarded as the standard measure for testing the rate of oxygen transfer in gas-liquid dispersions, experimental results differ and further research is needed.

Gassing-Out Method. This method was first introduced by Bartholemew et al.[18] for the measurement of $K_L a$ in an uninoculated fermentation broth. Liu[35,36] has applied the gassing-out method to correlate $K_L a$ with various operational variables of a fermentor, such as pH, temperature, gas superficial rate, and power consumption.

The method is very simple because only one measuring device, a DO electrode, is needed. Unlike the sulphite-oxidation method, the gassing-out method is less sensitive to impurities, pH, and temperature, and thus more reliable. The solubility of oxygen in the aqueous phase is very small; hence the total amount of oxygen absorbed by water in this method is relatively small compared to the total oxygen present in the gas phase under normal operational conditions. The oxygen partial pressure in the gas phase can then be treated as a constant. The mass balance

$$\frac{dC}{dt} = K_L a(C* - C)$$

may be integrated with constant $C*$ and $K_L a$ to obtain

$$K_L a = \frac{1}{t_2 - t_1} \ln\left(\frac{C^* - C_1}{C^* - C_2}\right) \tag{6}$$

The plot of $\ln(C^* - C)$ versus time results in a straight line and its slope is equal to $K_L a$.

Dynamic Method. Taguchi and Humphrey[37], and Bandyopadhyay et al.[38,39] have proposed a dynamic technique for measuring the volumetric oxygen

transfer coefficient, K_La, in fermentation systems. The dynamic method
is based on following the dissolved O_2 concentration during a short
interruption of aeration of the system. Only a fast-response, sterilizable,
dissolved oxygen probe is required to obtain the necessary data.

Once the aeration is briefly interrupted, the decrease in dissolved
oxygen due to respiration is measured to obtain the rate of oxygen uptake
by the cells. Since this is an unsteady state or dynamic situation, the
change in dissolved oxygen concentration when the aeration is resumed
is given by

$$\frac{dC}{da} = K_La(C^* - C_{mean}) - rX \tag{7}$$

where X is the cell mass concentration and r is the specific oxygen
uptake per unit mass of cells. Equation (7) can be rearranged to

$$C = -\frac{1}{K_La}\left(\frac{dC}{dt} + rX\right) + C^* \tag{8}$$

Therefore, a plot of C versus $\left(\frac{dC}{dt} + rX\right)$ results in a straight line.
K_La and C^* can be determined as the reciprocal of the slope and the
intercept respectively.

Bandyopadhyay et al.[38,39] have pointed out that there was a discre-
pency in both oxygen uptake and K_La values between the oxygen balance
and the dynamic method. The values measured by the dynamic method appear
to be abnormally low. The reason for these lower values was due to
the fact that air bubbles still remain in the mash during the brief period
of no aeration. Nonetheless, the method has been successfully applied to
real fermentation systems. The main advantage of this method lies in
its simplicity; it requires only a measuring device, the dissolved O_2
probe. Hence, K_La is internally consistent and not subject to experi-
mental variation due to comparing measurements from different sensors.

PARAMETERS AFFECTING OXYGEN TRANSFER

A. Interfacial Area and Gas Holdup

An important factor for mass transfer is the gas-liquid interfacial area per unit volume over which mass transfer occurs. Various techniques for measuring interfacial area have appeared in the literature. Three physical methods including the light scattering, light reflection, and photographic techniques, and a chemical method will be discussed here.

The light scattering technique is based on the light scattering properties of gas bubblesin liquids. A parallel beam of light is passed through the dispersion and a photocell is placed at a distance, L, from it. Only the part of the beam which does not meet any obstacle, as gas bubbles, is detected by the photocell. An empirical correlation based on theoretical considerations which gives the light transmittance as a function of the interfacial area is derived as[8,9,31]:

$$4\ln\frac{I_o}{I} = aL \tag{9}$$

where I_o = incident-light intensity, I = emergent-light intensity, L = optical path length in centimeters, and a = interfacial area per cubic centimeter of dispersion. Lee and Meyrick[42] found that the minimum value of I/I_o, the ratio of emergent and incident light intensity, which can be measured with reasonable accuracy and reliability is not much less than 10^{-2}. This means that the maximum value of aL, the product of specific interfacial area and path length, is about 20. This method has also been reported as applicable only in dispersions with relatively low specific interfacial area that Lee and Meyrick[42] have reported is about 600 to 700 m^2/m^3.

Interfacial area in liquid-liquid dispersions has also been measured photographically. A similar expression was developed for liquid-liquid

systems as[43]

$$\ln \frac{I_o}{I} = \alpha aL \qquad (10)$$

where α is the scattering factor. For a given incident light wave length the scattering factor should be a unique factor of the relative refractive index of the liquid pair.

The specific interfacial area varies greatly with position in an agitated vessel. With this technique, a lengthy integration procedure has to be performed in order to obtain an overall interfacial area. Furthermore, insertion of the probe in the system disturbs the hydrodynamics of the dispersion

The light reflection technique has been employed for measuring interfacial area of bubble dispersions in liquids by Calderbank[8,9,41]. The technique is only suitable for measurements of a near the vessel wall and therefore not applicable to the measurements of average value in a vessel with large variations of interfacial area with position.

Van Dierendonck et al.[49] and Towell et al.[45] took photographs of the liquid content of the reactor through the transparent vessel wall or with an intrascope in the interior of the reactor. Kwaecki et al.[46] extracted bubbles from the reactor by means of a tube connected to a small, square-section column. The bubbles in the column were photographed. With this method, the specific interfacial area was calculated from the gas holdup, H_G, and the Sauter mean diameter, D_{SM}, measured on the photographs. The following equation was used.

$$a = \frac{6 \cdot H_G}{D_{SM}} \qquad (11)$$

A serious limitation of both photographic measuring techniques is that only local samples can be taken and that the hydrodynamics of the dispersion at the sampling point are disturbed.

The possibility of using radioisotopes for the measurement of interfacial area between liquids has been tested. The technique was first investigated at the Oak Ridge National Laboratory[47]. Here a radioisotope emitting short-range particle was contacted at an immiscible phase capable of interacting with the particles. Because of the short range of the particles, interaction was restricted to the region close to the interface. Thus, the product of the intereaction (such as a new chemical species or radiation) will be approximately proportional to the interfacial area. Preliminary investigations with tetrachloroethylene and alpha particles from polonium-210 gave inconclusive results due to low yields of chlorine. Considerable improvement resulted at Oak Ridge when a fluorocarbon was substituted as the target phase and the neutrons produced from the nuclear interaction between the alpha particles and fluorine were detected[48]. The general technique for measuring interfacial areas is limited by the necessity of high immiscibility between the phases as well as the availability of suitable isotope and target material. Mitsis et al.[49] have used tritiated water and xylene with scintillator which satisfies both the requirement of immiscibility between phases, and of having a short particle range. In stirred vessels the interfacial area between xylene containing a scintillator and tritiated water was measured as a function of stirrer speed by a scintillation counting technique. Because of the 6μ average range of the tritium betas the rate at which flashes are detected by a phototube is a function of the interfacial area. A calibration curve of count rate against known

interfacial area for unstirred phases in containers of various diameters gave a numerical estimate of the interfacial area for ten configurations. Further details should be referred to the paper by Mitsis et al.[49].

For the chemical method reactions in the liquid phase between gas and liquid with known kinetics are used. Westerterp et al. were the first to measure overall interfacial area in stirred tanks of gas-liquid dispersions with the chemical method. For this purpose, they used the absorption of oxygen in aqueous sodium sulphite solutions. The oxidation of the sulphite was catalyzed by copper ions. Reith and Beek[50,51,52] have studied the measurement of interfacial area by the rate of oxidation of aqueous sodium sulphite solutions catalyzed by cupric ions. The reaction rate is found to be influenced by the oxygen, sulphite and catalyst concentrations, temperature and pH. With this method, an overall interfacial area in the whole vessel was obtained. However, it has the disadvantage that a systematic investigation of the liquid phase properties (such as viscosity and interfacial tension) on the interfacial area is virtually impossible, since the addition of surface active or viscous components would make a new and time consuming investigation of the kinetics of the chemical reaction necessary[52].

Reviews of the extensive literature on the subject by Towell et al.[45], Reith[52], and Valentine[53] reflect the diversity of systems used such as liquids differing in dispersion characteristics, vessels of different types and geometries, and various measuring techniques, which makes the comparison of the various correlations in the literature very difficult. Their results show that unfortunately, different measuring techniques lead to totally different interfacial areas with very few exceptions, even though measured under identical geometrical, physical, and operational conditions.

Also closely related to the interfacial area is the gas holdup which is defined as the volumetric gas void fraction. Many researchers have examined the effects of the interfacial area and gas holdup on mass transfer processes.

By bubbling various gases through liquids, Calderbank[41] attempted to determine the dependency of the oxygen transfer coefficient on the diffusivity of small and large bubbles. A stirred tank with a six-bladed impeller was employed for the absorption of gases in aqueous solutions of glycerol, glycol and ethyl alcohol. The following correlations were obtained as[41]

$$K_L \propto D_L^{2/3} \tag{12}$$

for small bubbles of diameter less than 2mm, and

$$K_L \propto D_L^{0.68} \tag{13}$$

for large bubbles of diameter 2mm to 5mm; where D_L is the diffusivity in cm^2/sec. Since, the mass transfer coefficient K_L is independent of bubble size and liquid turbulence, Calderbank[41] thus concluded that the mass transfer coefficient $K_L a$ depends on the interfacial area.

Gas holdup in perforated plate columns has been extensively studied by Fair et al.[54], and Kitai et al.[55]. Fair et al.[54] found that the gas holdup increases significantly when sieve trays were inserted into the bubble column. Oxygen transfer data and gas holdup for perforated plate multistage tower systems were reported by Kitai et al.[55]. The difference in gas holdup between Na_2SO_3-air system and water-air system was not distinct, although a slightly better dispersion was observed in Na_2SO_3 solution. The effects of the column diameter on the gas holdup and oxygen transfer coefficient were found to be very small. A rather remarkable difference caused by the plate types employed in the column was detected. In their results, a 30% higher gas holdup was obtained with a plate of 2mm hole diameter than

that with a plate of 10 mm hole diameter. Akehata[56] found that gas holdup of a baffled bubble column was higher than that without the baffle plate. This is attributed to the small bubble size which resulted from the higher frequency of bubble breakage and partly to the hindering effect of baffle plates. Very high gas holdups were measured right beneath the baffle plates.

The effect of liquid properties on the gas holdup and mass transfer coefficient in bubble columns was studied by Akita and Yoshida[57]. The gas holdup varies with viscosity and density of liquid, surface tension, and the superficial gas velocity. Experimental data lead to the following correlation[57]:

$$\frac{H_G}{(1-H_G)^4} = 0.20 \left(\frac{gD_T^2 \rho_L}{\gamma}\right)^{1/8} \left(\frac{gD_T^3}{\nu_L}\right)^{1/12} \left(\frac{V_s}{\sqrt{gD_L}}\right)^{1.0} \tag{14}$$

where γ, ν_L, D_T, V_s, and g represent the surface tension, kinematic viscosity of liquid, column diameter, superficial gas velocity, and gravitational constant respectively. Equation (14) can also be simplified to the expression

$$\frac{H_G}{(1-H_G)^4} = 0.20 \ N_{Bo}^{1/8} \ N_{Ga}^{1/12} \ N_{Fr} \tag{15}$$

where N_{Bo}, N_{Ga}, and N_{Fr} are the dimensionless Bond number, Galileo number, and Froude number respectively. Since the gas holdup in aqueous solutions of electrolytes was found to be slightly larger than in electrolyte solutions, it is also suggested by them that 0.25 instead of 0.20 be taken as the value of the leading constant in the right hand side of equations (14) and (15). As to the mass transfer coefficient, $K_L a$, was affected by liquid phase diffusivity and the column diameter and is proportional to the gas holdup to the 1.1 power.

In a subsequent paper by Akita and Yoshida[58], the equation of specific interfacial area was obtained as

$$a = \frac{1}{3} \left(\frac{gD_T^2 \rho_L}{\gamma}\right)^{0.5} \left(\frac{gD_T^3}{\nu_L}\right)^{0.1} \frac{H_G^{1.13}}{D_T} \tag{16}$$

which is simplified to

$$\frac{aD_T}{H_G^{1.13}} = \frac{1}{3} N_{Bo}^{0.5} N_{Ga}^{0.1} \tag{17}$$

An extensive literature review on the gas holdup in bubble columns was made by Mashelkar[59]. Some results are summarized as: (1) holdup varies directly with the superficial gas velocity; (2) holdup is independent of the column diameter; (3) electrolytes can raise the holdup to values 30% higher than those of nonelectrolytes; (4) perforated plates in the column increase holdup significantly; (5) holdup is unlikely to be affected by the temperature and pressure; (6) foaming systems exhibit unusually high holdup.

With regard to the variation of the gas holdup with superficial gas velocity, a correlation for air-water system was given as[59]

$$H_G \propto \frac{V_s}{30 + 2V_s} \tag{18}$$

Figure 2 was constructed with the available data in the literature. However, with a closer examination, one easily ascertains that for data in the upflow region of airlift systems Mashelkar's correlation actually overestimates the mean by about 10%. It is thus recommended that in the upflow region of airlift systems a factor of 0.90 be introduced in Mashelkar's correlation[59], that is,

$$H_G = 0.90 \left(\frac{V_s}{30 + 2V_s}\right) \left(\frac{1}{\rho_L}\right) \left(\frac{\gamma}{72}\right)^{1/3} \tag{19}$$

where ρ_L is the liquid density and γ, surface tension of the liquid.

A sieve tray column is a special type of tower fermentor in which the sieve trays serve as static mixers. Other types of motionless mixers have recently been developed; however, research on their application in tower fermentors is just beginning. Oxygen transfer in a sieve tray column and a Koch mixer tower system was studied by Hsu[60]. Gas holdup was found to be much greater in the sieve tray and Koch mixer columns; indicating that the sieve plate and motionless mixer help in trapping more gas in the column and lead to a higher gas phase dispersion. Based on the result shown in Figure 3, one realizes that, as gas flow rate increased, a column equipped with motionless mixers or sieve plates is preferred to a bubble column.

Calderbank[61] investigated the gas void fraction on sieve plates 6.3 and 14 centimeters in diameter. The mean bubble diameter was constant up to a gas holdup of 0.35. At gas void fractions above 0.4, the gas bubble volume increased rapidly with the gas void fraction. This increase was primarily due to bubble coalescence. The interfacial area was measured as a function of gas holdup in a bubble column of 9.3 cm in diameter. For gas holdup in the range of 0.05 to 0.25, the interfacial area was directly proportional to the gas holdup. However, for gas holdup greater than 0.25, the interfacial area decreased and leveled off. The following correlation was proposed in CGS units by Calderbank[41]

$$a = 1.44 \left[\frac{(P/V)^{0.4} \rho_\ell^{0.2}}{\gamma^{0.6}} \right] \left(\frac{V_s}{V_t} \right)^{0.5} \tag{20}$$

where (P/V) = power dissipated per unit volume of liquid medium, V_s = superficial gas velocity, V_t = terminal bubble rise velocity, ρ_ℓ = liquid density, and γ = interfacial tension in dynes/cm.

Van Dierendonck et al.[44] proposed the following correlation for all the gas-liquid tower systems investigated

$$\frac{D_{SM}^2 \rho_L g}{\gamma} = [1.2 + 260 \frac{\mu(N-N_o)d}{\gamma}]^{-2} \qquad (21)$$

provided that $0<(N-N_o)$ d<1.5 m/sec; where D_{SM}- sauter mean diameter of bubbles, N = agitator speed, N_o = minimum agitator speed for dispersion gas bubbles, $N \geq N_o$, μ = viscosity. In the range of $N>2N_o$, for pure liquid, a different correlation was given as

$$\frac{D_{SM}^2 \rho_L}{\gamma} = 0.45 \qquad (22)$$

For details of the information given above, one should refer to the original paper by van Dierendonck et al[44].

The airlift fermentor has recently received much attention and is claimed as one of the most promising designs. The volumetric gas holdup was determined from the static pressure gradient in the annulus and draft tube regions by Hatch[11]. In a pilot scale airlift fermentor with Candida intermedia growing on n-alkane, the gas holdups in the draft tube and annular regions were found to be functions of sparger gas flow rate. From the experimental data[11], one can obtain the following correlations as

$$H_D = 0.277 \cdot \log V_s - 0.097 \qquad (23)$$

for the draft tube region, and

$$H_A = 0.222 \cdot \log V_s - 0.09 \qquad (24)$$

for the annular region. Figures 3 and 4 show the correlation of gas holdup with respect to the superficial gas velocity based on cross-sectional area of the draft tube region.

For airlift fermentors packed with motionless Koch mixers[62], the overall gas holdup was a monotonically increasing function of the air flow rate in either an air-water system or an air-5% Na_2SO_3 solution. The magnitudes of gas holdup measured in the air-5% Na_2SO_3 system are about double the values in the air-water system.

Other similar designs based on the airlift principle are also found in the literature. Recent work on the thin-channel rectangular airlift fermentor has shown the bubble collision frequency for the system to be 1/4 the value for the concentric airlift fermentor which indicates a smaller bubble coalescence for the rectangular system[63]. A larger interfacial area is thus expected for the thin-channel rectangular airlift fermentor.

Using a baffle to divide the cylinder into an upflow and a downflow region, the split airlift fermentor has been experimentally studied[64]. It was found that, in all positions tested, the gas holdup changes linearly with the superficial gas velocity. The gas holdup in the downflow region is a linear increasing function of the superficial gas velocity for values of holdup from 0.0092 to 0.1950; the values of gas holdup at positions lower than two-thirds of the baffle height range from 0.0092 to 0.2740; the values of gas holdup for the upper one-third of the baffle height are a linear function of the superficial gas velocity up to a gas velocity of 650 cm/min; above the gas velocity of 650 cm/min, the gas holdup tails off indicating an unmeasurable gas holdup for high gas velocities in the head region.

In summary, the mass transfer coefficient is dependent on the interfacial area. The interfacial area is related to the gas holdup and is highly sensitive to the fermentor design, physical properties, and the superficial gas velocity. The interfacial area is also affected by the bubble coalescence and redispersion rates.

B. Sparger Design

On designing a gas sparged column, one of the important factors which must be taken into consideration is the dimensions of the gas sparger. It is at the sparger that the bubbles are created and frictional losses through the orifice take place. A successful sparger design in terms of minimizing the energy loss while maximizing the interfacial area may greatly benefit oxygen transfer efficiency.

Consider the case of gas emerging from a simple submerged orifice at very low flow rates. Bubbles form at the orifice periodically, grow to a certain size, and break away. The bubble size can be described by[53]

$$d_b = 1.82 \ [\frac{d_o \gamma g_c}{\Delta \rho \cdot g}] \tag{25}$$

where d_o = orifice diameter, γ = interfacial tension, $\Delta \rho = \rho_L - \rho_g$, difference in density, g = gravitational constant, and g_c = conversion factor. At this stage, bubble size is independent of gas flow rate, and the frequency of bubble formation is proportional to the gas flow rate.

At higher gas flow rates, the frequency levels off and the bubble volume increases. Finally, a point is encountered where distinct bubbles do not form; rather, a chain bubbling process is noted, where the larger bubbles breakup several inches above the orifice. Leibson et al.[65] employed a high speed motion picture camera to take pictures of the air bubbles formed in water and aqueous butanol solution. They found that, in the turbulent flow region, the mean bubble size was found to be described in CGS units by:

$$d_b = \frac{0.71}{N_{Re}^{0.01}} \tag{26}$$

Figure 5 shows the effect of the orifice Reynolds number and orifice size to the mean bubble size[11]. The mean bubble size generated at the orifice

can be minimized by either maintaining the orifice Reynolds number above 2100 or by utilizing orifice diameter less than 0.1 mm. However, before specifying the optimum orifice size, it is necessary to consider the pressure losses through the orifice. Potter[66] showed that the total pressure drop is related to the gravity force, surface tension, frictional loss, and accel-erational force. Since the pressure loss due to the acceleration force is negligible and the gravity force is independent of the orifice size, the dependency of the pressure drop with respect to orifice size is described in CGS units by[11]:

$$\Delta P = (\frac{2\gamma}{r}) + 0.28 \; (\frac{V_o}{c})^2 \; (\frac{\rho_g}{\rho_L}) \tag{27}$$

where ΔP = total pressure drop through the orifice, in cm water, γ = surface tension, r = bubble radius, V_o = orifice gas velocity, c = orifice constant $\simeq 0.7$, ρ_g = gas density, and ρ_L = liquid density. The first term in equation (27) is the pressure loss due to surface tension and the second term is the fractional pressure drop across orifice.

At very high orifice Reynolds numbers, the power dissipation in the liquid phase around the sparger becomes significant. Interfacial area is increased due to the high frequency of bubble breakage. Levich[67] showed that bubbles breakup when the external dynamic pressure exceeds the internal capi-llary pressure of the bubble as

$$\frac{\rho_L V_L^2}{2} > \frac{\gamma}{r_c} \tag{28}$$

where V_L = liquid velocity at bubble surface, and r_c = radius of curvature. The ratio of the internal force to surface tension is defined as the Wever number. The bubble starts to break up when the Weber number exceeds a

critical value which was experimentally determined to be 2.4 by Hu and Kintner[68]. It is therefore apparent that the equilibrium bubble size decreases as the local liquid velocity is increased.

The role of liquid turbulence and mixing in aeration towers on bubble size is shown by the work of Mashelkar and Sharma[69]. Gas-liquid interfacial areas in bubble columns were measured at various orifice gas velocities. For very low superficial gas velocities (less than 30 cm/min), the interfacial area in the column was found to be a strong function of the orifice diameter and a weak funciton of the gas flow rate through the orifice. The mean bubble size in the column remains essentially constant. At moderate superficial gas velocities $(30 < V_S < 600$ cm/min), the orifice gas velocity was found to affect the interfacial area in the column. In this range, coalescence begins to influence the bubble size distribution more than the orifice diameter. At high superficial gas velocities (greater than 600 cm/min), the orifice diameter and orifice gas velocity were found to have little effect on the interfacial area. As the superficial gas velocity is increased, the gas holdup is increased and coalescence becomes more rapid.

As far as the orifice geometry is concerned, circular orifices have the advantage that they admit an accurate assessment of the surface-tension effect. In industrial operations, however, use of noncircular slots for bubble formation is frequently encountered. A systematic study of the influence of noncircular orifices on bubble formation has been made by Krishnamurthi et al.[70] and reviewed by Kumar and Kuloor[71]. They have compared the bubble volume obtained by using alternatively, a standard circular orifice of arbitrary diameter and two sets of orifices of other geometries like triangular, square, etc., chosen to have either equal perimeters or equal areas with the

standard one. Their study, which was confined to low flow rates (less than 0.05 cm^3/sec), indicated that the bubble volumes obtianed from the circular orifice did not correspond exactly to those from the noncircular orifices whether compared on an equal-perimeter or equal-area basis. They were closest for orifices of equal areas. On extending the study to high flow rates (up to 200 cm^3/sec), Ramakrishnan et al.[72] found that an orifice having a noncircular geometry given bubble volumes equal to those obtianed from a circular orifice of the same area. They thus concluded that any theory for the formation of bubbles from circular orifices can also be extended to situations where noncircular orifices are involved[71,72].

Deckwer et al.[73] have studied the mixing and mass transfer in two tall bubble columns. Bubble column I had a diameter of 20 cm and a total height of 723 cm. A plate with 56 nozzles of 1 mm diameter was used as gas sparger. Bubble column II had a diameter of 15 cm and a height of 440 cm. The gas was sparged by a glass sintered porous plate with a mean pore diameter of 150 mm. The mass transfer coefficients tested for bubble column II at variour liquid flow rates were about double those in bubble column I. They explained that the remarkable difference was attributed to the gas spargers employed which provided for different gas holdups with different bubble size distributions and hence, different specific interfacial areas were obtained.

Deckwer and Burckhart[74] observed that the oxygen transfer coefficients in bubble columns equipped with sintered plates (mean pore diameter: 0.01 mm) were considerably higher than those obtained from bubble columns with nozzles (1 mm diameter) as gas distributor. The measured $K_L a$ values can be correlated as[74]

$$K_L a = A^B V_s \tag{29}$$

The coefficient A depends only on the gas distributor and the liquid phase properties. That is to say the oxygen transfer coefficient $K_L a$ is a

function of the type of gas sparger employed. Figure 7 depicts the measured $K_L a$ values at various gas flow rates for sintered plates and nozzles.

Many researchers have studied the oxygen transfer capabilities of various types of spargers in search for one which can produce a high oxygen transfer rate from the bubble phase to the liquid. Eckenfelder[75] found that the values of $K_L a$ measured with various types of spargers by ths sulfite-oxidation method did not differ appreciably when compared on the basis of power consumption per unit volume of liquid. Since no mechanical agitators were employed in the work, the power consumption for each sparger is basically the power required for sparging air into liquid.

Oels and Schügerl[76] have examined the influence of four different types of gas distributors on the performance of bubble column fermentors. Results have shown that the gas holdup, interfacial area, and voluemtric mass transfer coefficient all increase in the sequence of perforated plate, porous plate, injector nozzle, and ejector nozzle. The highest interfacial area, volumetric mass transfer coefficient, and oxygen transfer rate are by all means achieved in antifoam-free culture medium by ejector nozzle because the ejector nozzle produces the highest energy dissipation density. Therefore, they are convinced that the ejector nozzle is a very effective gas distributor with high volumetric energy consumption; however, with low volumetric energy consumption, the porous plate is the most economical gas distributor tested.

In summary, at low flow rates in the quiescent regime, the sparger design may be important. In this region, the bubble size is independent of gas flow rates and the frequency of bubble formation is proportional to the gas flow rate. Coalescence in the liquid is not high enough to govern the quality of the dispersion. Thus a porous or sintered plate with pore sizes in the range of 10 to 100 microns gives a much higher interfacial area than

a single nozzle. However, in the turbulent regime, where superficial gas velocity exceeds 10 cm/sec, the sparger design becomes trivial, because the dispersion quality is governed solely by the mixing effect created by liquid turbulence[59]. In dealing with a non-mechanical airlift system, a reasonable uniform distribution of orifices over the vessel cross section is desirable even though the gas flow rate may be so high as to induce liquid recirculations. By and large, before running a gas-liquid contact device, considerable effort should still be spent on the sparger design.

There is much literature on the design of gas spargers. Useful articles for design engineers are those by Hatch[11], Leibson et al.[65], Kumar and Kuloor[71], Eckenfelder[75], Oels and Schügerl[76], and Fair[77].

C. Column Height and Diameter

The column height and diameter are significant factors in designing an aeration tower. The height and diameter of the column influence the overall gas-liquid interfacial area by altering the hydrodynamics, the gas residence time, and the expansion of bubbles.

Yoshida and Akita[78] examined the effects of column height and diameter on the volumetric liquid-phase mass transfer coefficient in bubble columns 7.7 cm to 60 cm in diameter. In all cases tested, neither $K_L a$ nor the gas holdup depends on the ungassed liquid height appreciably. The oxygen transfer coefficient $K_L a$ was found to increase with increasing column diameter. In the 7.7 cm diameter column, plug flow was observed at fairly low superficial gas velocities. In columns with larger diameter, however, no plug flow was observed, and more violent motion and more downward movement of fluids along the wall existed. Bubbles near the wall showed very complicated motion which might enhance mixing and thus the mass transfer rate.

Freedman and Davidson[79] have found that the transition from
bubbly to slug flow tends to occur at low gas holdups in small diameter
columns. This indicates that not only can larger bubbles or slugs
exist in smaller diameter columns, but they are also formed at lower
superficial gas velocities or gas holdups. A liquid circulation pattern
at the column wall has also been noted. The liquid downward flow
along the wall was accounted for by differences in hydrostatic head
at the wall and column center. The intensity of the downward flow
is a direct function of column height and it also leads to a local
liquid turbulence to promote bubble breakup. In other words, the
column height indirectly leads to an increase in interfacial area.
However, according to Calderbank[80], in the study of carbon dioxide
dissolved in a 10 ft high bubble column of water containing various
amounts of glycerol, as the column height increases, an increase in
bubble coalescence is subject to happen which, on the contrary, de-
creases the overall interfacial area.

Calderbank[81] demonstrated that the degree to which column
height affects coalescence is very dependent on the liquid phase
composition by measuring rates of coalescence of carbon dioxide
bubbles rising through a 4 inch square tower which was 10 ft high
and filled with water. Interfacial area, gas holdup, and bubble
diameter were measured as a function of vertical position. When
hexanol was added to inhibit coalescence, the interfacial area
was found to increase by a factor of two in the top section
of the column although the gas holdup remained virtually constant.
In the lower section of the column, the addition of hexanol had
no effect on the interfacial area.

Recently, Blanco et al.[82] investigated mass transfer in columns 8 cm and 25 cm in diameter using the sodium sulfite oxidation method. The oxygen transfer coefficient was higher in the 25 cm diameter column than in the 8 cm diameter column. As to the effect of column height on the oxygen transfer coefficient, no appreciable difference was noted for different column heights.

Wallis[83] reviewed the influence of walls and column diameter on bubble rise velocity and found the following equations to apply for bubbles rising in an inviscid liquid[83]:

$$V_b = V_\infty \qquad \text{for } d_b < 0.125 \, D_T$$

$$V_b = V_\infty (1.13e^{-d_b/D_T}) \qquad \text{for } 0.125 \, D_T < d_b < 0.6 \, D_T$$

and

$$V_b = V_\infty [0.496(D_T/d_b)^{\frac{1}{2}}] \quad \text{for } d_b > 0.6 \, D_T \qquad (30)$$

where V_b = bubble rise velocity, V_∞ = bubble rise velocity in an infinite pool, d_b = bubble diameter, and D_T = column diameter. Furthermore, Wallis concluded that once the bubble diameter reaches 60% of the column diameter, the bubbles behave as slug flow bubbles. For bubbles approaching the column diameter, the rise velocity is reduced by as much as 50%. This allows larger bubbles to exist in free rise. For example, if the terminal bubble rise velocity for air bubbles in pure water were reduced from 30 to 15 cm/sec by the influence of vessel containing walls, the critical bubble radius would be increased to 7.2 cm. It is thus apparent that larger, stable

bubbles or slugs can exist in free rise as the column diameter is decreased.

In order to predict the effects of the geometric design and operating parameters on the oxygen transfer rate and performance ratio, a series of experiments were performed by Hatch and co-workers[14,84,85,86,87,88] in a bench-scale airlift unit for _Bacillus subtilis_ fermentations using glucose as the carbon source. The column used was a pyrex glass pipe of 10 cm inside diameter and 120 cm tall. Results show that the optimum diameter ratio of draft tube diameter to column diameter is 0.7, and the area ratio of upflow to downflow regions is 0.83. The effect of medium height on mass transfer coefficients was also studied. The results show that at high draft tube superficial gas velocities, there appears to be no effect of medium height on the mass transfer coefficient. However, at lower gas velocities, say 400 cm/min or less, higher mass transfer coefficients were obtained for lower liquid height to diameter ratio columns. Recently, a mathematical model was developed to describe oxygen transfer in an airlift fermentor consisting of a 30 cm diameter stainless steel column five meters in height with an internal cylinder 20.6 cm in diameter and 260 cm tall[11,88]. The effect of the draft tube diameter was examined by using the mathematical model to simulate the effect of the downflow/upflow area and the draft tube height on the performance ratio as well as overall oxygen transfer coefficient. The computer simulation shows that as the downflow/upflow area ratio is decreased, the performance ratio reaches a maximum at the area ratio of 0.8 and the overall oxygen transfer rate increases continuously over the range of area ratios tested. The performance ratio increases slowly until the ungassed liquid height is approached while the draft tube height increases. The performance ratio then increases exponentially with increasing draft

tube height. Therefore, as far as the maximum performance ratio is concerned, the draft tube height should be increased until restriction of fluid flow in the circulation loop through the head region takes place[11,14].

Orazem[89] examined the effect of baffle height on the mass transfer coefficient in a split cylinder airlift fermentor which was 6 inches in diameter. Baffles of various heights were employed to vertically split the tower into two equal sections. The baffles were placed 2.44 inches above the bottom of the column to allow an opening with a cross-sectional area 1.09 times that of the upflow and downflow cross-sectional areas. The maximum oxygen transfer coefficient was observed in the system equipped with a baffle 2 feet high. The oxygen transfer coefficient, $K_L a$, is shown as a function of baffle height in Figure 8. The author also suggested that the presence of an optimal baffle height for oxygen transfer merit further study of multistage systems.

In summary, the overall effect of column height on interfacial area is determined by the effects of coalescence, liquid turbulence, and the expansion of gas bubbles. It is concluded from the literature that over the ranges of column heights studied, these effects tend to counterbalance. However, as the column diameter decreases, the bubble rise velocity is reduced. This allows bigger bubbles or slugs to be formed which lowers the overall interfacial area. When designing an aeration tower for mass transfer, it is advantageous to use a column diameter large enough that the bubble rise velocity is unaffected.

D. Oxygen Partial Pressure

Oxygen transfer rate is governed by the equation,

$$\frac{dC}{dt} = K_L a \, (C^* - C) \tag{31}$$

where C^* is a function of the oxygen partial pressure. According to Henry's

law, at equilibrium the partial pressure of oxygen in the gas phase is pro-

portional to the amount of oxygen dissolved in the liquid phase, that is,

$$C^* = \frac{P_{O_2}}{H_c} = \frac{P_T}{H_c} Y \tag{32}$$

Therefore, equation (31) may write:

$$dC = K_L a (\frac{P_T}{H_c} Y - C) \, dt \tag{33}$$

Either an increase in the total pressure by externally pressurizing the

gas phase or an increase in the oxygen partial pressure by using commercial

oxygen will result in an increase in oxygen transfer rate. Hence, commercial

oxygen offers considerable potential in aerobic fermentations where

oxygen transfer is limiting. A pronounced advantage lies in the fact that

pressurization can be obtained with negligible energy expenditure to in-

crease the dissolved oxygen at saturation condition to very high levels,

thus enhancing the oxygen transfer rate[90].

A 50% increase in the interfacial area is reported by using pure oxygen

instead of air[91]. Also, the oxidation rate of sodium sulfite solution by

pure oxygen was about seven times higher than that by air, which can be

attributed to the increase in the interfacial area for pure oxygen aeration[62].

Deckwer et al.[92] have pointed out that in designing a tall bubble column,

the axial pressure is one of the critical factors which should be taken into

account. Ho[93] has proposed a model for the oxygen transfer in airlift

fermentors in which the oxygen partial pressure in the gas phase is considered

a function of the vertical position and gas holdup. This model shows results

of the dissolved oxygen concentration distribution qualitatively in agree-

ment with those found by Hatch[11].

As far as cell growth is concerned, however, in conventional fermentors,

the microorganisms normally grow in an environment where the dissolved

oxygen concentration ranges from 1 to 10 mg/1. Yet, with pressurized
oxygen transfer systems using commercial oxygen, it is quite feasible to
reach a dissolved oxygen concentration of 100 mg/1[90].

EFFECT OF HYDROCARBON PHASE ON OXYGEN TRANSFER

Yoshida et al.[94] have determined values of $K_L a$ in both an agitated vessel and a bubble column for the aqueous dispersions of kerosene, a liquid paraffin, toluene, oleic acid, and powdered polyvinylchloride. The oxygen concentration in the feed and exit streams of the bubble column were measured to find the oxygen uptake rate of each liquid mixture. They assumed the oil and water phase were in equilibrium such that the liquid dispersions can be regarded as a single phase. Further study by Yamane and Yoshida[95] showed that indeed small oil droplets, when placed in the aqueous phase, reach an oxygen equilibrium so rapidly that the assumption stands. The dynamic method for determining $K_L a$, which involves recording the oxygen concentration in the medium following a step change in the gas phase oxygen partial pressure, was used in batchwise experiments for the PVC -in-water system. $K_L a$ decreased with increasing oil fraction for the kerosene, paraffin, and PVC powder dispersions; but for the toluene and oleic acid dispersions, $K_L a$ decreased slightly, then increased with increasing oil fraction.

Yoshida et al.[94] pointed out that the spreading coefficient, $S_{o/\ell A} = \gamma_{\ell/A} - (\gamma_{o/A} + \gamma_{o/\ell})$, is negative for the kerosene- and paraffin-water systems, but positive for the toluene- and oleic acid-water systems. They thus suggested that for positive spreading coefficients, the dispersed phase may act like a surface active agent, and increase the interfacial area while decreasing the mass transfer coefficient, K_L. At low oil fractions, the effect of hydrocarbon phase on K_L may dominate. They showed that the surfactant Tween 85 has an effect on oxygen transfer similar to that of toluene and oleic acid. Gas holdups for the toluene and oleic acid systems

showed trends similar to the K_La values, indicating that the increase in K_La may at least be partially due to an increase in interfacial area. Gas holdup in the kerosene and paraffin in water systems varied little with oil fraction, indicating that the decrease in K_La was likely due to a decrease in K_L. They proposed that this apparent decrease in K_L be attributed to oil drops partially covering the gas bubble surfaces. The diffusive or convective oxygen transfer rate through these oil drops would be expected to be slower than through the continuous phase. The PVC powder had a greater effect on K_La than did the oil drops, perhaps due to the inability of oxygen to be transported through the solid or a more pronounced effect on the fluid motion of the continuous phase.

Coty et al.[96] applied the sodium sulfite oxidation method to study the oxygen uptake rate of mixtures containing hexadecane and a mineral salts medium in which the oil phase was continuous. They found the oxygen transfer rates from air to mixtures containing 50% and 66% oil in airlift fermentors were much larger than to the medium without oil. However, if the solubility of oxygen in the hexadecane is assumed to be six times greater than in the medium as suggested by Matsumura et al[97], the Henry's law constant, H_c, is calculated on the basis of a weighted average of these solubilities, and the oxygen concentration in both liquids is assumed to be zero, then K_La values for the pure medium and the 50% oil mixture are about the same, while those for the 66% oil mixture are about twice the K_La values for the pure medium. They also observed that phase inversion may take place at $\phi = 0.40$. It appears that an increase in the dispersed phase volume fraction causes a decrease in the volumetric oxygen transfer coefficient to the liquid mixture, regardless of which liquid phase is dispersed.

The equilibrium distribution of oxygen in the water and n-paraffin phases has been measured under isothermal conditions at 25°, 30°, 35°, and 40°C. From the study, Matsumura et al.[97] were able to show that oxygen is 7 to 9 times more soluble in n-paraffin than in water. They measured the gas phase oxygen partial pressure change in a closed agitated vessel with a draft tube as oxygen was absorbed by the liquid mixture. The partial pressure data were then fitted with the solution to the model equations and correlations were developed. They assumed the pathway of oxygen transfer was from air to water to oil, and that the oil phase was in equilibrium with the water phase oxygen concentration present at the oil-water interface. They observed the volumetric oxygen transfer coefficients in both phases increased with increasing oil fraction. The correlations they obtained are[97]

$$(K_L a)_{wg} = (1.75 \times 10^{-2} e^{0.115\phi} - 0.8 \times 10^{-3} e^{-46.9\phi}) \, N^{1.0} V_S^{1/3} \qquad (34)$$

$$(K_L a)_{wh} = \frac{1}{1 + H_{wh}(\frac{1}{\phi} - 1)} (K_L a)_{wg} \qquad (35)$$

where N = rotation speed of impeller in rounds per second, ϕ = oil volume fraction, V_S = superficial gas velocity in cm/sec, and H_{wh} = partition coefficient of oxygen between water and hydrocarbon phase. Furthermore, the effect of temperature on the equilibrium distribution of oxygen was represented by the following expression with errors less than 15%[97],

$$C_w = 3.3 \times 10^{-3} C_o \exp\left(\frac{10^3}{230 + T}\right) + 5.0 \times 10^{-6} \qquad (36)$$

where C_w = oxygen concentration in the water phase, C_o = oxygen concentration in the hydrocarbon phase, and C_o ranges from 0.9×10^{-4} to 8×10^{-4} g-mole/liter.

Yoshida et al.[43] have taken into account the possibility of cells utilizing a considerable amount of oxygen from oil which spreads at the air-water interface. From the following two oxygen balances,

$$\frac{dC_w}{dt} = (K_La)_{gw} (C_g - C_w) + (K_La)_{ow}(C_o - C_w) - \beta R_w \qquad (37)$$

$$H_{wh} \frac{dC_o}{dt} = (K_La)_{go} (C_g - C_o) + (K_La)_{ow} (C_w - C_o) - \beta R_o \qquad (38)$$

where $H_{wh} = \dfrac{H_c V_o}{V_w}$ $\beta = \dfrac{V_w + V_o}{V_w}$, H_{wh} is the equilibrium constant for the dissolved oxygen between the water and oil phases, and (K_La) represents the volumetric oxygen transfer coefficient between the phases denoted as subscripts, they obtained the dissolved oxygen concentration in the course of cells cultivation as

$$\tilde{C}_w = C_g - \frac{[(K_La)_{go} + (K_La)_{ow} \beta R_w - (K_La)_{o2} \beta R_o}{(K_La)_{gw}(K_La)_{go} + (K_La)_{go}(K_La)_{ow} + (K_La)_{ow}(K_La)_{gw}} \qquad (39)$$

$$\tilde{C}_o = C_g - \frac{[(K_La)_{go} + (K_La)_{ow}] \beta R_o - (K_La)_{ow} \beta R_w}{(K_La)_{gw}(K_La)_{go} + (K_La)_{go}(K_La)_{ow} + (K_La)_{ow}(K_La)_{gw}} \qquad (40)$$

Note that $\tilde{C}_w$ and $\tilde{C}_o$ are functions of the volumetric oxygen transfer coefficients and respiration rate of the cells. During cultivation of Candida rugosa, the measured values of $\tilde{C}_w$ decreased with cell growth and returned to the initial level after exhaustion of the substrate. The oxygen transfer coefficient between the gas and water phase, $(K_La)_{gw}$ decreased gradually with cell growth and increased after exhaustion of the substrate. Also, $(K_La)_{gw}$ decreased parallel to the decreasing amount of oil. They explained the decrease in $(K_La)_{gw}$ during fermentation was due to the blockage caused by the flock of oil and cells adsorbed at the air-liquid interface. Since $(K_La)_{gw}$ value increased after the oil was used up, this may reflect a relief of the blocking effect.

In summary, it is quite likely that the hydrocarbon phase spreads at the gas-liquid interface to influence the oxygen transfer rates under certain circumstances. However, further research is needed.

EFFECT OF CELL PHASE ON OXYGEN TRANSFER

In a hydrocarbon fermentation medium, not only are aqueous and oil phases present, but also respiring cells; their presence has a pronounced effect on the oxygen transfer phenomena. Limited studies have been undertaken on the effect of growing cells on the rate of biological reactions which are associated with oxygen transfer.

Oxygen from the gas phase enters the liquid and diffuses to the cell surface while nutrients in the liquid are also diffusing to the surface to support the biological reaction of cell metabolism. Reaction occurs at the respiratory sites on and within the cell surface. The mass transfer processes can be discussed as follows:

$$N_{O_2} = K_L a_b (C - C)$$

$$= K_m a_m (C - C_m)$$

$$= K_m' a_m C_m \qquad (41)$$

where K_i's and a_i's are the appropriate mass transfer coefficients and interfacial areas respectively. The last term represents reaction on the cell surface, a_m. Equation (41) can be rearranged to a series of resistances:

$$\frac{C^*}{N_{O_2}} = \frac{1}{K_L a_b} + \frac{1}{K_m a_m} + \frac{1}{K_m' a_m} \qquad (42)$$

therefore,

$$R_T = R_1 + R_2 + R_3 + \text{etc.} \qquad (43)$$

The magnitude of the interfacial resistance depends on the properties of the interfacial film. Usually, the mass transfer coefficient is considered as inversely proportional to the thickness of the liquid film. It used to be widely held that one of the functions of agitation

in submerged systems was to increase the mass transfer rate by decreasing the film thickness. This effect has been shown to be negligible by Calderbank and co-workers[41,61,98]. They also observed that agitation intensity has no influence on the mass transfer rate once it is sufficient to ensure that the gas bubbles and microorganisms are freely suspended. The question as to whether the controlling resistance is the rate of oxygen transfer from gas to liquid or from the liquid to the organism is a matter of the relative interfacial areas, provided that the oxygen concentration of the bubbles is not seriously depleted. This requirement is usually satisfied, since, of the oxygen supplied in the air stream, it is rarely that more than 10 to 15% is actually utilized by the organisms[99].

Brierley and Steel[100] measured oxygen transfer coefficients by the gassing-out method. They found that the rate of solution of oxygen was reduced markedly by addition of filamentous mycelium and paper pulp, but not by the addition of sago pellets. Therefore, they concluded that the morphology of the solid phase largely determined its physical effect upon the oxygen transfer rate.

Wise et al.[101] have observed that the presence of microorganisms can increase by over 40% the oxygen transfer rate at low Reynolds number flow. The increase was reported to be due to the cells or inert particles disrupting the gas-liquid interface surrounding the gas bubble and thus decreasing the interfacial resistance. They have found that neither cell viability nor the cell-liquid interfacial resistance significantly influences the increas in oxygen mass transfer rate.

Van der Kroon[102] has observed that suspended solid particles had a greater effect on the oxygen transfer rate. The presence of suspended solids greatly reduced the rate of sulfite oxidation reaction.

Mimura and co-workers[23] used both the dynamic and mass balance methods in stirred tank batch cultivations in which the media initially contained 1% n-hexadecane by volume. K_La values found by the dynamic method showed a decrease as the fermentation proceeded and as cell concentration increased. However, K_La values found by making a gas phase oxygen balance increased slightly as the growth progressed. They found that when the hexadecane had been exhausted in the fermentation, the value of K_La returned to its initial value. The researchers thus postulated that as growth increased, cells form flocs with oil droplets which accumulated at the gas-liquid interface. This decreased the available interfacial area for oxygen transfer to the liquid and also enabled the cells to take up oxygen directly from the gas or from the interfacial film. During hydrocarbon fermentations cells adsorb to the surface of the oil drops and the interfacial tension between aqueous and hydrocarbon phases decreases as fermentation proceeds[103]. The decrease in the interfacial tension may cause the spreading coefficient to become positive allowing the oil to form a film at the gas-liquid interface[104,105]. For example, the decrease of interfacial tension during batch fermentation of Candida lipolytica on n-hexadecane leads to the spreading coefficient values shown in Fig. 10. The organisms then adsorb to the hydrocarbon film at the air-liquid interface to block the available oxygen transfer pathway.

Prokop et al.[105] have observed similar results during a batch cultivation in a stirred draft tube fermentor with an initial hydrocarbon volume fraction of 5%. They used an oxygen balance on the gas phase to determine the oxygen uptake of the broth and a weighted mean Henry's law constant to determine K_La values with the dynamic method.

In summary, the presence of microorganisms may have a significant effect on the oxygen transfer rate by changing hydrodynamic motion and by blocking the mass transfer route. It is still not certain at this stage what effect the presence of cells has on the rate of oxygen transfer across the interfaces that are present in the hydrocarbon fermentation.

FERMENTOR DESIGN

From a chemical engineering point of view, a fermentor is a reactor which brings into contact gas and liquid phases, providing adequate mixing and heat exchange as well as sufficient mass transfer of oxygen and substrates to and from the microorganisms in a suitable nutritional and physiological environment. In designing a fermentor, the materials of construction must first be considered such that they will not adversely affect, nor be adversely affected by, the desired microbial activity, either by interaction with the fermentation broth or by harboring unwanted organisms. They must be resistant to corrosion by the nutrient medium and products, and to the effect of sterilization temperatures. The actual construction of the equipment from suitable materials must also take account of these factors and of the stresses imposed by pressurization and the weight of vessel contents. Provision for the regulation of temperature and of air supply, for charging and discharging the vessel contents, for inoculation, for the control of pH and foaming, and for controlled addition of sterilized nutrients or other materials during the course of fermentations must be devised simultaneously[107].

The earliest large-scale fermentors as described by de Becze[108] were typical large cylindrical tanks with air injected at the base. This design was soon modified by the use of impellers to increase the effect of mixing and dispersion of gas phase. A reduction in the consumption of compressed air by a factor of five resulted. The addition of mechanical agitation was also found to provide better mixing of the medium and higher oxygen transfer rates than those of the gas sparged tank. The mechanically agitated fermentor, therefore, became standard in the early years of the fermentation industry.

Though the mechanically agitated, fully baffled fermentors equipped with an open-blade turbine have prevailed for quite a long while, this design has not found appreciable application to hydrocarbon fermentation because of the homogeneity problems. Einsele et al.[109] have investigated the agitation and aeration in hydrocarbon fermentations using a flat-blade turbine fermentor and a second fermentor with forced circulation and an emulsifying device. High oxygen transfer rates and 25% higher productivities were obtained with the circulation fermentor due to its good vertical mixing. Katinger[110] has also reported results which indicate that both intensity of mixing and the pattern of circulation influence performance in hydrocarbon fermentations. Humphrey and Erickson[4] have also pointed out that a recycle fermentor in which the fermentor contents periodically pass through a region of intense mixing may provide the desired quality of micromixing for hydrocarbon fermentation. They proposed the region of intense mixing should be designed to generate the desired degree of interfacial area and should also provide for mixing between drops. On this basis, a combination of an open-blade turbine with a draft tube to induce liquid circulation, such as the Waldhof type, is employed more frequently in hydrocarbon fermentation.

Recently, a recycle fermentor with mechanically-driven external circulation has been tested for hydrocarbon fermentation[4,111]. Normally, a pump or a Venturi contactor[111] will meet the requirement of providing good homogeneity through intensive axial flow in this type of fermentors.

While a number of novel fermentor designs have been proposed for the purpose of increasing the oxygen transfer rate, the quality of mixing, as well as minimizing the power requirement, one of the most promising

was found to be the nonmechanically-agitated airlift fermentor which was first patented by Lefrancois and co-workers[112]. Normally, the airlift design consists of an upflow region where gas bubbles and liquid flow upwards cocurrently and a downflow region where gas-liquid motion can be cocurrent and countercurrent as well. The air is sparged at the base of a rising column which immediately lowers the density of the upflow regions. Because of the pressure difference between the upflow and down-flow region, a recirculating flow pattern is formed. As the sparged air flow rate is further increased, the liquid flow rate in the circulation loop increases and bubbles entrained above the downflow region are carried downwards by the liquid motion. Oxygen transfer can therefore take place in both the upflow and downflow regions as well as the region above the draft tube, namely, the head region.

The literature has evidenced various fermentor designs based on the airlift principle. One of the first bench scale airlift fermentors con-sisted of an inverted 5 liter bottle with an airlift tube inserted at the base[113]. Air was sparged at the base through the airlift tube and thence a liquid recirculation formed.

Blakebrough et al.[114] used the sulfite oxidation method to measure oxygen transfer rates in airlift tubes 74 to 367 cm in height and 1.5 to 2.67 cm in diameter. Air was introduced at the base of the airlift tubes below the liquid recirculation inlet and the two phase mixture was discharged from the top of the airlift tubes into a gas-liquid sepa-ration tank. A reservoir was located below the separator to maintain a constant liquid head at the bottom of the airlift tube. By raising or lowering the reservoir the liquid recirculation rate could be varied independently of the air flow rate. Although oxygen transfer rates over 200 millimoles/liter-hour were measured in the airlift tube, approximately

70% of the liquid volume was in the separator and reservoir which lowered the overall oxygen transfer rate to the order of 60 to 80 millimoles/ liter-hour. It was concluded that a number of airlift tubes served by the same reservoir should be built to decrease the dead volume and provide a higher overall oxygen transfer rate.

Laine et al.[115] reported on the production of yeast on hydrocarbons using an airlift fermentor consisting of a column, an air sparger, and a central draft tube to separate upflow and downflow regions. The central draft tube acted as an airlift by coninuously recirculating media up the draft tube and down the annular space between the draft tube and outer column.

A pilot scale concentric airlift fermentor has been extensively studied[11,88]. The fermentor consisted of a 30 cm diameter stainless steel column 5 meters in height with an internal draft tube of 20.6 cm in diameter and 260 cm in height. 200 liter continuous cultures of Candida intermedia utilizing n-alkanes without vitamin supplementation were used for the oxygen transfer studies. The oxygen transfer coefficients measured were found to vary from 200 to 780 millimoles/l-hr-atm depending on location within the fermentor, the fermentor geometry, and the sparged air flow rate. Interesting enough is that Hatch has observed a 50% increase in mass transfer rate for the airlift fermentor with a draft tube compared to studies without a draft tube.

An alternate design to the concentric airlift fermentor is the thin-channel rectangular airlift fermentor[63]. The rectangular airlift consists of a rectangular vessel containing a vertical planar baffle which is placed parallel to the side wall at or near the midpoint. Two spargers are placed parallel to the baffle at the bottom edge and opposite the bottom edge of the baffle in the upflow region. The rectangular

airlift is claimed to have the following operational advantages over concentric airlift: (1) construction is simple permitting nesting of more than one unit, (2) coalescence of bubbles in the upflow region is reduced by a factor of four, (3) bubble entrainment to the downflow region may be enhanced, (4) performance ratios of magnitude greater than ten are indicated in comparison to those ranging from four to five pounds oxygen transferred per horsepower-hour for the concentric airlift fermentors.

Another design is the external recycle airlift fermentor[88,116,117]. Air is sparged at the bottom of the primary column which is treated as the gas-liquid upflow region. The bubbles rise up into a large head region and recirculate down an external column. The external recycle airlift is of simple construction; two columns connected by a common head space and bottom region. The external recycle system has the advantage of easier control of heat transfer, liquid flow rate, and liquid motion.

A split cylinder airlift fermentor was designed for oxygen transfer and fluid mechanics studies[64]. The split airlift consisted of a cylindrical vessel which was split into two equal cross-sectional areas by a vertical baffle. Air is sparged at the base of one compartment. Liquid recirculation can be induced from the upflow compartment to the head region and down in the downflow compartment. The design of split fermentor suggests a minimum internal wetted surface area because of the split cylinder with no internal cooling and heating coils. The reduced wetted area per unit volume of liquid medium increased the liquid velocity which enhanced bubble break-up and increased the interfacial area for mass transfer as well. The performance ratio obtained is constant at 14 lb. O_2/hp-hr for superficial gas velocities up to 500 cm/min, the performance ratio decreases with increasing velocity. Fig. 11 shows comparison of the performance ratio of various fermentor designs.

So far, a number of airlift designs have been applied in industry. In Japan, the Kanegafuchi Chemical Company has built an external recycle airlift fermentor of 1000 liter volume[116]. Imperial Chemical Industries has also tested a very similar 1000 liter airlift of the external circulation design[88,117]. A rectangular airlift fermentor has recently been installed by Betz Laboratories for waste water treatment at Philadelphia[88,117]. A commercial-scale concentric airlift fermentor of 50,000 liter volume was constructed by Gulf Research and Development Co. at Pittsburgh[88,118].

In summary, the production of protein from n-alkanes is currently one of the leading processes in producing protein from non-traditional carbon substrates. In the interest of obtaining high yields in the fermentation process, it is necessary to ensure simultaneously in the aerated and mixed submerged culture[119]:

1) that the concentration of the sparingly soluble oxygen is above the critical concentration;

2) that the cell mass, oil phase, and gas bubble suspended in the medium is sufficiently dispersed by means of mixing with a minimum amount of energy consumption;

3) that the mechanical damage to the population at intensive rates of agitation and aeration should be kept to the minimum.

Research is needed in the area of optimal fermentor design which may simultaneously meet the above requirements for cell growth.

CONCLUSION

Much has been said and written about the oxygen transfer in agi-
tated and aerated fermentation systems, and very thorough reviews have
been available[5,7,8,9,11,14]. However, for mass transfer processes in
the hydrocarbon fermentation, more factors have to be considered because
of the second liquid phase. Oxygen, for example, can be transported from
the gas phase directly to cells at the gas-liquid interface, to the dispersed
liquid phase, or to the continuous aqueous phase. Oxygen also is distri-
buted between the two liquid phases and consumed by cells at the liquid-
liquid interface and in the aqueous phase.

Since many complex physico-chemical and biological processes take
place in fermentations with two liquid phases, it is extremely difficult,
if not impossible, at this stage of development to fully understand what
effect the presence of a second liquid phase has on the rate of oxygen
transfer across the interfaces that are present in a hydrocarbon fermen-
tation. So far, a great number of investigators have chosen to treat
systems with two liquid phases as if there was only one phase by assuming
oxygen equilibrium between the liquids or by neglecting mass transfer to
the dispersed phase. Indeed, in further studies of hydrocarbon systems
where the oil fraction is greater than 2%, it is suggested that the
hydrocarbon phase should be regarded as a distinct phase in the system.
The need of the treatment becomes obvious when the oil fraction is
fairly large.

In hydrocarbon fermentations, oxygen transport is very important.
The biomass productivity per unit volume is usually limited by either
substrate transport or oxygen transport. Since high mass transfer rates
can be obtained in the tower fermentation system, it may be a very

desirable system for the large scale production of single cell protein from petroleum hydrocarbons. The optimization of the productivity per unit volume in the tower fermentor with respect to substrate transfer and oxygen transfer rate is desirable; however, process efficiency must also be considered.

NOMENCLATURE

a = interfacial area per unit volume of liquid dispersion, cm^2/cm^3

a_b = gas-liquid interfacial area per unit volume of liquid dispersion, cm^2/cm^3

a_m = cell-liquid interfacial area per unit volume of liquid disperison, cm^2/cm^3

C = dissolved oxygen concentration, mg O_2/ℓ

C_m = saturated oxygen concentration at cell surface, mg O_2/ℓ

D = dispersion coefficient, cm^2/sec

D_L = oxygen diffusivity in the liquid phase, cm^2/sec

D_{SM} = Sauter mean diameter, cm

D_T = column diameter, cm

d_b = bubble diameter, cm

d_o = orifice diameter, cm

g = gravitational constant, cm/sec^2

g_c = gravitational conversion factor, dimensionless

H_c = Henry's law constant, ℓ - atm/mg O_2

H_G = gas holdup, dimensionless

H_{wh} = partition coefficient of oxygen between water and hydrocarbon phase, ℓ - atm/mg O_2

I = emergent - light intensity, candela

I_o = incident-light intensity, candela

K_L = mass transfer coefficient in liquid film surrounding the gas bubble, cm/sec

K_m = mass transfer coefficient in liquid medium surrounding the cell, cm/sec

K'_m = mass transfer coefficient at the cell surface, cm/sec

L = optical path length, cm

N	=	agitator speed, round/sec
N_o	=	minimum agitator speed for dispersion gas bubbles, round/sec
N_{Bo}	=	Bond number ($= \dfrac{\rho_L g D_T^2}{\gamma}$), dimensionless
N_{Fr}	=	Froude number ($= \dfrac{V_s}{\sqrt{g D_L}}$), dimensionless
N_{Ga}	=	Galileo number ($= \dfrac{g D_T^3}{\nu_L}$), dimensionless
N_{Re}	=	Reynolds number ($= \dfrac{\rho_g V_s d_o}{\mu_g}$), dimensionless
P	=	power consumption, horsepower
P_T	=	pressure, atm
R	=	rate of production of a chemical species, mg O_2/ℓ - sec
r	=	specific oxygen uptake rate by cells, mg O_2/mg cell - sec
r_c	=	radius of curvature, cm
$S_{o/\ell A}$	=	oil spreading coefficient at air-water interface, dyne/cm
T	=	temperature, °C
t	=	time, sec
V	=	volume of the mixing vessel containing the agitated fluids, ℓ
V_b	=	bubble rise velocity, cm/sec
V_L	=	liquid flow rate, cm/sec
V_o	=	orifice gas velocity, cm/sec
V_s	=	superficial gas velocity, cm/sec
V_t	=	terminal bubble rise velocity, cm/sec
V_∞	=	bubble rise velocity in an infinite pool, cm/sec
v	=	velocity, cm/sec
X	=	cell concentration per unit volume of liquid dispersion, mg cell/ℓ
Y	=	mole fraction of oxygen in the gas phase, mole O_2/mole gas

α =   the scattering factor, dimensionless

γ =   surface or interfacial tension, dyne/cm

μ =   viscosity, g/cm-sec

v_L =   kinematic viscosity, cm^2/sec

ρ =   fluid density, g/cm^3

ϕ =   oil volume fraction, dimensionless

Superscripts

$*$ =   at equilibrium

Subscripts

g   =   of the gas phase

L   =   of the liquid phase

m   =   of the microorganism phase

o   =   of the oil phase

W   =   of the aqueous phase

REFERENCES

1. MacLean, G. T., "Oxygen Transfer in Aerated Systems Containing One and Two Liquid Phases", M.S. Thesis, Kansas State University (1976)

2. Humphrey, A. E., "A Critical Review of Hydrocarbon Fermentations and Their Industrial Utilization", Biotechnol. Bioeng., 9, 3 (1967)

3. Mimura, A., "Recent Problems in Petroleum Fermentations: Biochemical Engineering Problems", J. Ferment. Technol., 48, 449 (1970)

4. Humphrey, A. E., and L. E. Erickson, "Kinetics of Growth on Aqueous-Oil and Aqueous-Solid Dispersed Systems", J. Appl. Chem. Biotechnol., 22, 125 (1972)

5. Wang, D. I. C., and A. E. Humphrey, "Developments in Agitation and Aeration of Fermentation Systems", Progress in Industrial Microbiology, (ed.) Hockenhull, D. J. D., Vol. 8, p. 1, J. & A. Churchill Ltd., London (1968)

6. Humphrey, A. E., "Current Developments in Fermentation", Chem. Engng. p. 98, December 9 (1974)

7. Finn, R. K., "Agitation and Aeration", Biochemical and Biological Engineering Science, (ed.) Blakebrough, N., Chapter 4, p. 69, Academic Press, London and New York (1967)

8. Calderbank, P. H., "Mass Transfer in Fermentation Equipment", Biochemical and Biological Engineering Science, (ed.) Blakebrough, N., Chapter 5, p. 102, Academic Press, London and New York (1967)

9. Calderbank, P. H., "Mass Transfer", Mixing (II),(ed.) Uhl, V. W., and J. B. Gray, Chapter 6, p. 1, Academic Press, New York and London (1967)

10. Bajpai, R. K., "Experimental and Analytical Studies of Drop-Size Distributions in Hydrocarbon Fermentations", PhD Thesis, Indian Institute of Technology, Kanpur (1975)

11. Hatch, R. T., "Experimental and Theoretical Studies of Oxygen Transfer in the Airlift Fermentor", PhD Thesis, Massachusetts Institute of Technology (1973)

12. Yamane, T., "Mechanisms of Substrate Uptake and Kinetic Model of Microbial Growth in Hydrocarbon Fermentation with Two Liquid Phases", J. Ferment. Technol., 52, 689 (1974)

13. Erickson, L. E., T. Nakahara, and A. Prokop, "Growth in Cultures with Two Liquid Phases: Hydrocarbon Uptake and Transport", Process Biochem., 10, No. 5, 9 (1975).

14. Hatch, R. T., "Fermentor Design", Single-Cell Protein II, (ed.) Tannenbaum, S. R., and D. I. C. Wang, p. 46, The MIT Press, Cambridge, Massachusetts (1975).

15. Prokop, A. and M. Sobotka, "Insoluble Substrate and Oxygen Trnasport in Hydrocarbon Fermentation", Single-Cell Protein II, (ed.) Tannenbaum, S. R. and D. I. C. Wang, p. 126, The MIT Press, Cambridge, Massachusetts, (1975

16. Hromatka, O., H. Ebner, and C. Csoklich, "Vinegar Fermentation. IV. Influence of Complete Interruption of Aeration on the Submerged Fermentation", Enzymologia, 15, 134 (1951)

17. Hixon, A. W. and E. L. Gaden, Jr., "Oxygen Transfer in Submerged Fermentation", Ind. Eng. Chem., 42, 1792 (1950)

18. Bartholomew, W. H., E. O. Karow, M. R. Sfat, and R. H. Wilhelm, "Design and Operation of a Laboratory Fermentor", Ind. Eng. Chem., 42, 1801 (1950)

19. Whitaker, S., "The Transport Equation for Multi-Phase Systems", Chem. Eng. Sci., 28, 139 (1973)

20. Gray, W. G., "A Derivation of the Equations for Multi-Phase Transport", Chem. Eng. Sci., 30, 229 (1975)

21. Mimura, A. and I. Takeda, "Biochemical Engineering Analysis of Hydrocarbon Fermentation. (IV) Effect of Dissolved Oxygen on a Hydrocarbon Assimilating Yeasts", J. Ferment. Technol., 50, 250 (1972)

22. Moo-Young, M., T. Shimizu, and D. A. Whitworth, "Hydrocarbon Fermentations Using Candida Lipolytica. I. Basic Growth Parameters for Batch and Continuous Culture Conditions", Biotechnol. Bioeng., 13, 741 (1971)

23. Mimura, A., I. Takeda, and R. Wakasa, "Some Characteristic Phenomena of Oxygen Transfer in Hydrocarbon Fermentation", Biotechnol. Bioeng. Symp., No. 4, 467 (1973)

24. Cooper, C. M., G. A. Fernstrom, and S. A. Miller, "Performance of Agitated Gas-Liquid Contactors", Ind. Eng. Chem., 36, 504 (1944)

25. Maxon, W. D. and M. J. Johnson, "Aeration Studies on Propagation of Baker's Yeasts", Ind. Eng. Chem., 45, 2554 (1953)

26. Schultz, J. S. and E. L. Gaden, Jr., "Sulfite Oxidation as a Measure of Aeration Effectiveness", Ind. Eng. Chem., 48, 2209 (1956)

27. Friedman, A. M. and E. N. Lightfoot, Jr., "Oxygen Absorption in Aerated Tanks. New Correlation for Open Flat-Bladed Impellers", Ind. Eng. Chem., 49, 1227 (1957)

28. Hamer, G. and N. Blakebrough, "Turbine Impellers as Gas-Liquid Contacting Devices", J. Appl. Chem., 13, 517 (1963)

29. Blakebrough, N. and K. Sambamurthy, "Performance of Turbine Impellers in Sparger Aerated Fermentation Vessels", J. Appl. Chem., 14, 413 (1964)

30. Blakebrough, N. and K. Sambamurthy, "Mass Transfer and Mixing Rates in Fermentation Vessels", Biotechnol. Bioeng., 8, 25 (1966)

31. Robinson, R. G. and A. J. Engel, "An Analysis of Controlled-Cycling Mass-Transfer Operations", Bio. Eng. Food Process, Chem. Eng. Prog. Symp. Series, 69, 129 (1966)

32. Finn, R. K., "Agitation-Aeration in the Laboratory and in Industry", Bacteriol. Review, 18, 254 (1954)

33. Pirt, S. J., D. S. Callow, and W. A. Gillett, "Oxygen Absorption Rates in Sodium Sulfite Solutions. Comparison of Cupric and Cobaltous Ions as Catalysts", Chem. Ind. (London), 730 (1957)

34. Greenhalgh, S. H., W. J. McManamey, and K. E. Porter, "A Comparison of Oxygen Mass Transfer into Sodium Sulphite Solution and a Biological System", J. Appl. Chem. Biotechnol., 25, 143 (1975)

35. Liu, M. S., R. M. R. Branion, and D. W. Duncan, "Oxygen Transfer to Water and to Sodium Sulfite Solutions", J. Water Pollut. Contr. Fed., 44, 34 (1972)

36. Liu, M. S., "Oxygen Trnasfer in a Fermentor", PhD Thesis, University of British Columbia (1973)

37. Taguchi, H. and A. E. Humphrey, "Oxygen Transfer in Fermentation Processes", Kagaku Kogaku, 30, 869 (1966)

38. Bandyopadhyay, B., A. E. Humphrey, and H. Taguchi, "Dynamic Measurement of the Volumetric Oxygen Transfer Coefficient in Fermentation Systems", Biotechnol. Bioeng., 9, 533 (1967)

39. Bandyopadhyay, B., "Development of a Dynamic Technique for Measuring Volumetric O_2 Transfer Rates in Aerobic Fermentations--Its Utility and Limitations", PhD Thesis, University of Pennsylvania (1969)

40. Miller, T. L. and M. J. Johnson, "Utilization of Normal Alkanes by Yeasts", Biotechnol. Bioeng., 8, 549 (1966)

41. Calderbank, P. H., "Physical Rate Process in Industrial Fermentation. I: The Interfacial Area in Gas-Liquid Contacting with Mechanical Agitation", Trans. Inst. Chem. Engrs., 36, 443 (1958)

42. Lee, J. C. and D. L. Meyrick, "Gas-Liquid Interfacial Areas in Salt Solutions in an Agitated Tank", Trans. Inst. Chem. Engrs., 48 (2), T37 (1970)

43. Trice, V. G., Jr. and W. A. Rodger, "Light Transmittance as a Measure of Interfacial Area in Liquid-Liquid Dispersions", AIChE J., 2, 205 (1956)

44. Van Dierendonck, L. L., J. M. H. Fortuin, and D. Venderbos, "Specific Contact Area in Gas-Liquid Reactors", Fourth European Symposium on Chemical Reaction Engineering, Brussels (1968)

45. Towell, G. D., C. P. Strand, and G. H. Ackerman, "Mixing and Mass Transfer in Large-Diameter Bubble Columns", Proc. AIChE – I. Chem. E. Symposium, No. 10, p. 97, Inst. Chem. Engrs., London (1965)

46. Kawecki, W., T. Reith, J. W. Van Heuven, and W. J. Beek, "Bubble Size Distribution in the Impeller Region of a Stirred Vessel", Chem. Eng. Sci., 22, 1519 (1967)

47. Robertson, C. S., Jr. and P. J. Birbara, "Interfacial Area by Alpha Dosimetry", Unclassified, ORNL K T-256, Unpublished.

48. Bressee, J. C. and C. V. Chester, "The Use of Radioisotopes for the Measurement of Interfacial Area", 2nd. U. N. Intern. Conf. on the Peaceful Uses of Atomic Energy (1958)

49. Mitsis, G. J., R. R. Plebuch, and K. F. Gordon, "A Scintillation Method for Determining Liquid-Liquid Interfacial Areas", AIChE J., 6, 505 (1960)

50. Reith, T. and W. J. Beek, "Gas Holdups, Interfacial Areas, and Mass-Transfer Coefficients in Gas-Liquid Contactors", Fourth European Symposium on Chemical Reaction Engineering, Brussels (1968)

51. Reith, T. and W. J. Beek, "Oxidation of Aqueous Sodium Sulfite Solutions", Chem. Eng. Sci., 28, 1331 (1973)

52. Reith, T., "Interfacial Area and Scaling-Up of Gas-Liquid Contactors", Brit. Chem. Eng., 15, 1559 (1970)

53. Valentine, F. H. H., Absorption in Gas-Liquid Dispersions, E. & F. N. Spon. Ltd., London (1967)

54. Fair, J. R., A. J. Lambright, and J. W. Andersen, "Heat Transfer and Gas Hold-Up in a Sparged Contactor", Ind. Eng. Chem. Process Design Develop., 1, 33 (1962)

55. Kitai, A., R. Okamoto, and A. Ozaki, "The Performance of Perforated Plate Column as a Multistage Continuous Fermentor. (III) Determination of Oxygen Transfer Coefficient", J. Ferment. Technol., 47, 348 (1969)

56. Akehata, T., "Distributions of Gas Hold-Up in Baffled and Unbaffled Bubble Columns", Bulletin of Tokyo Inst. of Technol., No. 122, 13 (1974)

57. Akita, K. and F. Yoshida, "Gas Holdup and Volumetric Mass Transfer Coefficient in Bubble Columns", Ind. Eng. Chem. Process Design Develop., 12, 76 (1973)

58. Akita, K. and F. Yoshida, "Bubble Size, Interfacial Area, and Liquid-Phase Mass Transfer Coefficient in Bubble Columns", Ind. Eng. Chem. Process Design Develop., 13, 84 (1974)

59. Mashelkar, R. A., "Bubble Columns", Brit. Chem. Eng., 15, 1297 (1970)

60. Hsu, K. H., "Growth of Mixed Cultures and Oxygen Transfer in Tower Systems with Motionless Mixers", M.S. Thesis, Kansas State University (1974)

61. Calderbank, P. H., "Physical Rate Processes in Industrial Fermentation. Part II. Mass Transfer Coefficients in Gas-Liquid Contacting with and without Mechanical Agitation", Trans. Inst. Chem. Engrs., 37, 173 (1959)

62. Fan, L. T. and K. B. Wang, "Oxidation of Sulfite in an Air Lift Reactor Packed with Motionless Mixers", Presented at AIChE 81st National Meeting, Kansas City, MO, April 11-14 (1976)

63. Gasner, L. L., "Development and Application of the Thin Channel Rectangular Air Lift Mass Transfer Reactor to Fermentation and Waste-Water Treatment Systems", Biotechnol. Bioeng., 16, 1179 (1974)

64. Belfield, A. R., Jr., "Experimental Studies of Oxygen Transfer in a Split Cylinder Airlift", M.S. Thesis, University of Maryland (1976)

65. Leibson, I., E. G. Holcomb, A. G. Cacoso, and J. J. Jacmic, "Rate of Flow and Mechanics of Bubble Formation from Single Submerged Orifices", AIChE J., 2, 296 (1956)

66. Potter, O. E., "Bubble Formation under Constant Pressure Conditions", Chem. Eng. Sci., 24, 1733 (1969)

67. Levich, V. G., Physicochemical Hydrodynamics, Prentice-Hall, Inc., Englewood Cliffs, NJ (1962)

68. Hu, S. and R. C. Kintner, "The Fall of Single Liquid Drops through Water", AIChE J., 1, 42 (1955)

69. Mashelkar, R. A. and M. M. Sharmar, "Mass Transfer in Bubble and Packed Columns", Trans. Inst. Chem. Engrs., 48, T162 (1970)

70. Krishnamurthi, S., R. Kumar, and R. L. Datta, "Formation of Air Bubbles in Liquids. Effect of Orifice Geometry", Trans. Indian Inst. Chem. Engrs., 14, 78 (1961)

71. Kumar, R. and N. R. Kuloor, "The Formation of Bubbles and Drops", Advances in Chemical Engineering, (ed.) Drew, T. B., G. R. Cokelet, J. W. Hoopes, Jr., and T. Vermeulen, Vol. 8, p. 255, Academic Press, New York, NY (1970)

72. Ramakrishnan, S., R. Kumar, and N. R. Kuloor, "Bubble Formation. I. Bubble Formation under Constant Flow Conditions", Chem. Eng. Sci., 24, 731 (1969)

73. Deckwer, W.-D., R. Burckhart, and G. Zoll, "Mixing and Mass Transfer in Tall Bubble Columns", Chem. Eng. Sci., 29, 2177 (1974)

74. Deckwer, W.-D. and R. Burckhart, "Determination of Mass Transfer in Tower Fermenters", Fifth International Ferment. Symp., p. 63, Berlin (1976)

75. Eckenfelder, W. W., Jr., "Process Design of Aeration System for Biological Waste Treatment", Chem. Eng. Progress, 52, 286 (1956)

76. Oels, U. and K. Schugerl, "Influence of Different Types of Gas Distributors on the Performance of Bubble Column Fermentors", Fifth International Ferment. Symp., p. 64, Berlin (1976)

77. Fair, J. R., "Designing Gas-Sparged Reactors", Chem. Engng., p. 67 July 3 (1967)

78. Yoshida, F. and K. Akita, "Performance of Gas Bubble Columns", AIChE J., 11, 9 (1965)

79. Freedman, W., and J. F. Davidson, "Hold-up and Liquid Circulation in Bubble Columns", Trans. Inst. Chem. Engrs., 47, 251 (1969)

80. Calderbank, P. H., M. B. Moo-Young, and R. Bibby, "Coalescence in Bubble Reactors and Absorbers", Chem. Reaction Eng. Symp., p. 91 (1964)

81. Calderbank, P. H., "Gas Absorption from Bubbles", Chem. Engr., 45, CE209 (1967)

82. Blanco, J., L. Scotti, and J. C. Yarze, "Hold-up and Mass Transfer in a Highly Expanded Gas-Liquid Sparged Reactor", Ind. Eng. Chem. Research Results Service (1970)

83. Wallis, G. B., One-Dimensional Two-Phase Flow, McGraw-Hill, Inc., New York, NY (1969)

84. Hatch, R. T., "Mass Transfer Characteristics of an Airlift Fermentor", M.S. Thesis, Massachusetts Institute of Technology (1969)

85. Hatch, R. T., C. Cuevas, and D. I. C. Wang, "Oxygen Absorption Rates in Airlift Fermentors: Laboratory and Pilot Studies", Presented at 158th National American Chemical Society Meeting, New York, NY, September 8-12 (1969)

86. Wang, D. I. C., and R. T. Hatch, "Engineering Developments in the Production of Single-Cell Protein", Proceedings of International Symposium on Conversion and Manufacture of Foodstuffs by Microorganisms, p. 24, Saikon Publ. Co. Ltd., Tokyo, Japan (1971)

87. Wang, D. I. C., R. T. Hatch, and C. Cuevas, "Engineering Aspects of Single-Cell Protein Production from Hydrocarbon Substrates: The Airlift Fermentor", Proceedings of the 8th World Petroleum Congress, Vol. 5, p. 149, Applied Science Publishers Ltd., Essex, England (1971)

88. Hatch, R. T. and D. I. C. Wang, "Oxygen Transfer in the Airlift Fermentor", Presented at 1st Chemical Congress of the North American Continent, Mexico City, December (1975)

89. Orazem, M. E., "Effect of Column Height of Oxygen Transfer in Airlift Fermentor", Proceedings of the Sixth Biochemical Engineering Symposium, Published by Iowa State University (1976)

90. Speece, R. E., and P. G. Lim, "Commercial Oxygen Applications in Industrial Fermentation", Presented at American Chemical Society Annual Meeting, Chicago, IL, August (1973).

91. Onda, K., H. Takenchi, and Y. Maeda, "The Absorption of Oxygen into Sodium Sulfite Solution in a Packed Column", Chem. Eng. Sci., 27, 449 (1972)

92. Deckwer, W.-D., "Non-Isobaric Bubble Columns with Variable Gas Velocity", Chem. Eng. Sci., 31, 309 (1976)

93. Ho, C. S., "Mathematical Model of Oxygen Transfer in Airlift Fermentors", Proceedings of the Sixth Biochemical Engineering Symposium, Published by Iowa State University (1976)

94. Yoshida, F., T. Yamane, and Y. Miyamoto, "Oxygen Absorption into Oil-in-Water Emulsions", Ind. Eng. Chem. Process Design Develop., 9, 570 (1970)

95. Yamane, T. and F. Yoshida, "Comments on Oxygen Absorption into Oil-Water Emulsions", J. Ferment. Technol., 52, 445 (1974)

96. Coty, V. F., R. L. Gorring, I. J. Heilweil, R. J. Leavitt, and S. Serinivasan, "Growth of Microbes in an Oil Continuous Environment," Biotechnol. Bioeng., 13, 825 (1971)

97. Matsumura, M., M. Obara, H. Yoshitome, and J. Kobayashi, "Oxygen Equilibrium Distribution and Its Transfer in an Air-Water-Oil System," J. Ferment. Technol., 50, 742 (1972)

98. Calderbank, P. H., and S. J. R. Jones, "Physical Rate Processes in Industrial Fermentation--Part III. Mass Transfer from Fluids to Solid Particles Suspended in Mixing Vessels", Trans. Inst. Chem. Engrs., 39, 363 (1961)

99. Blakebrough, N., "Mass Transfer in Aerobic Microbial Systems", Brit. Chem. Eng., 12, 78 (1967)

100. Brierley, M. R. and R. Steel, "Agitation-Aeration in Submerged Fermentation. Part 2. Effect of Solid Disperse Phase on Oxygen Absorption in a Fermentor", Appl. Microbiol., 7, 57 (1959)

101. Wise, D. L., D. I. C. Wang, and R. I. Matelles, "Increased Oxygen Mass Transfer Rates from Single Bubbles in Microbial Systems at Low Reynolds Numbers", Biotechnol. Bioeng., 11, 647 (1969)

102. Van der Kroon, G. T. M., "The Influence of Suspended Solids on the Rate of Oxygen Transfer in Aqueous Solutions", Water Research, 2, 26 (1968)

103. Mimura, A., S. Watanabe, and I. Takeda, "Biochemical Engineering Analysis of Hydrocarbon Fermentation. III. Analysis of Emulsification Phenomena", J. Ferment. Technol., 49, 255 (1971)

104. Erickson, L. E., T. Nakahara, J. R. Gutierrez, G. T. MacLean, and L. T. Fan, "Modelling and Characterization of Hydrocarbon Fermentations", Presented at Joint US/USSR Conference on Data Acquisition and Processing for Laboratory and Industrial Measurements in Fermentation Processes, University of Pennsylvania, Philadelphia, August 12-15 (1975)

105. Erickson, L. E., J. R. Gutierrez, and T. Nakahara, "Growth of Cultures with Two Liquid Phases in Tower Systems", Fifth International Ferment. Symp., P. 132, Berlin (1976)

106. Prokop, A., M. Sobotka, J. Panos, and K. Pecka, "Batch Kinetics and Oxygen Consumption of Candida lipolytica 4-1 on n-Alkanes", Folio Microbial., 19, 125 (1974)

107. Blakebrough, N., "Fundamentals of Fermentor Design", Pure and Appld. Chem., 36, 305 (1973)

108. De Becje, G., and A. J. Liebmann, "Aeration in the Production of Compressed Yeast", Ind. Eng. Chem., 36, 882 (1944)

109. Einsele, A., H. W. Blanch, and A. Fiechter, "Agitation and Aeration in Hydrocarbon Fermentations", Biotechnol. Bioeng. Symp., No. 4, 455 (1973)

110. Katinger, H. W. D., "Influence of Interfacial Area and Nonutilizable Hydrocarbons on Growth Kinetics of Candida sp. in Hydrocarbon Fermentations", Biotechnol. Bioeng. Symp., No. 4, 455 (1973)

111. Bauer, W. G., A. G. Frederickson, and H. M. Tsuchiya, "Mass-Transfer Characterisitcs of a Venturi Liquid-Gas Contactor," Ind. Eng. Chem. Process Design Develop., 2, 178 (1963)

112. Lefrancois, L., C. G. Mariller, and J. V. Mejane, "Effectionnements aux procedes de Cultures fongiques et de Fermentations Industrielles", Brevet D'Invention, France #1,102,200, Delivree le 4 Mai (1955)

113. Lundgren, D. G., and R. T. Russell, "An Air-Lift Laboratory Fermentor", Appl. Microbiol., 4, 31 (1955)

114. Blakebrough, N., P. G. Shepherd, and I. Nimmons, "Equipment for Hydrocarbon Fermentations", Biotechnol. Bioeng., 9, 77 (1967)

115. Laine, B., C. Vernet, and G. Evans, "Recent Progress in the Production of Protein from Petroleum", Proc. of 7th. World Petroleum Congress, Vol. 8, Part 2, 197, Elsevier Publishing Co. Ltd., Essex, England (1967)

116. Kanazawa, M., "The Production of Yeast from n-Paraffins", Single-Cell Protein II, (ed.) Tannenbaum, S. R., and D. I. C. Wang, P.438, The MIT Press, Cambridge, Massachusetts (1975)

117. Gow, P. G., J. D. Littlehailes, S. R. L. Smith, and R. B. Walter, "SCP Production from Methanol: Bacteria", Single-Cell Protein II, (ed.) Tannenbaum, S. R., and D. I. C. Wang, P. 370, the MIT Press, Cambridge, Massachusetts (1975)

118. Cooper, P. G., R. S. Silver, and J. P. Boyle, "Semi-Commercial Studies of a Petroprotein Process Based on N-Paraffins", Single-Cell Protein II, (ed.) Tannenbaum, S. R., and D. I. C. Wang, P. 454, The MIT Press, Cambridge, Massachusetts (1975)

119. Lrngyel, Z. L., "Problems of Mixing and Aeration in Submerged Culture Processes", Int. Chem. Eng., 10, 252 (1970)

120. Hughmark, G. A., "Holdup and Mass Transfer in Bubble Columns", Ind. Eng. Chem. Process Des. Develop., 6, 218 (1967)

121. Carleton, A. J., R. J. Flain, J. Rennie, and F. H. H. Valentin, "Some Properties of a Packed Bubble Column", Chem. Eng. Sci., 22, 1839 (1967)

122. Fukuda, H., Y. Sumino, and T. Kanzaki, "Scale-Up of Fermentors", J. Ferment. Technol., 46, 829 (1968)

123. Miura, Y., "Transfer of Oxygen and Scale-Up in Submerged Aerobic Fermentation", Advances in Biochemical Engineering, (ed.) Ghose, T. K., A. Fiechter, and N. Blakebrough, Vol. 4, P. 3, Springer-Verlag Berlin, Heidelberg (1976)
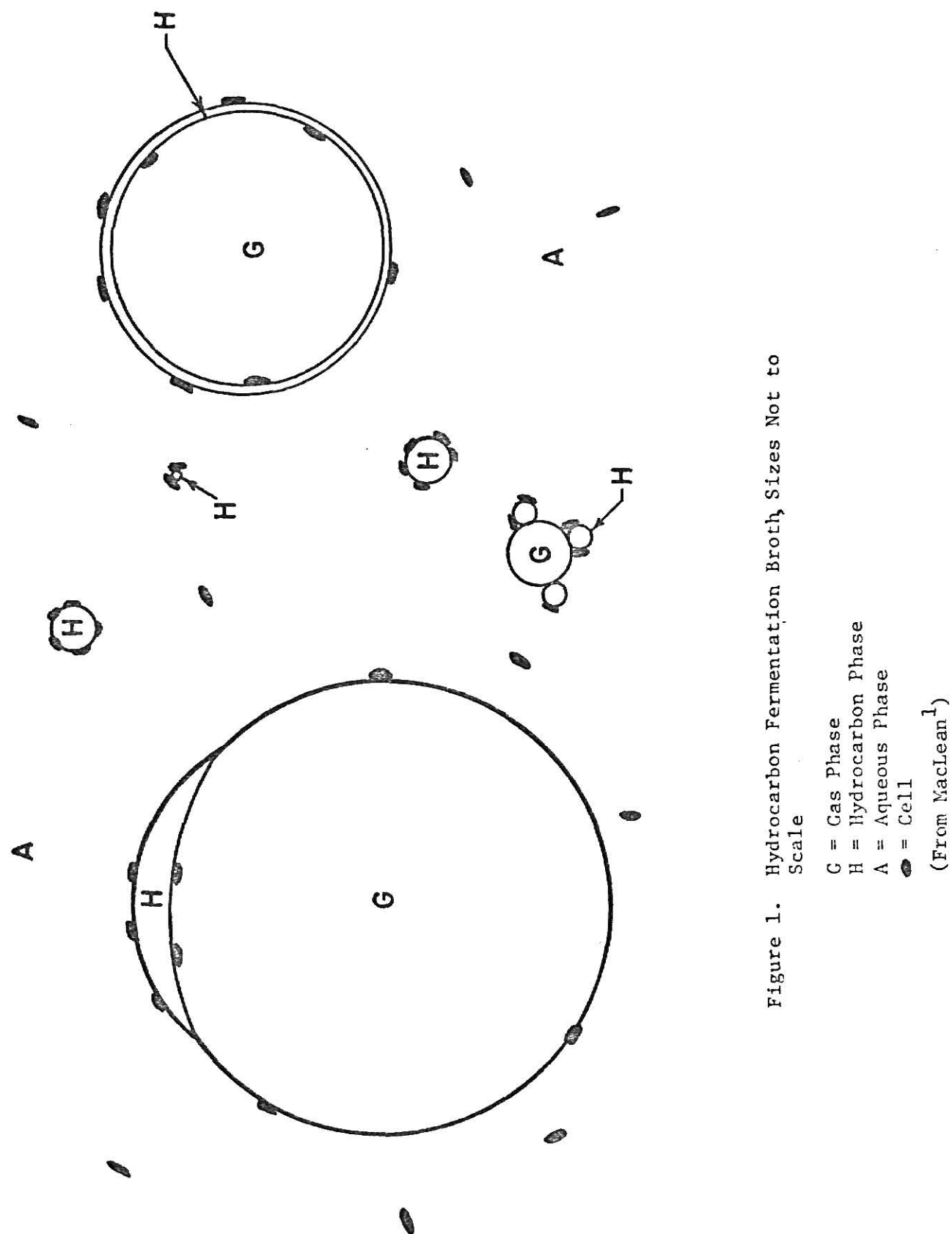
Figure 1. Hydrocarbon Fermentation Broth, Sizes Not to Scale

G = Gas Phase
H = Hydrocarbon Phase
A = Aqueous Phase
● = Cell

(From MacLean[1])
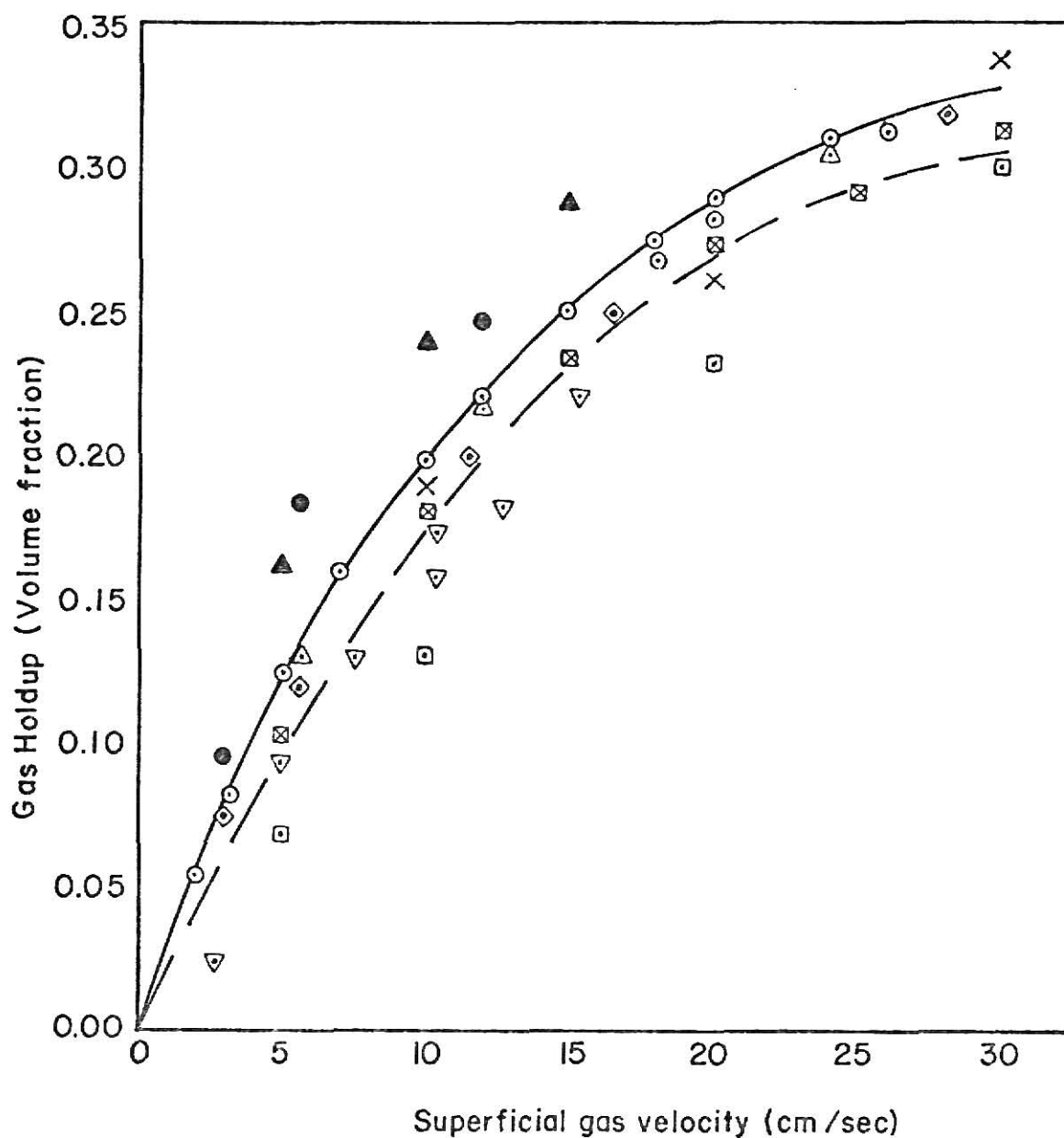
Fig. 2. Correlation of gas holdup data.

Solid line — Mashelker[59]

▽ — Belfield[64]

◇ — Yoshida and Akita[78]

△ — Towell et al.[45]

● — Fair et al.[54]

⊠ — Hatch[11]

⊡ — Fan and Wang[62]

⊙ — Hughmark[120]

✕ — Reith and Beek[50]

△ — Carleton et al.[121]
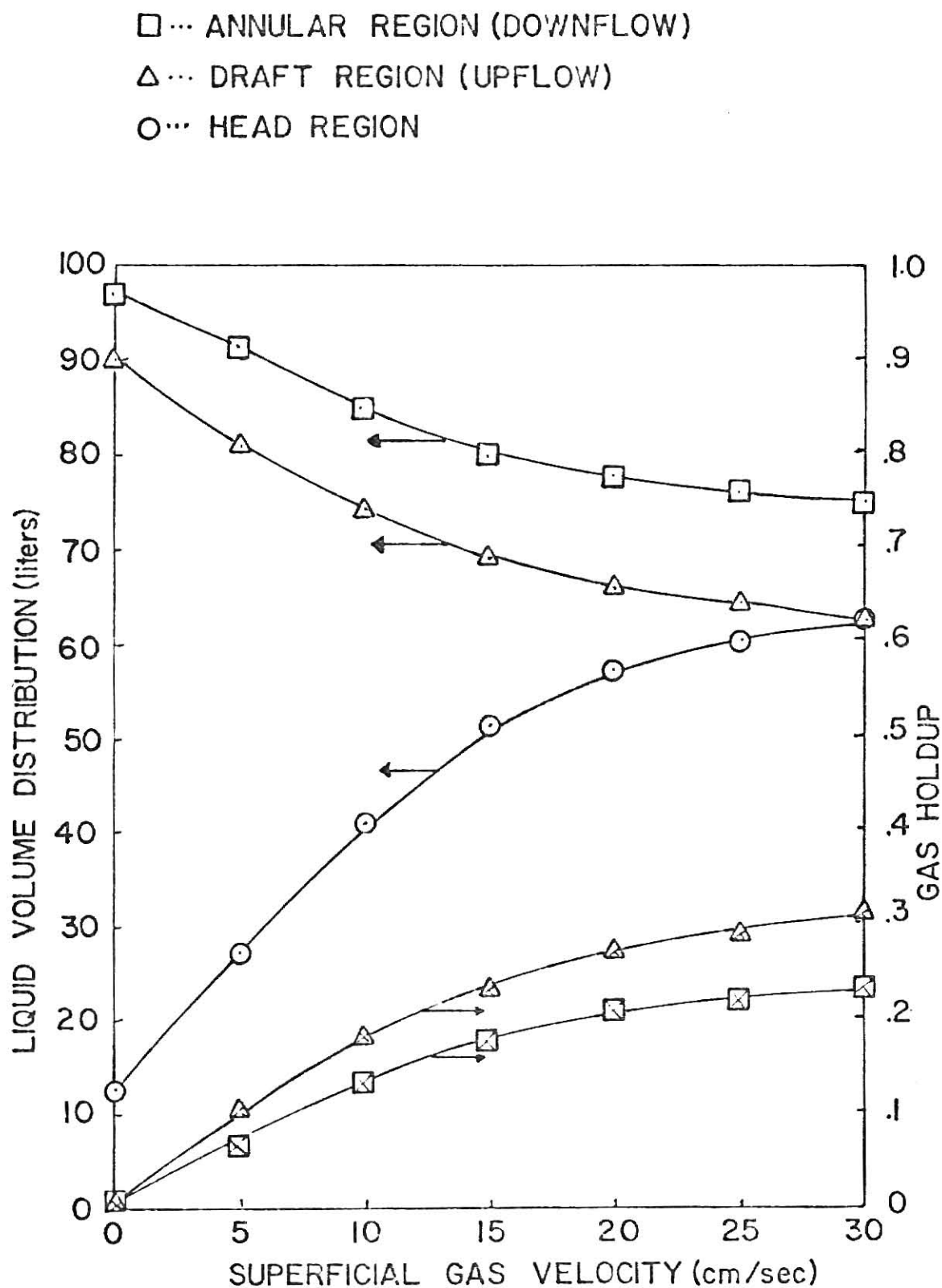
Fig. 3.   Gas holdup distribution in the concentric airlift fermentor.
(From Hatch[11])
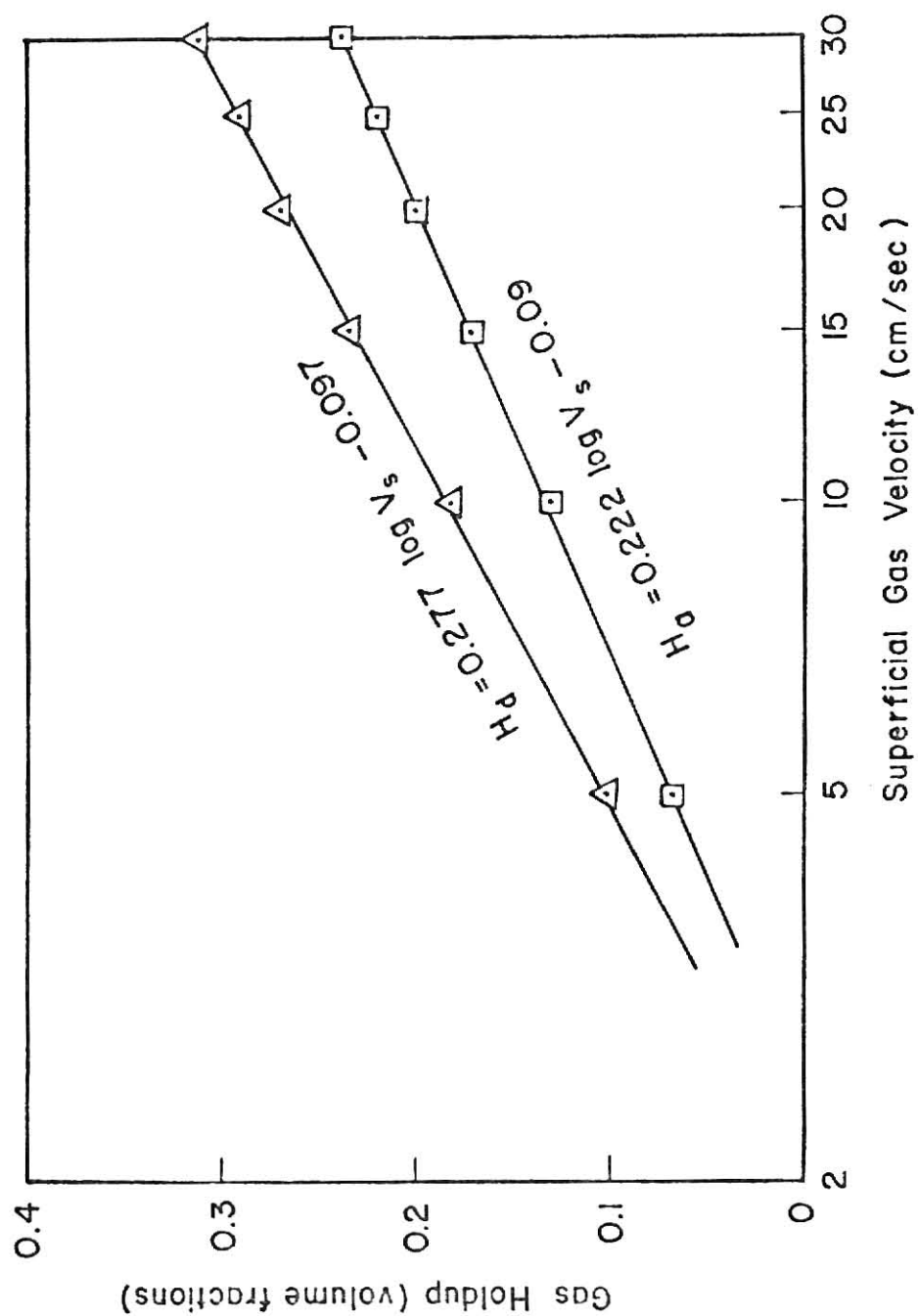
Fig. 4. Correlation of gas holdup with draft tube superficial gas velocity in the concentric airlift fermentor. (Data from Hatch[11])

△ draft tube, ⊡ annular region.
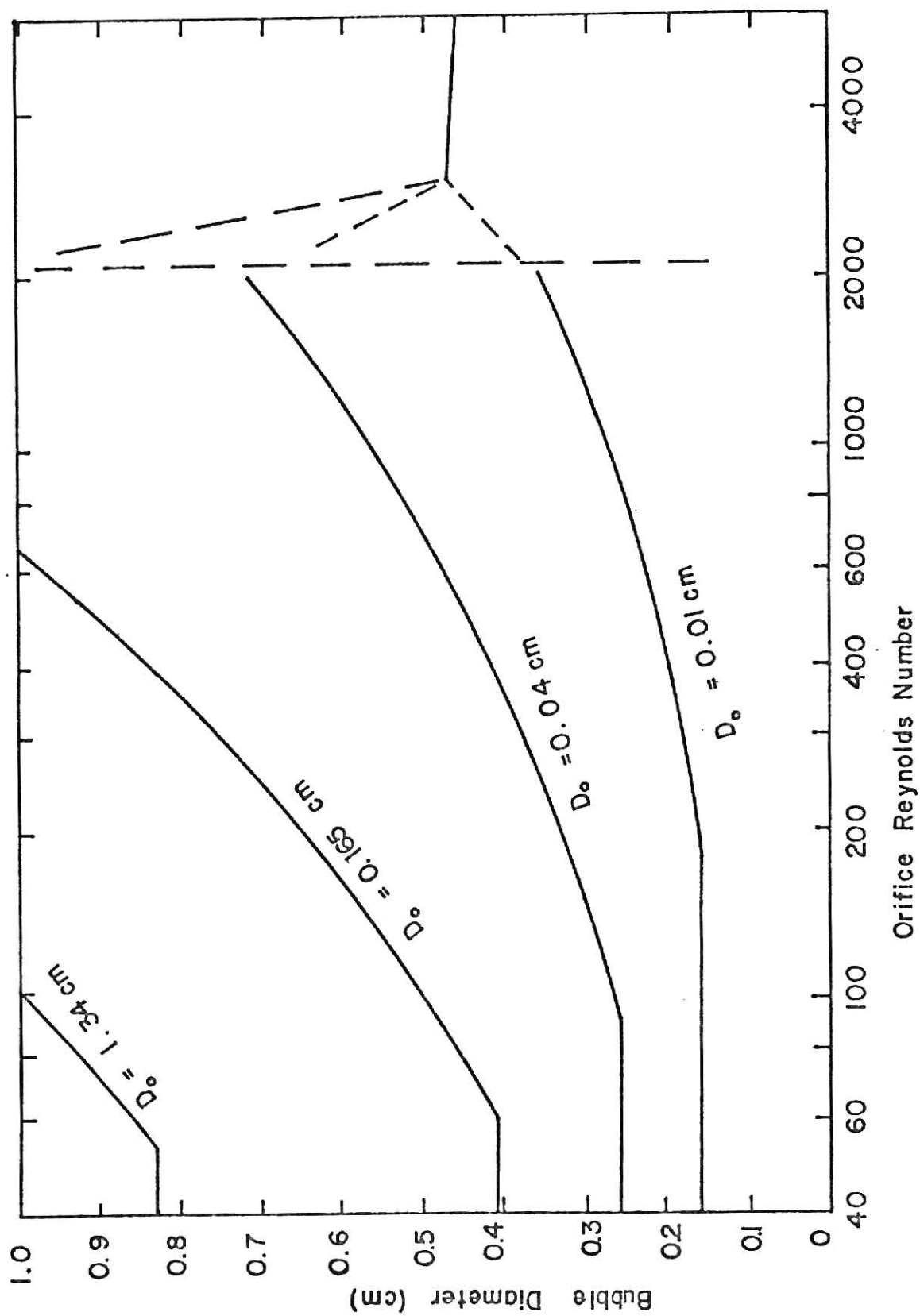
Fig. 5. Bubble diameter as a fuction of orifice Reynolds number with orifice diameter as parameter. (From Hatch[11])
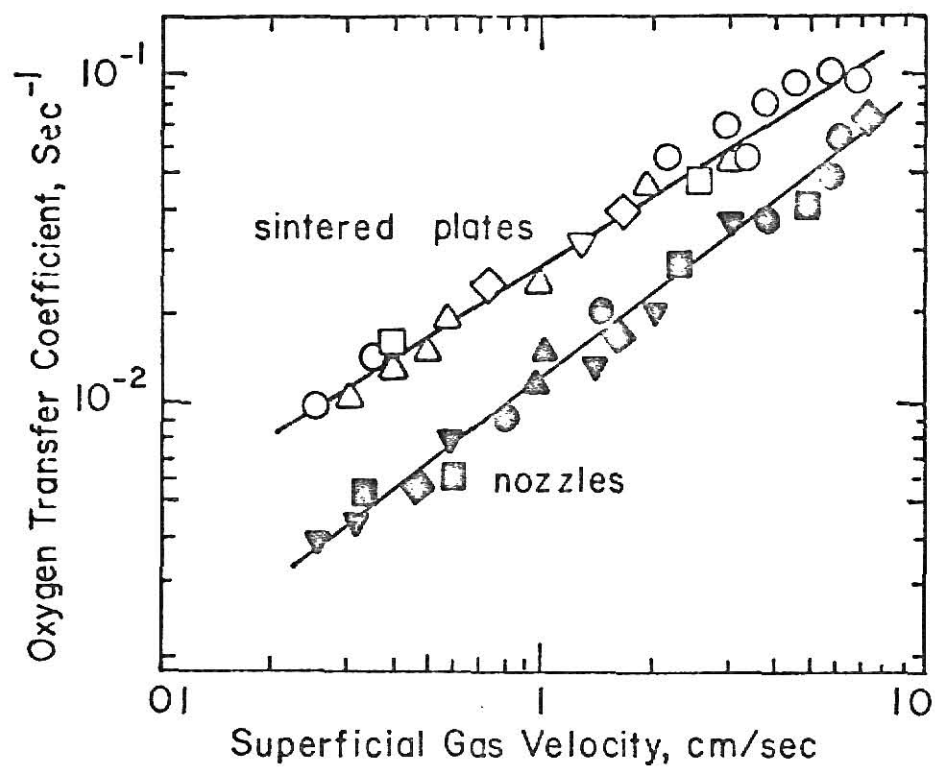
Fig. 6. K_La values at various liquid flow rates for nozzles and sintered plates as gas dispersers. (From Deckwer and Burckhart[74])
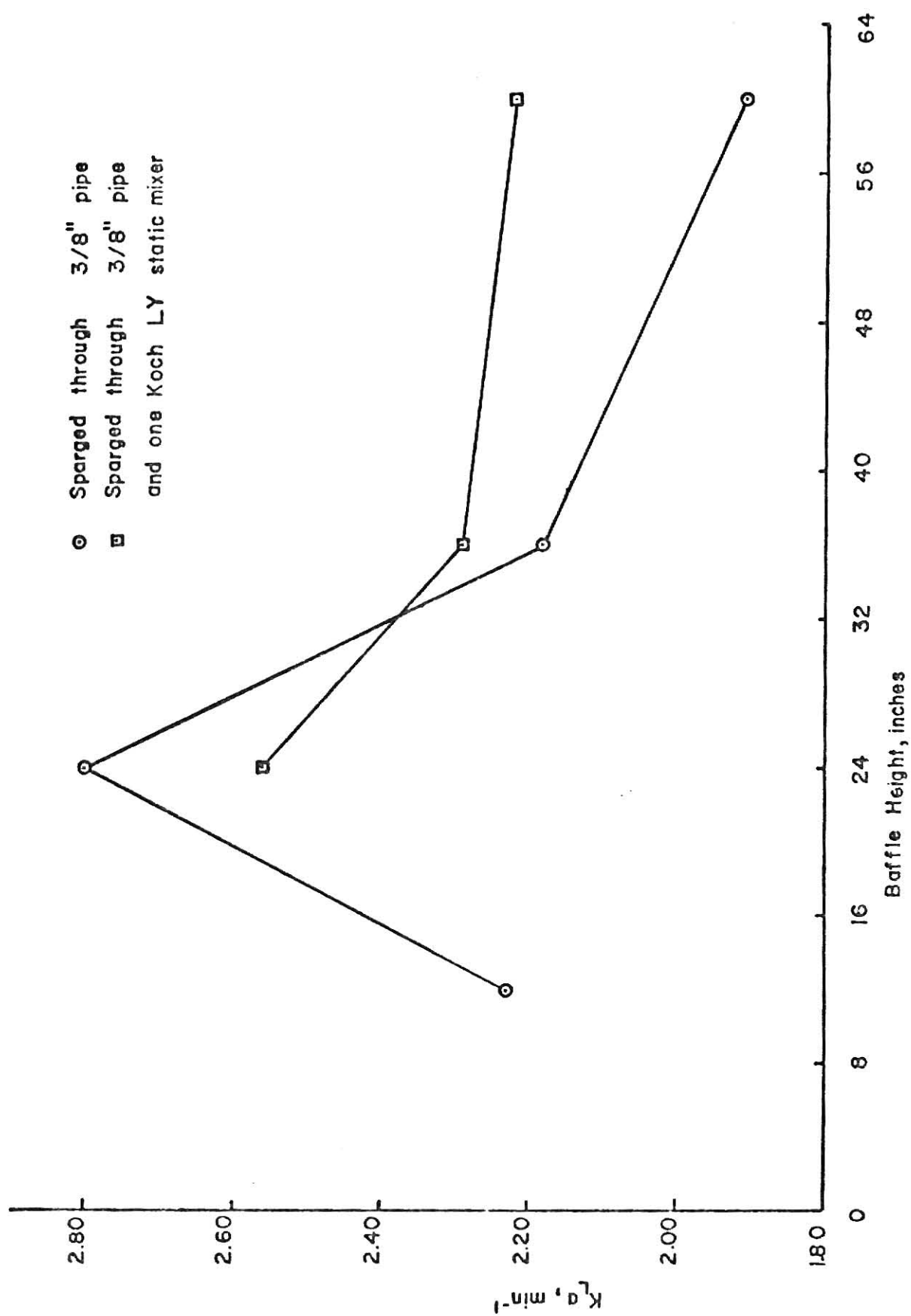
Fig. 7. The effect of baffle height on the mass transfer coefficient. (From Orazem[89])
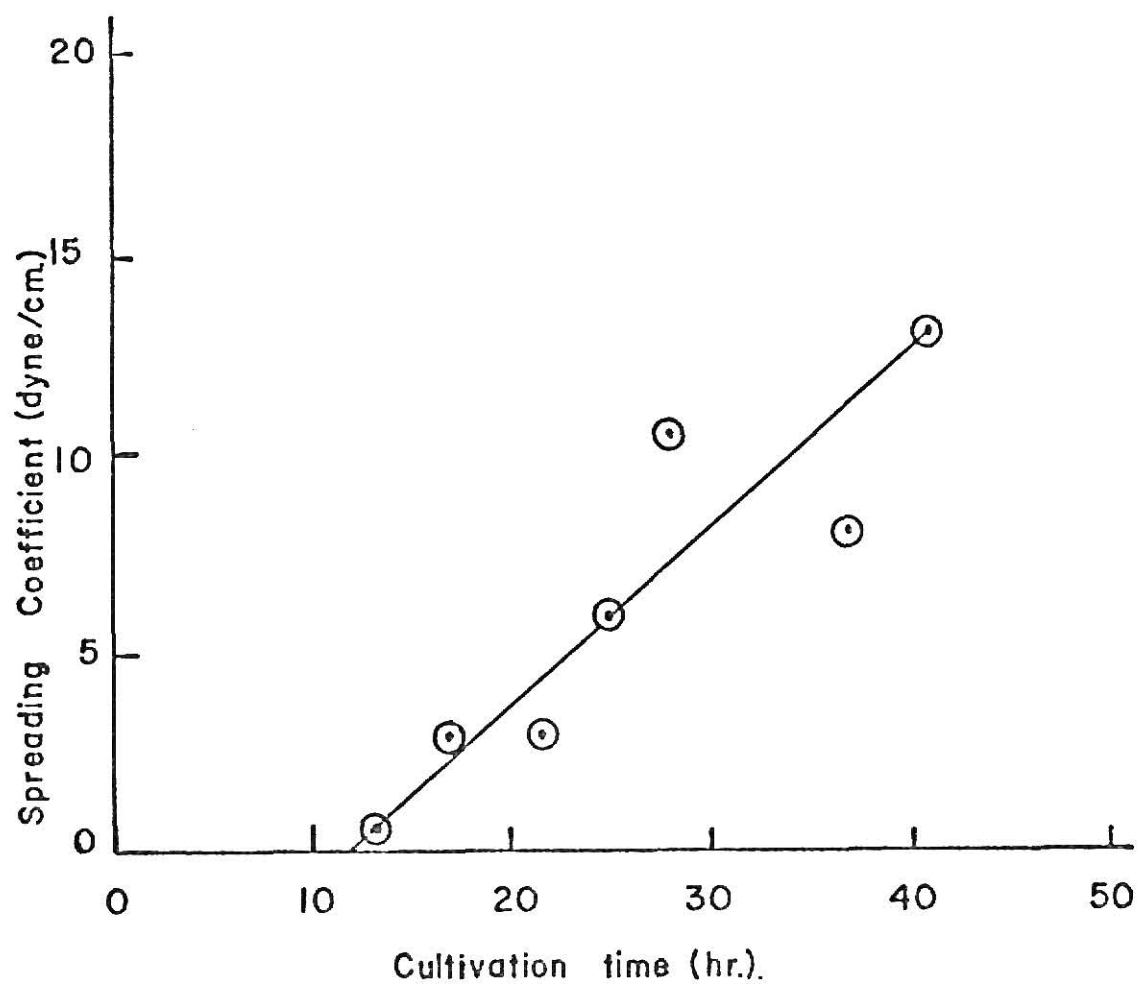
Fig. 8. Effect of cultivation on spreading coefficient during batch fermentation (From Erickson et al.[105])
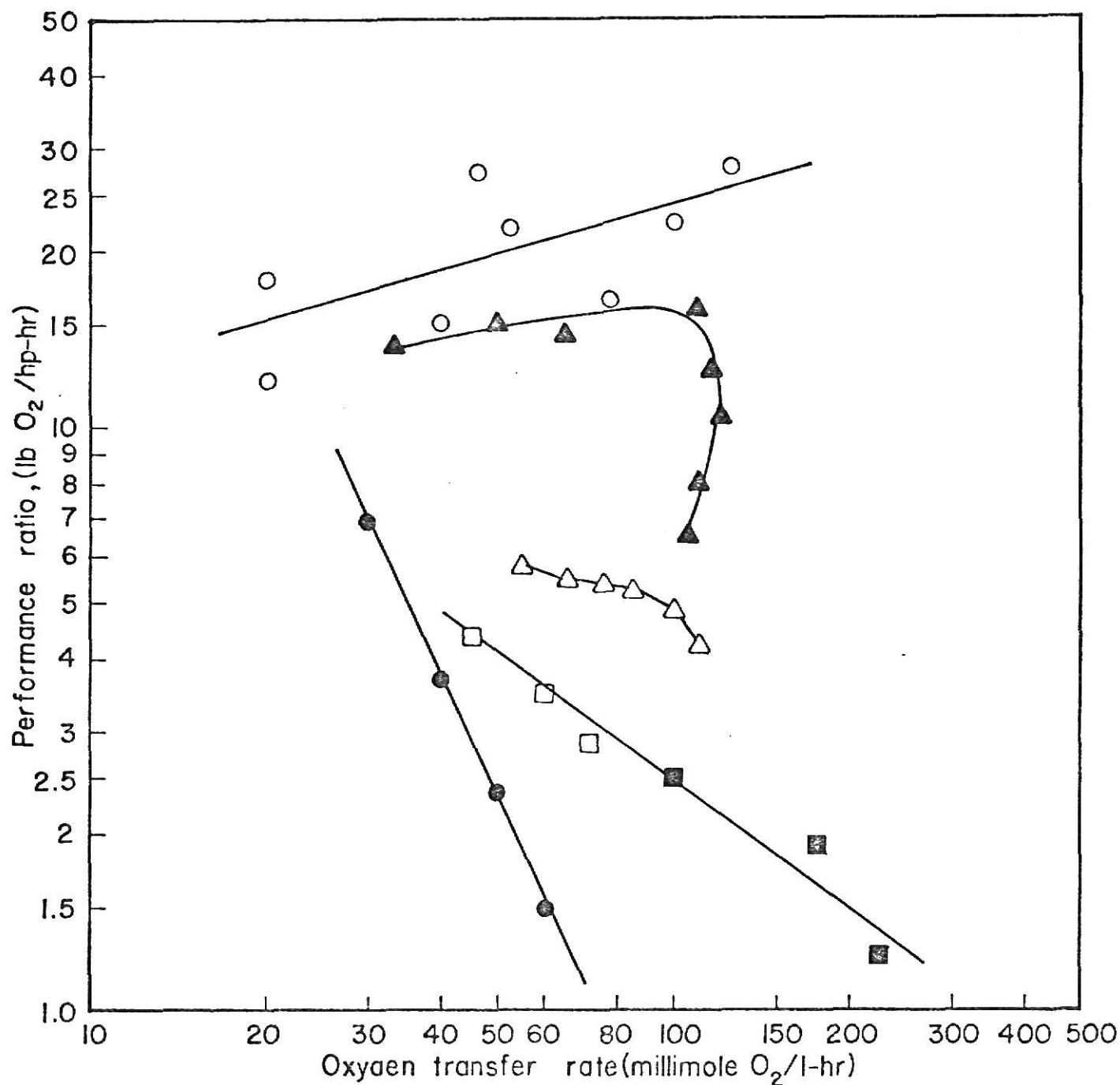
Fig. 9. A comparison of the performance ratios of various fermenter designs as a function of oxygen transfer rate.

▲ — Split cylinder airlift fermentor (Belfield[64])
△ — Concentric airlift fermentor (Hatch[11])
□ — 100 l. stirred tank (Fukuda[122])
▨ — 4000 l. stirred tank (Fukuda[122])
● — Rectangular airlift fermentor (Gasner[63])
○ — Aeration tower (Hatch[11,14])

CHAPTER III

HYDROCARBON SUBSTRATE TRANSFER IN TOWER FERMENTORS WITH TWO LIQUID PHASES

INTRODUCTION

The utilization of various hydrocarbons by microorganisms has recently received a good deal of attention. Normally, hydrocarbon fermentations involve at least four phases which contribute in various measures to cell growth. Growth will be affected by many factors in the dispersed systems that do not exist in single liquid phase systems for which much of the theory on continuous culture has been based. For example, one must consider the size, number and distribution of drops, distribution of growth limiting substrate between the continuous and the dispersed phases, fraction of cells in the continuous phase and at the dispersed phase interface, mass transfer between phases, frequency of coalescence and breakup of drops, cell adsorption and desorption at the surface of the oil drops, and so forth. For these reasons the dispersed phase culture system is considered more complex than the homogeneous single aqueous phase system.

The processes by which the utilizable hydrocarbons are transported to the cells and the uptake of hydrocarbon by the cells are important because hydrocarbon substrate transport and uptake can limit growth rates. A number of excellent reviews on the hydrocarbon uptake and transport in fermentations with two liquid phases have appeared[1-6]. The literature on hydrocarbon transport and uptake during single cell cultivation is reviewed from an engineering viewpoint.

HYDROCARBON TRANSPORT IN AERATED TOWER FERMENTORS

Problems of mass transfer in biological growth systems containing hydrocarbon as a rate limiting substrate are very complex. Not only substrate uptake by microorganisms but also the hydrodynamics in aerated tower fermentors can be strongly influenced by the presence of hydrocarbon phase. This section deals with the hydrocarbon transport with an emphasis to the drop size distribution, and possibilities of hydrocarbon phase spreading at air-water interface and over cell walls as well. The following section will deal with the uptake of hydrocarbon substrate by microorganisms.

A. Oil Drop Size Distribution

In the fermentation with liquid hydrocarbons, the hydrocarbon phase is dispersed as drops in the aqueous medium. These drops continuously coalesce and redisperse with each other giving rise to a distribution of oil drop sizes. Indeed, a thorough knowledge of drop size distributions is essential before a rational design and scale-up of hydrocarbon fermentors may be conducted.

A number of methods for measurement of drop sizes in liquid-liquid dispersions have been proposed. Several methods are primarily performed by physical means, e.g. by microscopic inspection[7,8], by Coulter counting[9,10], by light transmission or light scattering techniques[11,12], by direct photography[13,14,15,16], and by sedimentation analysis[17,18].

Shinnar[7] used direct microscopic inspection to measure drop size distributions of Shell-wax dispersed in water in a heated vessel. Quickly cooling the sample taken from the system fixed the dispersion,

which could then be observed and be counted under a microscope. The
direct microscopic observation technique was later applied to measure-
ment of n-alkane fermentations[8]. Since the possibility of coalescence
could not be negated in the process, Yoshida and Yamada[13] used a flow
cell adjoining the vessel to photograph the dispersions in a kerosene-
water system.

Direct photography of drops in an agitated system has been utilized
by many researchers to measure drop size distributions[14,19,20]. A
review of these techniques prior to 1961 is available[24]. Chen and
Middleman[14] took photographs by using a photoelectric probe with a
synchronized flash unit. Ward[15] and Scott et al.[16] also followed similar
methods for their studies. Sedimentation analysis which takes advantage
of the specific weight difference between dispersed and continuous
phases, was developed by Wang and Ochoa[17] for n-hexadecane fermentation.
A combination of sedimentation analysis with radioactive tracer in
simulated systems was used by Podlech and Borzani[18].

When the volumetric fraction of dispersed phase is not large, photo-
graphic measurements of drop size may be successful. For large fractions
of dispersed phase, however, coalescence takes place. Three types of
measuring techniques have been presented to avoid coalescence. The
first method was utilized by Van Heuven and Hoevenaar[21] and based on
the property of lowering interfacial tension by detergents between the
phases. The detergent method can be used for both pure chemical as
well as fermentation systems. The second method, called the gelatin-
embedding technique, stabilizes the dispersions by the solidifying-
gelatin in which the drops of the dispersed phase are embedded. The
method was first employed by Katinger[22] and later by Prokop et
al.[12,23,24]. It consisted of taking samples directly from the fermentor

into a semi-molten gelatin solution which was then immediately solidified by dipping into ethanol-dry ice mixture. The drops were prevented from coalescing by the high viscosity and the stabilizing effect of solidifying gelatin. The third method[9,25] is to use an interfacial polycondensation reaction to encapsulate the droplets. Sebacoyldichloride is dissolved in the dispersed organic phase. After a steady state dispersion is attained in water, a small amount of a strong solution of hexamethylenediamine in water saturated with sodium laurylsulfate is added to the continuous phase. Thus a thin polymer film is formed which encapsulates the droplets. The technique, proposed by Madden and McCoy[25], has the disadvantage that a reactant has to be added to the dispersed phase before making the dispersion. This can affect the interfacial tension and coalescence frequency.

Gelatin, encapsulation and detergent methods have been compared in biological as well as non-biological systems. The detergent method has been found to be easier to conduct in both systems and also allows a better accuracy in the region of small droplets[11].

Bajpai[6] reviewed a number of experimental studies on the drop size distribution in hydrocarbon fermentation systems. Prokop and co-workers[12,23,24] have presented drop size distributions observed in batch fermentations of Candida lipolytica on gas-oil and n-hexadecane dissolved in dewaxed gas-oil. A positively skewed distribution is reported and large numbers of tiny drops ($<3\mu$m) are observed. Distributions of drop sizes in samples taken from different positions of large vessels show no spatial dependence. Dispersed phase fraction and inoculum size were found to have a strong influence over the drop size distributions. Distributions differ greatly at various times during fermentation which is due to different interfacial tensions and biomass concentrations as well. Similar

observations were pointed out by Katinger[22] from his study of drop

size distributions during the course of fermentation with gas-oil and

hexadecane as substrates.

Blanch and Einsele[26] measured the drop size distribution during the

growth of Candida tropicalis on pure n-hexadecane both in circulation

system and in flat-blade turbine system. Highly skewed distributions were

obtained which were affected by biomass concentration and the stage of

fermentation. Sauter-mean diameter of oil droplets in the circulation system

did not show good correlation with the Weber number.

Yoshida and Yamada[13] studied dispersion of kerosene in water in bubble

columns and in a turbine agitated tank. Sauter-mean diameter which did not

depend on sampling position, however, was found to be affected by power

input and fraction of the dispersed phase.

Podlech and Borzani[18] studied the diesel oil-water system using a

radiometric technique. An empirical parameter was used to characterize

the drop size distributions which were found to be unsymmetrical. Podlech

et al.[27] observed a marked influence of the presence of oxygen on the drop

size distribution in diesel oil-water systems. The oil drop size distri-

bution, measured by the radiometric method, using a scintillation counter,

is correlated by the following equation

$$F = 100(1 - 10^{-\alpha BH/r^2}) \tag{1}$$

where F = oil fraction in the form of drops with radius equal to or larger

      than r,

    α = experimental parameter that defines the drop size distribution,

    H = distance from the radiation detector to the tank bottom,

and $B = \dfrac{9\mu_c}{2g \cdot \Delta\rho} = 1.9702 \times 10^{-4}$ cm $\cdot$ sec.

Recently, an empirical correlation of oil drop size distribution in hydrocarbon-water systems was given as[28]

$$\beta = \frac{\alpha \cdot 10^{-bN} \cdot \phi}{K + \phi}$$ (2)

where β = drop size distribution; ϕ = hydrocarbon volume fraction ; N = impeller speed and α, b, K = empirical constants.

Wang and Ochoa[17] have measured distribution of n-hexadecane drop size during cultivation of Candida intermedia. Existance of cells as well as detergents was found to greatly influence the specific surface area of hydrocarbon droplets. The drop size distribution, however, was not affected by changes in cell concentration above 0.5 grams dry weight of cells per liter of cultivation medium.

The formation and maintenance of dispersions involves a balance of breakup and coalescence of the dispersed droplets in a continuous phase that is in turbulent flow. The breakup of droplets can occur either by viscous shear forces or by turbulent pressure fluctuations. Clay[29] has proposed turbulence as the primary factor of breakup. Hinze[30] have expressed the forces controlling droplets deformation and breakup in terms of the Weber number. Breakup occurs when the Weber number exceeds a critical value which, in turn, depends upon the mechanism of droplet breakage. For a dispersion in turbulent flow the critical Weber number is nearly unity. Calderbank[31] further elaborated the work of Hinze and showed that viscous forces may be ignored in the dispersions of gases and liquids[32].

Detailed investigations of dispersions in agitated and baffled vessels have been made by Vermeulen and co-workers[33]. They have recognized the physical properties of the two fluids, volume fraction of the dispersed phase, agitation speed, and factors associated with the agitator geometry

as the pertinent variables influencing the drop size in the agitated, baffled system. They observed an increase in agitator speed reduces the drop size both for liquid-liquid and gas-liquid dispersions; a decrease in interfacial tension decreases drop size; the viscosity of the continuous phase has no influence for liquid-liquid systems but significantly affects gas-liquid systems where the increase in viscosity increases the bubble size; the viscosity of the dispersed phase increases the drop size but its effect is inconclusive in gas-liquid systems because of the nearly equal viscosities of the gases used; the density differences are not important in liquid-liquid systems and the gas density is not important in gas-liquid system; the mean drop size decreases with decrease in volume fractions of the dispersed phase both for liquid-liquid and gas-liquid systems. Vermeulen et al.[33] have also listed ten dimensionless variables which possibly influence the nature of the dispersions obtained. Six of these were employed for the correlation; they are the Weber number, Reynolds number, volume fraction of the dispersed phase, viscosity ratios, density ratios, amd length ratios. The other four were used but found not to improve the correlation. The correlation for liquid-liquid dispersions shows[32,33]

$$\frac{N^2 \rho' L^{4/3} D^{5/4}}{\gamma f_\phi^{5/3}} = 0.016 \tag{3}$$

where N = angular velocity of the agitator, revolutions/sec.,

$\rho' = 0.4\rho_c + 0.6\rho_d$,

L = paddle diameter, cm.,

f_ϕ = ratio of actual mean drop diameter to its diameter at $\phi = 0.1$.,

and γ, ϕ, D, ρ represent the interfacial tension, volume fraction, drop diameter, and liquid density respectively.

Bouyatiotis and Thorton[34] presented a correlation for a 7-inch diameter baffled vessel, 6-blade turbine, with a turbine diameter of 0.225 feet operated for the organic liquids (γ = 8.5 to 34 dyne/cm, ρ_D = 43.1 to 56.4 lb. mass/ft^3, μ_d = 1.18 to 1.81 cp.) dispersed in water, in the absence of mass transfer, as follows:

$$D_{SM} = D_p^{\,0} + 1.18\phi_D \left(\frac{\gamma^2 g_c^2}{\mu_c^2 g}\right) \left(\frac{\Delta\rho\gamma^3 g_c^3}{\mu_c^4 g}\right)^{-0.62} \left(\frac{\Delta\rho}{\rho_c}\right)^{0.05} \tag{4}$$

where $D_p^{\,0}$ is given by

$$\frac{(D_p^{\,0})^3 \rho_c^2 g}{\mu_c^2} = 29.0 \left(\frac{(P/V)^3 g_c^3}{\rho_c^2 \mu_c^4 g}\right)^{-0.32} \left(\frac{\rho_c \gamma^3 g_c^3}{\mu_c^4 g}\right)^{0.14} \tag{5}$$

where D_{SM} = Sauter-mean diameter, ϕ_D = fraction of organic liquids, γ = interfacial tension, μ_c = viscosity of the continuous phase, ρ_c = density of the continuous phase, and (P/V) = power input per unit liquid volume.

Calderbank[35] has investigated liquid-liquid dispersions and showed that the Sauter-mean diameter is strongly dependent on interfacial tension, volume fraction of dispersed phase, and power per unit volume. The correlation that Calderbank[35] presented is

$$D_{SM} = 0.224 \left[\frac{\gamma^{0.6}}{(P/V)^{0.4} \rho_c^{0.2}}\right] \phi_D^{0.5} \left(\frac{\mu_D}{\mu_c}\right)^{0.25} \tag{6}$$

During the course of fermentation, the oil mean drop size changes suggesting that it is strongly influenced by the cell density and interfacial tension. Wang and Ochoa[17] found that the drop size distributions in presence of _Candida intermedia_ were very different from those in absence of cells. Bajpai[6,36] observed a considerable drop in mean drop size at fairly low cell densities, about 1 mg/ℓ, which may be attributed to a decrease of interfacial tension. Figure 1 shows the change of interfacial tensions during a hydrocarbon fermentation.

In summary, among physical properties influencing mean drop size, the interfacial tension is most important and the viscosity of the dispersed phase is of second importance. The volume fraction of dispersed phase is another variable which significantly affects the drop size distribution. The literature indicates that the interfacial area and the Sauter-mean diameter increase with increases in volume fraction of dispersed phase[8,12,17,22,23,24]. The shape of the drop size distribution depends on agitation intensity and the type of fermentor. Systems with intense mechanical agitation appear to have a strongly skewed distribution in which the number of small drops is very large[23,24]. With airlift systems the Sauter-mean diameter is larger and the drop size distribution is closer to a normal distribution[3,22]. Comprehensive reviews of the literature on this subject are available[2,3,4,6,32,36].

B. Oil Spreading at Air-Water Interface

The spreading coefficient provides a measure as to whether the oil phase tends to displace the water film originally surrounding bubbles. For oil (o) at the interface between air (A) and water (ℓ), the spreading coefficient is given by[37]

$$S_{o/\ell A} = \gamma_{\ell/A} - (\gamma_{o/A} + \gamma_{o/\ell}) \tag{7}$$

where γ's are the appropriate interfacial tensions. Spreading of oil at the air-water interface occurs when the spreading coefficient is numerically zero or greater. The velocity of the spreading is directly proportional to the value of $S_{o/\ell A}$ and inversely proportional to the sum of the viscosities of the fluid. Figure 2 shows that the spreading coefficient increases during the course of fermentation which implies oil spreading at air-water interfaces, although pure hexadecane does not spread on water[40].

Prokop et al.[23] and Velankar et al.[39] have measured the interfacial tension of the culture broth and found that interfacial tension decreased in the course of fermentation. The variation of interfacial tension with time is different in each of these batch fermentations. Prokop et al.[23] observed a significant decrease of interfacial tension at the beginning period of cultivation of Candida lipolytica on gas oil followed by a gradual increase as fermentation proceeded. Velankar et al.[39] observed, however, that the interfacial tension decreased gradually during the fermentation of Pseudomonas aeruginosa on heptane. Prokop et al.[23] also reported that a maximum accumulation of extra-cellular free fatty acids was observed in the early period of fermentation. They thus suggested that long-chain extra-cellular fatty acids might play an important role in the decrease of interfacial tension. In the same paper, they also reported undetectable interfacial tension when the cells were not separated from the broth. The major difficulty in accurately measuring the interfacial tension of a sample containing cells arises from the absence of a clear interface.

Erickson et al.[40] have employed the following procedure to investigate the effect of cells on the interfacial tension. A definite amount of cells which were obtained by centrifuging and resuspending in distilled water was added to 7 ml oil and 29 ml phosphate buffer (pH 5-8) in a shaking flask. After 30 minutes shaking, the mixture was transferred to a small beaker which was 3.2 cm in diameter. The beaker containing the sample was allowed to stand until the oil-water interface became as clear as possible. When the amount of cells was small, all cells appeared to adsorb at the interface. The interfacial tension between oil and water was found to decrease as the amount of cells increased. This result is qualitatively in agreement with that shown in Figure 1.

Erickson et al.[41] observed that the oil concentration measured in a Koch mixers tower with external forced circulation varied with position in the tower and return flow as shown in Figure 3. The top sampling point was located 9 cm below the overflow to the circulation arm; therefore, samples from it might not be representative of the liquid surface. Larger concentrations of oil and cells have frequently been observed in the return flow and upper portion of the tower. This observation provides further evidence in favor of the concept of the oil phase spreading at the air-water interface. The bubbles rapidly carry the spreading oil up the draft tube and this results in relatively higher oil concentrations in the head region and the return flow.

Hattori et al.[42] in examining the performance of a draft tube fermentor which was a conventional agitated fermentor with draft tube as shown in Figure 4, found that the oil concentration also varied with position in the fermentor, as well as with agitation speed. With agitation at 150 rpm, the maximum oil concentration was found at the middle of draft tube; however, with agitation at 250 rpm, good mixing of the oil phase was attained and a slightly higher oil concentration was observed in the head region rather than in the draft tube as shown in Figure 5. This may further support the concept of the oil phase spreading at the air-water interface because of the high oil concentration measured in the head region.

In summary, it is quite likely that the hydrocarbon phase spreads at the gas-liquid interface under certain circumstances.

C. Oil Spreading at Cell Surfaces

The thermodynamic criterion for the spreading of oil (o) in contact with the liquid medium (ℓ) and the cell wall of microorganisms (m) is

given by the spreading coefficient, $S_{o/m\ell}$, as follows

$$S_{o/m\ell} = \gamma_{w/\ell} - \gamma_{m/o} - \gamma_{o/\ell} \qquad (8)$$

where the γ's are the appropriate interfacial tensions.   If $S_{o/m\ell}$ is

negative or zero, oil will not displace the immiscible aqueous liquid from the

cell wall by spreading; but, oil spreading on the cell wall tends to occur for

positive values of $S_{o/m\ell}$.

Zettlemoyer and associates[44] studied the spreading phenomenon at

interfaces of Teflon/oil/water/air. Their analysis reached negative

spreading coefficients at the Teflon/oil/water interfaces for various

oils such as tetradecane, hexadecane, and several mineral oils; indicating

that these oils cannot displace water in such systems.   However, an

interesting observation was that these oils can displace water by spreading

if a fourth phase of air is introduced to form a Teflon/oil/water/air

interface. For example, if a cell originally covered by an aqueous film

and adsorbed on the bubble surface comes in contact with an oil droplet,

an interface of cell wall/oil/liquid/air is established which may lead to

the spreading of oil droplets over the cell wall.

Microscopic observations indicate that cells are frequently found

at oil-water interfaces in hydrocarbon fermentations. It is quite

possible that cells have some lipophylic regions where oil spreads and

other regions where the aqueous phase is preferred by the cells.

Few investigations have been performed in measuring the free energy

of cell walls. Because this information can provide further knowledge

on the mechanism of hydrocarbon fermentation, it is strongly urged that

experiments be carried out.

HYDROCARBON UPTAKE IN CULTURES WITH TWO LIQUID PHASES

The mechanism of liquid hydrocarbon uptake by microorganisms is an important problem in hydrocarbon fermentation. The literature on hydrocarbon fermentation indicates that cell growth on hydrocarbon takes place by a variety of substrate transport pathways. Among those, three different pathways for hydrocarbon uptake by cells are frequently encountered, that is: (1) direct contact of the cells with large oil droplets, (2) direct contact of the cells with submicron droplets, and (3) uptake of dissolved hydrocarbons in the aqueous phase.

It appears that direct contact of cells and oil droplets of various sizes is the predominant mechanism of substrate transport. However, some researchers[45,46,47] have reported that the uptake of dissolved hydrocarbon should not be negated when short chain hydrocarbons are involved as the substrate.

Erdtsieck et al.[45] pointed out that the uptake of dissolved hydrocarbon should not be neglected when dodecane and undecane were employed as the carbon source for cell growth. Yoshida, Yamane and Yagi[46,47] demonstrated by experiments that Candida tropicalis uptook hydrocarbons dissolved in the aqueous phase rather than liquid hydrocarbons. They studied the growth rate of Candida tropicalis in two different fermentors: one was the shaking flask containing both the aqueous medium and liquid hydrocarbons; the other, a rotating disk fermentor containing the aqueous medium into which vapors of n-paraffins from C_6 to C_{18} were supplied continuously without forming any liquid hydrocarbon phase. Comparison of the specific growth rate of Candida tropicalis between two systems shows no appreciable distinction indicating negligible effect of direct contact between cells and liquid hydrocarbons. However, with a careful investigation of the picture of Candida tropicalis cultured

with liquid hydrocarbons in shaking flask, one can notice that no observable contact of cells with large oil drops occurred. This probably was caused by the existence of some undetectable surface active agents during cell growth.

Hamer[48] investigated the supply of n-heptane to bacteria as vapor in the air and concluded that gaseous hydrocarbons can be taken up either directly or in the form of a dissolved solute in the aqueous medium.

On the other hand, some experimental results on cell growth processes with two liquid phases support the mechanism of direct contact of cells and oil droplets. Johnson[49] concluded that microorganisms consumed hydrocarbons by direct contact with oil drops and denied the possibility of hydrocarbons dissolved in the aqueous phase being taken up by the microorganisms because of the very low solubilities in water of n-paraffins heavier than C_{10}.

Aiba et al.[8] assumed that the oil droplets most suitable for the uptake of microorganisms fall in the range of submicron oil droplets. They concluded by experiments that the rate of dissolution of hydrocarbons into the aqueous phase was negligible compared with the rate of decrease of hydrocarbons. They also found that the specific growth rate is independent of the initial hydrocarbon concentration, and the maximum cell concentration is proportional to the amount of hydrocarbon initially present.

In an attempt to explain the high rates of hydrocarbon transport with respect to its very low solubility in the aqueous phase, Goma et al.[50] proposed that the hydrocarbon is solubilized into the aqueous phase by the presence of surface active compounds

produced by the growing microorganisms. They introduced the concept of pseudo-solubility and attributed the high growth rate and high rates of substrate transport to the increased pseudo-solubility caused by the increasing amount of surface active compounds. They also deduced that solubilization was the first step of hydrocarbon assimilation by Candida lipolytica.

Moo-Young et al.[51,52] presented extensive experimental data on fermentation parameters for the cultivation of Candida lipolytica on n-dodecane. A model which is based on the assumption that cell growth kinetics is controlled by the degree of possible attachment between cells and oil droplets of submicron size, gave a good fit to their experimental data.

Wang and Ochoa[17] used the sedimentation technique to measure the interfacial area of the insoluble hydrocarbon droplets. They have found that the growth kinetics of yeast is directly related to the available interfacial area, impeller speed, and addition of surfactants. The interfacial area of the insoluble substrate during the fermentation varies linearly with the concentration of hydrocarbon and the concentration of cells.

Mimura et al.[53] observed that the affinity of a yeast cell for an oil droplet governs the cell's ability to grow on hydrocarbon. Accordingly, yeast cells with no affinity for oil droplets failed to grow on hydrocarbon while those which grew were found attached to oil droplets in the early stages of fermentation. An optimum oil drop size for the close association of the oil droplet with the cell was noted and such dispersion was named "biologically active hydrocarbon emulsion". Therefore, growth is greatly enhanced when the cells have a tendency to form dense flocs of submicron oil droplets with cells closely attached to their surfaces.

Surfactants frequently act to decrease the interfacial tension and increase the interfacial area. The adsorption of cells at oil-water interfaces and the rate of coalescence and redispersion of oil drops are also found to be affected by the existance of surfactants. Several researchers[17,53,54] used surfactants in their hydrocarbon fermentation experiments and found enhanced growth rates. Yoshida and co-workers[46,47] have shown that good growth rates can be obtained in colloidal emulsions containing only submicron oil droplets. Among all surfactants tested, they found that a mixture of 20 mg. Tween 20, 20 mg. sodium glycocholate, and 10 mg. lecithin per 100 mg. of water was the most effective in emulsification.

Erickson and Humphrey[55,56,57] have developed mathematical models which can be used to describe batch growth in fermentations with two liquid phases present in which the growth limiting substrate is dissolved in the dispersed phase. They have considered the possibilities of growth occurring at the surface of the dispersed phase and also in the continuous phase. Their results indicate that the interfacial area is a critical variable which must be considered in designs. Erickson et al.[58] and Shah et al.[59] modified their model by taking into account the drop size distribution, the rate of cell adsorption on the drop surface, the rate of desorption of cells from the drop surface, substrate transport between phases, phase equilibrium, and growth kinetics. The effect of coalescence and redispersion of oil drops is also considered. They have used a discrete uniform distribution and a discrete normal distribution which is obtained from an experimental distribution curve as drop size distribution. They have reported that the adsorption parameter can greatly influence growth in fermentors and that a much greater lag period exists for small values of the adsorption parameter

as compared to the larger values of this parameter because of the slower rate of adsorption of cells onto the drop surface where growth occurs.

Prokop et al.[60] have investigated experimentally the effects of inoculum size, dispersed phase volume, and substrate concentration on the batch growth of Candida lipolytica in a model system composed of n-hexadecane dissolved in a dewaxed gas oil. They performed sixteen different experiments and found that all of the batch growth curves exhibited a linear growth region with the length of the region ranging from 1.5 to 9.5 hours. Furthermore, they have shown that the rate of linear growth varied both with the change in the dispersed phase volume and initial dispersed phase substrate concentration. Shah et al.[59] have applied parameter estimation techniques to analyze the data obtained by Prokop et al.[60] and pointed out that the simple model of all growth occuring only at the oil drop surfaces with uniform dispersed phase substrate concentration is not adequate. They also concluded that either continuous phase growth or growth on small segregated drops or both contribute significantly to the linear growth rate especially when the dispersed phase substrate concentration is high.

Goma[61] proposed a mathematical model for the growth of Candida lipolytica on n-paraffins which are only slightly miscible with water and used at low concentrations. He also took physiological mechanism, and physical-chemical parameters into consideration. When growth occurred only from the dissolved substrate, the level of growth was independent of the conditions of agitation and aeration, but characte-ristic of the strain. The model can also be easily adapted to high concentrations of hydrocarbons.

Goma et al.[62] proposed that the microorganisms take up hydrocarbon in two stages. (I) When the cell growth starts, the hydrocarbons are in a macroemulsion (average drop size around 25μ). Some hydrocarbons are solubilized (less than 0.1 mg/ℓ). Growth occurs after assimilation of the most soluble of these alkanes. Delays in the uptake of the different hydrocarbons due to their different solubilities are observed. Specific pseudo-solubilization with a specific bio-surfactant occurs with each hydrocarbon. (II) With growth commencing on the most soluble alkanes, the surfactant decreases surface tension and increases the interfacial area between the carbon substrate and the aqueous phase. The hydrocarbon now exists as a microemulsion with a much greater interfacial area which allows the higher rate of dissolution and controls mass transfer. If the production of bio-surfactant is greater than the critical micellia concentration, an accumulation of micelles occurs in the aqueous phase. They have correlated the critical substrate concentration $S_{crit.}$, which represents the hydrocarbon potentially useful to the cell, as follows[62]:

$$S_{crit.} = 1 + \frac{18}{X} \tag{9}$$

where X is the biomass concentration. The value of $S_{crit.}$ is greater than the concentration of "pseudo-solubilized" hydrocarbon.

In summary, three pathways of substrate uptake by microorganisms have been suggested, they are: (1) direct contact of cells with large oil droplets, (2) direct contact of cells with submicron oil droplets, and (3) uptake of dissolved hydrocarbons in the aqueous phase. However, one should realize that the relative contributions of dissolved substrate, submicron droplets and larger droplets to substrate transport and growth

rate depend on the growth environment as well as experimental conditions and procedure. Besides, it is difficult to precisely determine the relative contributions of these processes.

CONCLUSION

The growth rate of microorganisms on hydrocarbons depends on the transfer rate of the substrate to and across the cell surface, as well as on biological, environmental, and genetic conditions. The transfer occurs in a system with four phases where cells, insoluble substrate, and aerated bubbles are treated as the dispersed phase while aqueous medium is the continuous phase. Knowledge of the hydrocarbon transfer in aerated tower fermentors is of extreme importance to biochemical engineers concerned with the design or operation of single-cell cultivation on hydrocarbon substrates.

Hydrocarbons being sparingly soluble in aqueous medium, exist in the form of drops. These drops are present in a turbulent environment and continuously breakup and coalesce giving rise to a distribution of drop sizes. Important variables which influence the oil drop size distribution include the interfacial tension and the turbulence of the broth. The volume fraction of dispersed hydrocarbon phase is another variable which significantly affects the interfacial area. Though much has been written on this subject, rational choice of hydrocarbon fermentor design has so far been hindered by inadequate knowledge of drop phenomena.

It has already been advocated in the literature that the hydrocarbon phase may spread at the air-water interface and at cell walls. Research is needed in this area in order to gain a better appreciation of the hydrocarbon uptake process during the course of fermentation.

Three possible pathways for hydrocarbon transport to microorganisms have been proposed, they are: (1) direct contact of the cells with large oil drops, (2) direct contact of the cells with submicron droplets, and (3) uptake of dissolved hydrocarbons in aqueous medium. The third pathway is small for the uptake of long-chain hydrocarbons because of their

very low solubilities in water. However, one should always keep in mind that the relative contributions of the three pathways to substrate transport and growth rate depend on the growth environment and experimental conditions.

NOMENCLATURE

a   =   interfacial area per unit volume of liquid dispersion, cm^2/cm^3

B   =   constant (= $9\mu_c/2g/\Delta\rho$ = 1.9702 x 10^{-4} cm $\cdot$ sec)

b   =   empirical constant in Eqn. (2), dimensionless

D   =   drop diameter, in Eqn. (3), cm

$D_p{}^{\circ}$ =   critical drop diameter as defined in Eqn. (5), cm

D_{SM} =   Sauter mean diameter, cm

F   =   oil fraction in the form of drops with radius equal to or larger than r , dimensionless

f_ϕ =   ratio of actual mean drop diameter to its diameter at ϕ = 0.1, dimensionless

g   =   gravitational constant, cm/sec^2

g_c =   gravitational conversion factor, dimensionless

H   =   distance from the radiation detector to the tank bottom, cm

H_c =   Henry's law constant, ℓ - atm/mg O_2

H_{wh} =   partition coefficient of oxygen between water and hydrocarbon phase, ℓ - atm/mg O_2

K   =   empirical constant in Eqn. (2), dimensionless

K_L =   mass transfer coefficient in liquid film surrounding gas bubble, cm/sec

L   =   paddle diameter, cm

N   =   agitator speed, round/sec

P   =   power consumption, horsepower

R_o =   specific oxygen uptake rate by cells from the oil phase, mg O_2/mg cell - sec

R_w =   specific oxygen uptake rate by cells from the aqueous phase, mg O_2/mg cell - sec

r   =   drop radius, cm

S   = substrate concentration, mg substrate/ℓ

$S_{o/\ell A}$ = oil spreading coefficient at gas-liquid interface, dyne/cm

V   = volume of the mixing vessel containing the agitated fluids, ℓ

x   = cell concentration per unit volume of liquid dispersion, mg cell/ℓ

α = empirical constant in Eqn. (2), dimensionless

β = $\left(\dfrac{V_w + V_o}{V_w}\right)$, dimensionless

γ = surface or interfacial tension, dyne/cm

μ = viscosity, g/cm-sec

Superscript

$\tilde{}$ = the measured value

Subscripts

c   = of the continuous phase

crit. = critical value

D   = of the dispersed phase

g   = of the gas phase

L   = of the liquid phase

ℓ = of the liquid phase

m   = of the microorganism phase

o   = of the oil phase

N   = of the aqueous phase

References

1. Humphrey, A. E., and L. E. Erickson, "Kinetics of Growth on Aqueous-Oil and Aqueous-Solid Dispersed Systems", J. Appl. Chem. Biotechnol., 4, 125 (1972)

2. Erickson, L. E., T. Nakahara, and A. Prokop, "Growth in Cultures With Two Liquid Phases: Hydrocarbon Uptake and Transport", Process Biochem., 10, No. 5, 9 (1975).

3. Prokop, A., and M. Sobotka, "Insoluble Substrate and Oxygen Transport in Hydrocarbon Fermentation", Single-Cell Protein II, (ed.) Tannenbaum, S. R., and D.I.C. Wang, P. 127, The MIT Press, Cambridge, Mass. (1975)

4. Yamane, T., "Mechanisms of Substrate Uptake and Kinetic Model of Microbial Growth in Hydrocarbon Fermentation with Two Liquid Phases", J. Ferment. Technol., 52, 689 (1974)

5. Humphrey, A. E., "A Critical Review of Hydrocarbon Fermentations and Their Industrial Utilization", Biotechnol. Bioeng., 9, 3 (1967)

6. Bajpai, R. K., "Experimental and Analytical Studies of Drop-Size Distributions in Hydrocarbon Fermentors", Ph.D. Thesis, Indian Institute of Technology, Kanpur (1975)

7. Shinnar, R., "On the Behavior of Liquid Dispersions in Mixing-Vessels", J. Fluid Mech., 10, 259 (1961)

8. Aiba, S., K. L. Haung, V. Moritz, and J. Someya, "Cultivation of Yeast Cells by Using n-Alkanes as the Sole Carbon Source: II. An Approach to the Mechanism of the Microbial Uptake of n-Alkanes", J. Ferment. Technol., 47, 211 (1969)

9. Morgan, P. W., Condensation Polymers: By Interfacial and Solution Methods, Interscience Publications, New York, N. Y. (1965)

10. Lien, T. R., and C. R. Phillips, "Determination of Particle Size Distribution of Oil-in-Water Emulsions by Electronic Counting", Environm. Sci. & Technol., 8, 588 (1974)

11. Bajpai, R. K., and A. Prokop, "A New Method of Measurement of Drop-Size Distribution in Hydrocarbon Fermentation", Biotechnol. Bioeng., 16, 1557 (1974)

12. Ludvik, M., and A. Prokop, "Size Distribution of Droplets of A Dispersed Phase at Fermentation", Collect. Czech. Chem. Commun., 40, 52 (1975)

13. Yoshida, F., and T. Yamada, "Average Size of Oil Drops in Hydrocarbon Fermentors", J. Ferment. Technol., 49, 235 (1971)

14. Chen, H. T., and S. Middleman, "Drop Size Distribution in Agitated Liquid-Liquid Systems", A.I.Ch.E. J., 13, 989 (1967)

15. Ward, J. P., "Turbulent Flow of Liquid-Liquid Dispersions: Drop Size, Friction Losses, and Velocity Distribution", Ph.D. Thesis, Oregon State University (1965)

16. Scott, L. S., W. B. Hayes, and C. D. Holland, "The Formation of Inter-
     facial Area in Immiscible Liquids by Orifice Mixers", A.I.Ch.E. J., 4,
     346 (1958)

17. Wang, D.I.C., and A. Ochoa, "Measurement on Interfacial Areas of
     Hydrocarbon in Yeast Fermentations and Relationships to Specific Growth
     Rates", Biotechnol. Bioeng., 14, 345 (1972)

18. Podlech, P.A.S., and W. Borzani, "Oil Drop Size Distribution in Hydrocarbon-
     Water System", Biotechnol. Bioeng., 14, 43 (1972)

19. Kintner, R. C., T. J. Horton, R. E. Granmann, and S. Ambekor, "Photo-
     graphy in Bubble and Drop Research", Can. J. Chem. Eng., 39, 235 (1961)

20. Brown, D. E., and K. Pitt, "Drop Size Distribution of Stirred Non-
     Coalescing Liquid-Liquid System", Chem. Eng. Sci., 27, 577 (1972)

21. Van Heuven, J. W., and J. C. Hoevenaar, "Measuring Techniques for the
     Determination of the Drop Size Distribution in Turbulent Liquid-Liquid
     Dispersions" Fourth European Symposium on Chemical Reaction Engineering,
     Brussels (1968).

22. Katinger, H.W.D., "Influence of Interfacial Area and Non-Utilizable
     Hydrocarbons on Growth Kinetics of Candida sp. in Hydrocarbon Fermen-
     tations", Biotechnol. Bioeng. Symp., No. 4, 485 (1973)

23. Prokop, A., M. Ludvik, and L. E. Erickson, "Growth Models of Cultures
     with Two Liquid Phases. VIII. Experimental Observations on Droplet
     Size and Interfacial Area", Biotechnol. Bioeng., 14, 587 (1972)

24. Prokop, A., and M. Ludvik, "Drop Size Frequency Distribution of Dispersed
     Hydrocarbon Phase in a Fermentation Process", Biotechnol. Bioeng. Symp.,
     No. 4, P. 349 (1973)

25. Madden, A. J., and G. L. Damerell, "Coalescence Frequencies in Agitated
     Liquid-Liquid Systems", A.I.Ch.E. J., 8, 233 (1962)

26. Blanch, H. W., and A. Einsele, "The Kinetics of Yeast Growth on Pure
     Hydrocarbons", Biotechnol. Bioeng., 15, 861 (1973)

27. Podlech, P.A.S., A.M.F.L.J. Bonomi, A.M.F. Gomes, and W. Borzani,
     "The Influence of Oxygen on the Oil Drop Size Distribution in Hydrocarbon-
     Water System", J. Ferment. Technol., 51, 917 (1973)

28. Borzani, W. and P.A.S. Podlech, "An Experimental Correlation Between
     the Oil Drop Size Distribution in Hydrocarbon-Water Systems, Oil
     Concentration, and Impeller Speed", Biotechnol. Bioeng., 18, 141 (1976)

29. Clay, P. H., "The Mechanism of Emulsion Formation in Turbulent Flow.
     I. Experimental Part; II. Theoretical Part and Discussion", Proc. Royal
     Acad. Sci. (Amsterdam), 43, 852, 979 (1940)

30. Hinze, J. O., "Fundamentals of the Hydrodynamic Mechanism of Splitting
     in Dispersion Processes", A.I.Ch.E. J., 1, 289 (1955)

31. Calderbank, P. H., "The Inter-Dispersion of Immiscible Fluid Phases", *British Chem. Eng.*, 1, 206 (1956)

32. Kumar, R., and N. R. Kuloor, "The Formation of Bubbles and Drops", *Advances In Chemical Engineering*, (ed.) Drew, T. B., G. R. Cokelet, J. W. Hoopes, Jr., and T. Vermeulen, Vol. 8, P. 255, Academic Press, Inc., New York, N. Y. (1975)

33. Vermeulen, T., G. M. Williams, and G. E. Langlois, "Interfacial Area in Liquid-Liquid and Gas-Liquid Agitation", *Chem. Eng. Progr.*, 51, 85 (1955)

34. Bouyatiotis, B. A., and J. D. Thorton, "Liquid-Liquid Extraction Studies in Stirred Tanks. Part I: Droplet Size and Hold-Up Measurements in a Seven-Inch Diameter Baffled Vessel", *Inst. Chem. Eng. Symp. on Liquid-Liquid Extraction*, P. 43, April, (1967)

35. Calderbank, P. H., "Physical Rate Processes in Industrial Fermentation. I. The Interfacial Area in Gas-Liquid Contacting with Mechanical Agitation", *Trans. Inst. Chem. Engrs.*, 36, 443 (1958)

36. Bajpai, R. K., A. Prokop, and D. Ramkrishna, "Dispersions in Hydrocarbon Fermentation. A Retrospective Study", *Biotechnol. Bioeng.*, 17, 541 (1976)

37. Davies, J. T., and E. K. Rideal, *Interfacial Phenomena*, Academic Press, New York, N. Y. (1961)

38. Yoshida, F., T. Yamane, and Y. Miyamoto, "Oxygen Absorption into Oil-in-Water Emulsions", *Ind. Eng. Chem. Process Des. Develop.*, 9, 570 (1970)

39. Velankar, S. K., S. M. Barnett, C. W. Houston, and A. R. Thompson, "Microbial Growth on Hydrocarbons-Some Experimental Results", *Biotechnol. Bioeng.*, 17, 241 (1975)

40. Erickson, L. E., J. R. Gutierrez, and T. Nakahara, "Growth of Cultures With Two Liquid Phases in Tower Systems", *Fifth International Ferment. Symp.*, P. 132, Berlin (1976)

41. Erickson, L. E., T. Nakahara, J. R. Gutierrez, G. T. MacLean, and L. T. Fan, "Modeling and Characterization of Hydrocarbon Fermentations", Presented at Joint US/USSR Conference on Data Acquisition and Processing for Laboratory and Industrial Measurements in Fermentation Processes, Univ. of Pennsylvania, Philadelphia, August 12-15, (1975)

42. Hattori, K., S. Yokoo, and O. Imada, "Performance of Draft Tube Fermentor for Hydrocarbon Fermentation", *J. Ferment. Technol.*, 52, 583 (1974)

43. Yoshida, T., K. Yokoyama, T. Imanaka, and H. Taguchi, "Oxygen Transfer in Hydrocarbon Fermentation", *Fifth International Ferment. Symp.*, P. 62, Berlin (1976)

44. Zettlemoyer, A. C., M. P. Aronson, and J. A. Lavelle, "Spreading at the Teflon/Oil/Water/Air Interfaces", J. Colloid & Interf. Sci., 34, 545 (1970)

45. Erdtsieck, B., and K. Rietema, Antonie van Leeuwenhoek , 35, Supplement Yeast Symp., F19 (1969)

46. Yoshida, F., T. Yamane, and H. Yagi, "Mechanism of Uptake of Liquid Hydrocarbons by Microorganisms", Biotechnol. Bioeng., 13, 215 (1971)

47. Yoshida, F., and T. Yamane, "Hydrocarbon Uptake by Microorganisms-A Supplementary Study", Biotechnol. Bioeng., 13, 691 (1971)

48. Hamer, G., "Volatile Organic Liquids as Carbon Substrates for Aerobic Fermentations. II. N-Heptane", J. Ferment. Technol., 46, 452 (1968)

49. Johnson, M. J., "Utilization of Hydrocarbons by Microorganisms", Chem. Ind. (London), P. 1532, September 3, (1964)

50. Goma, G., A. Pareilleux, and G. Durand, "Specific Hydrocarbon Solubilization During Growth of Candida-Lipolytica", J. Ferment. Technol., 51, 616 (1973)

51. Moo-Young, M., T. Shimizu, and D. A. Whitworth, "Hydrocarbon Fermentations Using Candida lipolytica. I. Basic Growth Parameters for Batch and Continuous Culture Conditions", Biotechnol. Bioeng.; 13, 741 (1971)

52. Moo-Young, M., and T. Shimizu, "Hydrocarbon Fermentation Using Candida lipolytica. II. A Model for Cell Growth Kinetics", Biotechnol. Bioeng., 13, 761 (1971)

53. Mimura, A., S. Watanabe, and I. Takeda, "Biochemical Engineering Analysis of Hydrocarbon Fermentation. III. Analysis of Emulsification Phenomena", J. Ferment. Technol., 49, 255 (1971)

54. Whitworth, D. A., M. Moo-Young, and T. Viswanatha, "Hydrocarbon Fermentations: Oxidation Mechanism and Nonionic-Surfactant Effects in a Culture of Candida lipolytica", Biotechnol. Bioeng., 15, 649 (1973)

55. Erickson, L. E., A. E. Humphrey and A. Prokop, "Growth Models of Cultures with Two Liquid Phases: I. Substrate in Dispersed Phase", Biotechnol. Bioeng., 11, 449 (1969)

56. Erickson, L. E., and A. E. Humphrey, "Growth Models of Cultures with Two Liquid Phases: II. Pure Substrate in Dispersed Phase", Biotechnol. Bioeng., 11, 467 (1969)

57. Erickson, L. E., and A. E. Humphrey, "Growth Models of Cultures with Two Liquid Phases: III. Continuous Cultures", Biotechnol. Bioeng., 11, 489 (1969)

58. Erickson, L. E., L. T. Fan, P. S. Shah, and M.S.K. Chen, "Growth Models of Cultures with Two Liquid Phases: IV. Cell Adsorption, Drop Size Distribution, and Batch Growth", Biotechnol. Bioeng., 12, 713 (1970)

59. Shah, P. S., L. E. Erickson, L. T. Fan, and A. Prokop, "Growth Models
     of Cultures with Two Liquid Phases: VI. Parameter Estimation and
     Statistical Analysis", Biotechnol. Bioeng., 14, 533 (1972)

60. Prokop, A., L. E. Erickson, and O. Paredes-Lopez, "Growth Models of
     Cultures with Two Liquid Phases: V. Substrate Dissolved in Dispersed
     Phase-Experimental Observation", Biotechnol. Bioeng., 13, 241 (1971)

61. Goma, G., A. Pareilleux, and G. Durand, "Mathematical Model for
     Growth of Candida-lipolytica on Paraffins", Czech. Acad. Sci. D.,
     276, 3491 (1973)

62. Goma, G., D. Al Ani, and A. Pareilleux, "Hydrocarbon Uptake by Micro-
     organisms", Fifth International Ferment. Symp., P. 131, Berlin (1976)
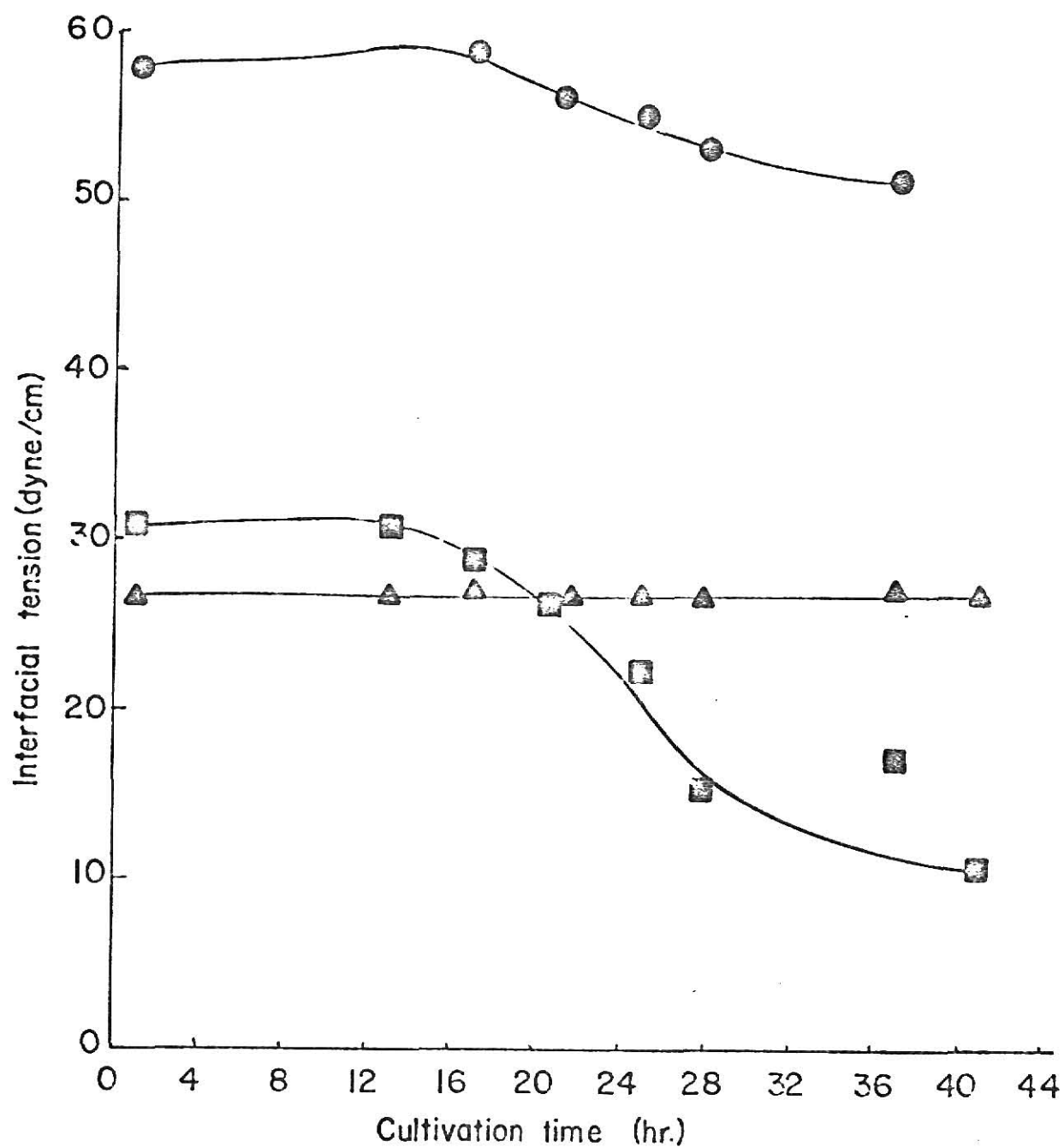
Fig. 1. Effect of cultivation on surface and interfacial tensions during fermentation (From Erickson et al.[41])

    ⬤ Interfacial tension between water and oil

    ▨ Interfacial tension between oil and air

    ▲ Interfacial tension between water and air.
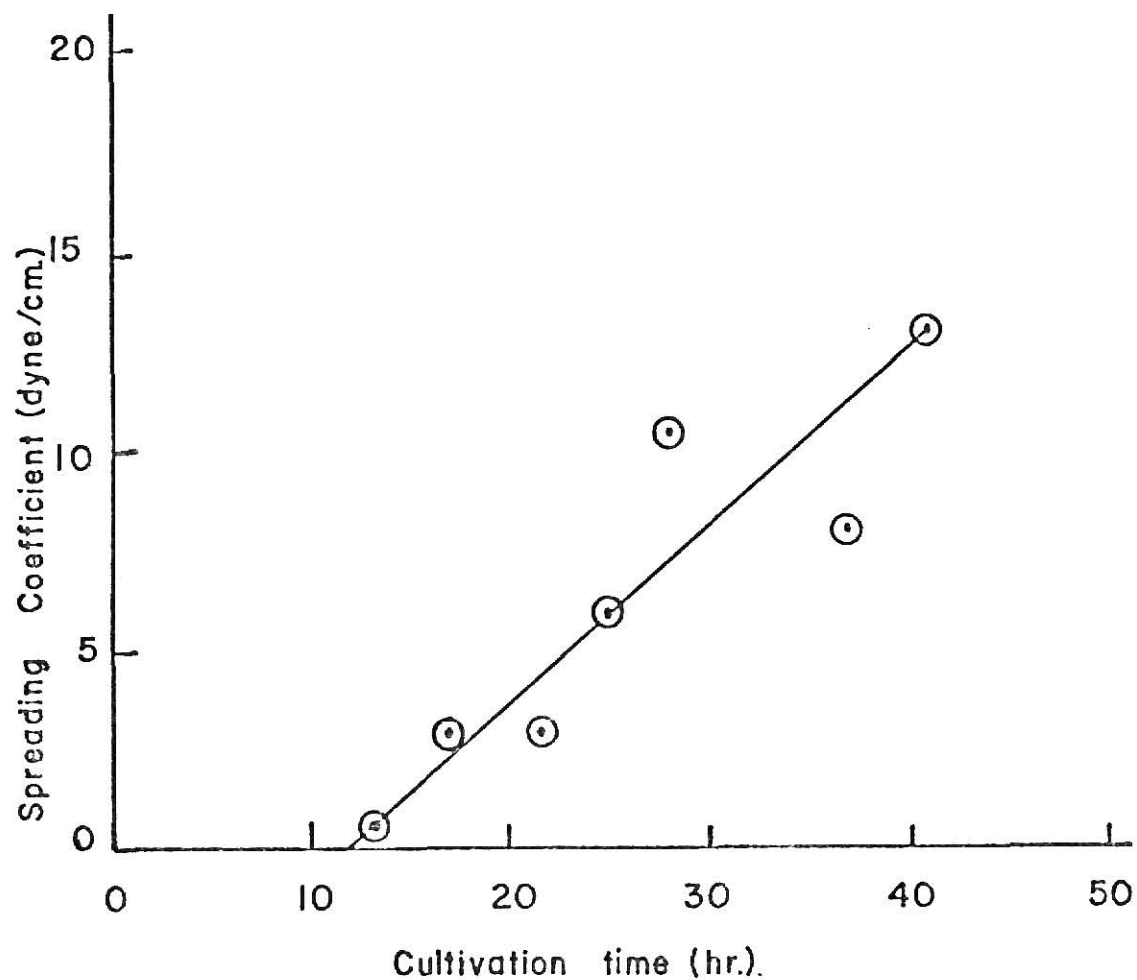
Fig. 2. Effect of cultivation on spreading coefficient during batch fermentation (From Erickson et al.[41])
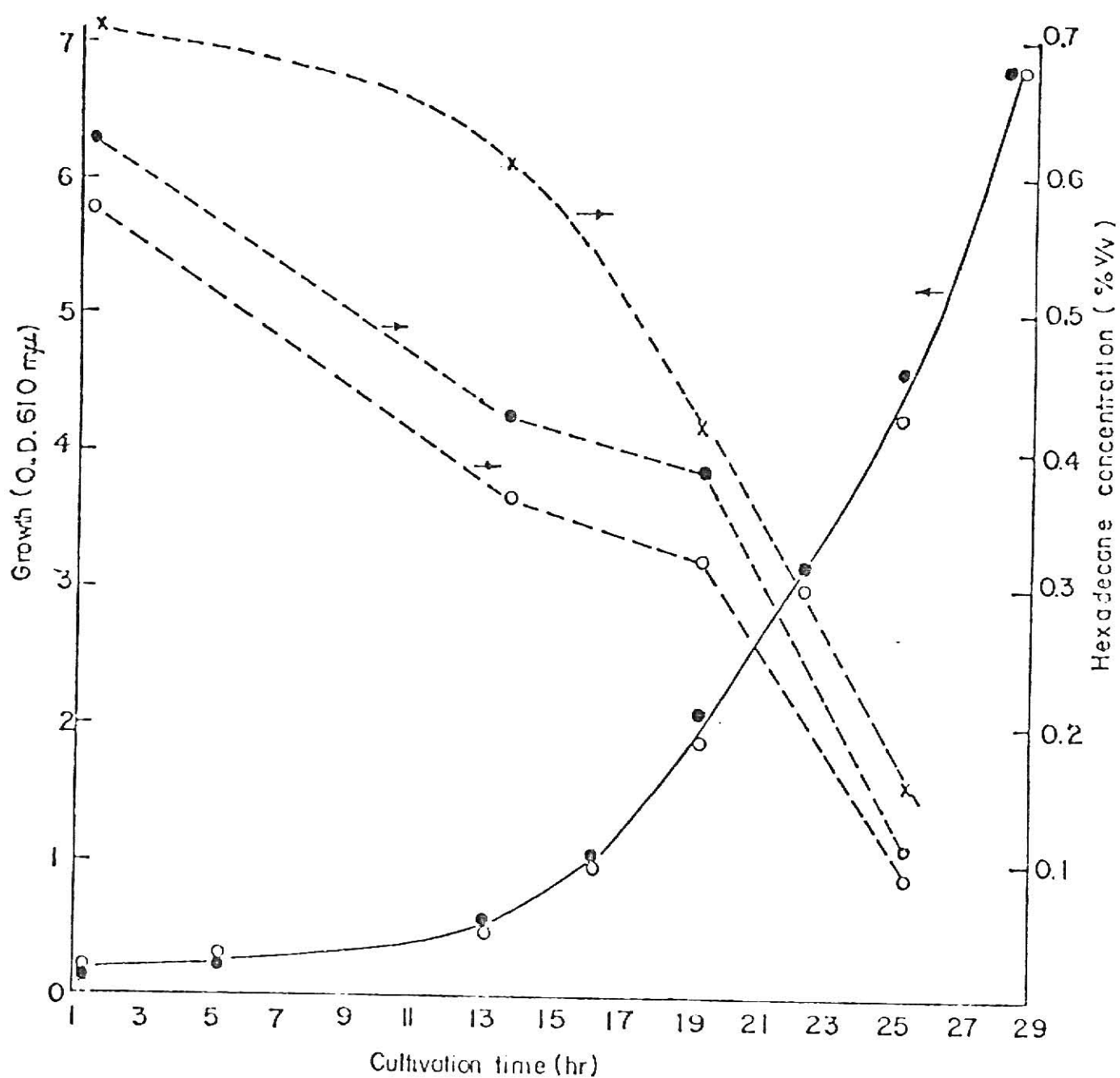
Fig. 3. Effect of cultivation on hexadecane concentration distribution

Koch mixers. (From Erickson et al.[40,41])

● Concentration at top

O Concentration at bottom

X Concentration at bottom of circulation arm.
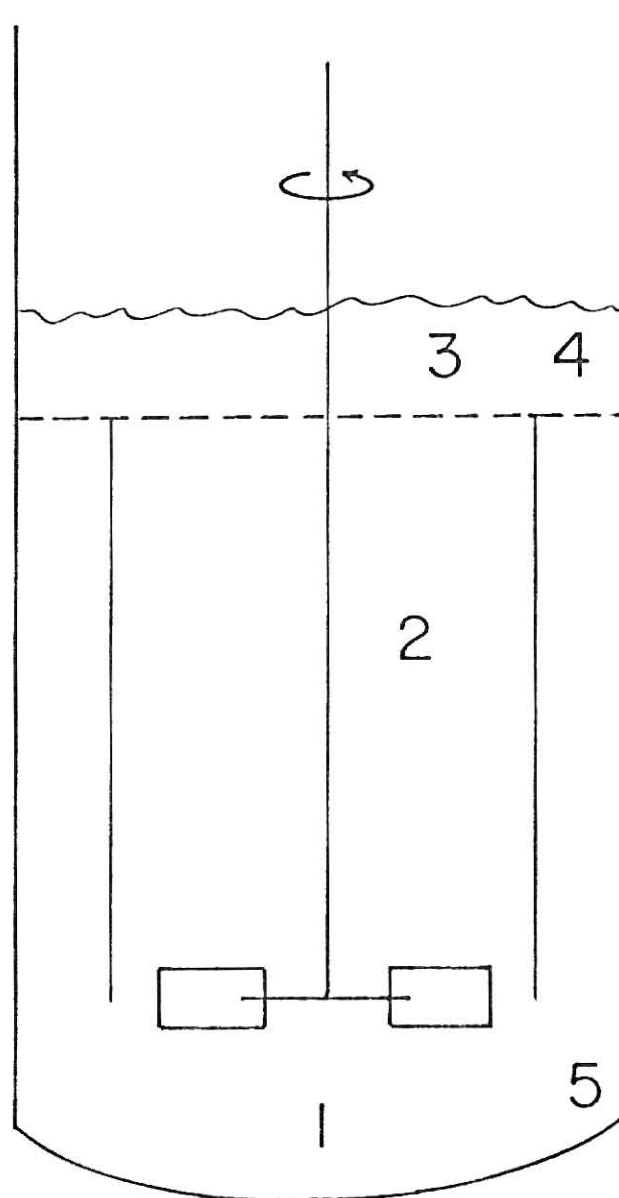
Fig. 4. Configuration of fermentor used by Hattori et al.[42] (From Hattori et al.[42])
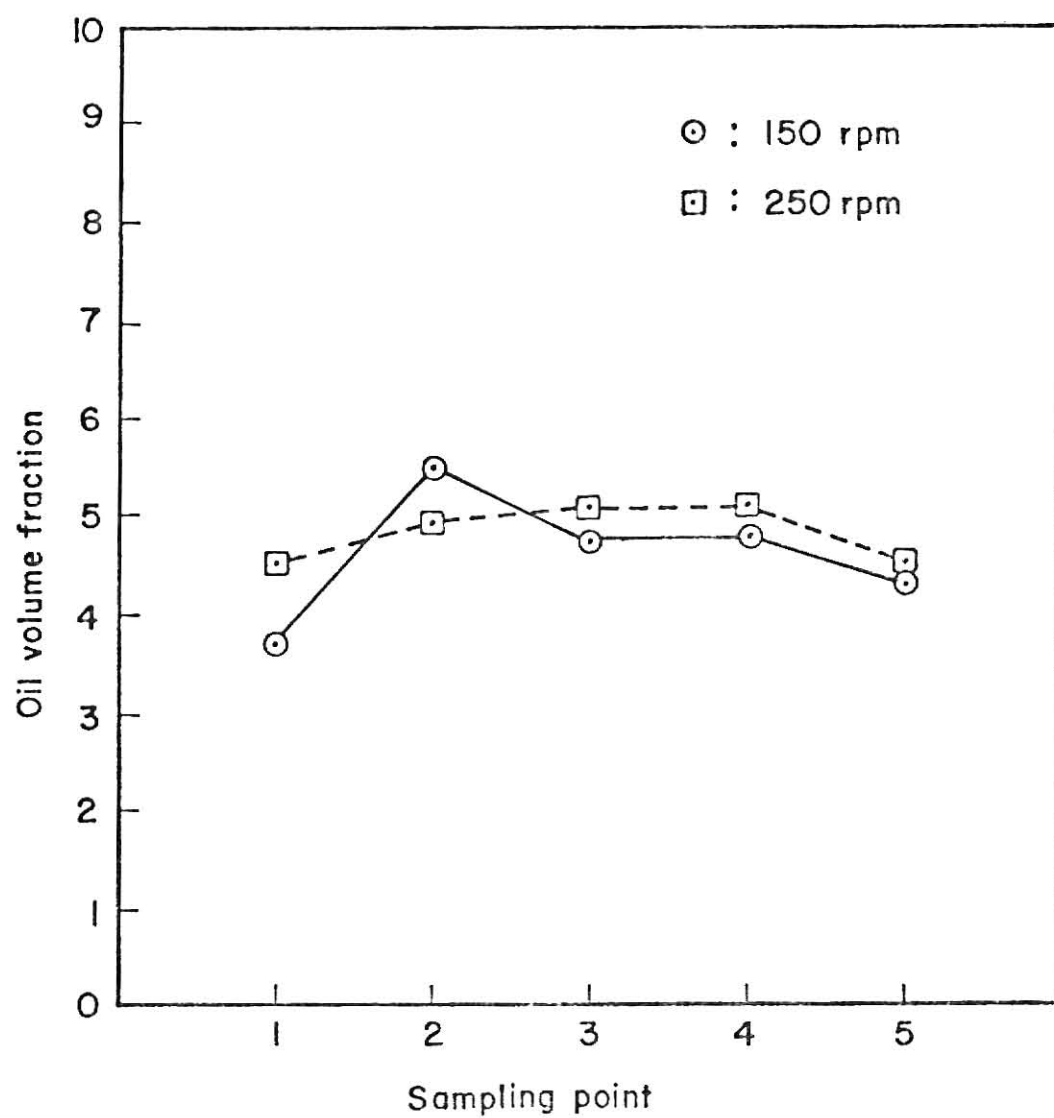
Fig. 5. Variation of oil fraction with position in fermentor
used by Hattori et al.[42] (From Hattori et al.[42])

CHAPTER IV

MODELING AND SIMULATION OF OXYGEN TRNASFER IN AIRLIFT FERMENTORS

INTRODUCTION

An impending food crisis has intensified research on cultivating edible yeasts on hydrocarbon substrates. Unlike microorganisms growing on carbohydrates, cell assimilating hydrocarbon substrates have a higher oxygen demand. On the basis of the same biomass production, a three times higher oxygen demand is reported for hydrocarbon fermentation than that for carbohydrate fermentation[1]. Because of the low solubility of oxygen in the aqueous phase, one of the most challenging fermentor design aspects is to continuously dissolve sufficient oxygen in the medium where the microorganisms grow. The rate of oxygen transport from the sparged gas phase to living organisms has frequently been the rate controlling factor in fermentations.

While a number of fermentor designs have been proposed for the purpose of increasing the oxygen transfer rate and minimizing the power consumption, one of the most promising was found to be the airlift fermentor which was first patented by Lefrancois and coworkers[2]. As shown in Figure 1, the concentric airlift fermentor[2-8] consists of two concentric cylinders with air sparged at the base of either the inner cylinder or the annular region. Three major regions of the airlift fermentor are:

1) the draft tube region, which is enclosed by the inner cylinder,

2) the annular region, which is the volume between two cylinders, and

3) the head region, which is the two-phase volume above the two regions. As air is sparged into the base of the draft tube region, the density of the dispersion in the draft tube is at once lower than that in the annular region, resulting in a pressure differential which induces the liquid circulation loop over the three regions. Some bubbles are entrained in the

annular region by the downward flow so that oxygen transfer can take place in all three regions. In some large scale airlift fermentations, air is sparged into the base of the annular region, forming a reverse recirculation loop which, due to smaller gap between the cylinders, has the advantage of reducing the hydrodynamic turbulence over the other concentric airlift with air sparged at the base of the draft tube region[9].

Alternate designs other than the concentric airlift such as the rectangular airlift[10], split cylinder airlift[11], and external recirculation airlift[12-14], have also been proposed. So far, a variety of airlift designs have been applied in industry. In Japan, the Kanegafuchi Chemical Company has built an external recycle airlift fermentor of 1000 liter volume[5,12]. Imperial Chemical Industries has also tested a very similar 1000 liter airlift of the external circulation design[5,13,14]. A rectangular airlift fermentor has recently been installed by Betz Laboratories for waste water treatment at Philadelphia[5,14]. A commercial-scale concentric airlift fermentor of 50,000 liter volume was constructed by Gulf Research and Development Co. at Pittsburgh[8].

The purpose of the present work is to model and simulate oxygen transfer in the concentric airlift fermentor. Most of the data are from Hatch's dissertation[3]. The model presented in this study is simple and can be adapted to systems other than the concentric airlift.

MODEL OF THIS STUDY

In airlift hydrocarbon fermentations, four phases are present; these are the aqueous medium, hydrocarbon phase, gas phase, and micro-organisms. Oxygen must be transported from the gas phase to the micro-organisms without interruption. Most researchers have treated systems with two liquid phases as if there is only one liquid phase by assuming oxygen equilibrium between the liquids or by neglecting mass transfer to the dispersed liquid phase. Mimura et al.[15] found that when the hydrocarbon volume fraction of the liquid dispersion is 2% or less, the liquid mixture can be treated as one phase. In the following study, the liquids are treated as a single phase, rather than separate phases.

In developing a model for the oxygen transfer from air bubbles to microorganisms in the culture medium of an airlift fermentor, it is neces-sary to consider the hydrodynamics of the heterogeneous gas-liquid opera-tions in the draft tube, head, and annular regions. Since several phases are present, the flow patterns are extremely complex. Exact mathematical models of the fluid flow and the oxygen transport in these operations pro-bably cannot be developed. Description of these systems will be based upon simplified concepts using flow models which assume complete mixing for each phase in each stage of the model.

The model of the steady state three-phase concentric airlift fermen-tor consists of a number of inter-connected theoretical stages as shown in Figure 2. In the head region a well-mixed reactor model is employed for each phase. The liquid velocities in the draft tube and annular regions of the concentric airlift of Hatch[3] were determined by the thermocouple response to hot water tracers injected at the base of the draft tube. The tracers were detected by two thermistors located one meter apart in

the upper half of the draft tube. The result[3] showed that in the draft tube and annular regions, the fluids frequently travel at velocities such that axial dispersion is small. The "tanks-in-series" model which Levenspiel[16] has referred to as an alternate approach to the dispersion model for dealing with small deviations from plug flow, can thus be employed to characterize the gas and liquid phases in the draft tube and annular ragions. As shown in Figure 2, for example, N stages can be assigned for the upflow draft tube region; M stages, for the downflow annular region; and another stage for the head region as well. The number of stages, i.e., N and M, can be adjusted, based on the amount of axial dispersion. The extent of axial dispersion may vary from phase to phase; that is, the values of N and M needed to model the axial dispersion in the gas phase may be different from those needed to model the axial dispersion in the liquid phase.

Under steady state conditions, the oxygen balance over a well-mixed stage, i, in the draft tube leads to

$$n_{i-1}Y_{i-1} - n_iY_i - K_La_i(C_i^* - C_i)(1 - H_{di})\frac{V_i}{m} = 0 \qquad (1)$$

for the gas phase, and

$$QC_{i-1} - QC_i + K_La_i(C_i^* - C_i)(1 - H_{di}) V_i - RX (1 - H_{di}) V_i = 0 \qquad (2)$$

for the liquid phase, where n = molar air flow rate, Y = mole fraction of oxygen in the gas phase, K_L = mass transfer coefficient, a = gas-liquid interfacial area per unit liquid mixture, C = dissolved oxygen concentration, C^* = oxygen concentration that is in equilibrium with gas phase oxygen concentration , H = gas holdup, V = total volume of the stage, m = molecular weight of oxygen, Q = volumetric liquid flow rate, R = specific oxygen uptake rate by microorganisms, X = cell concentration per unit liquid mixture

and the subscript refers to the stage number in the draft tube. Similar oxygen balances can also be written for the head and annular regions. These will be presented later in this section.

According to Henry's law, at equilibrium the partial pressure of oxygen in the gas phase is proportional to the amount of oxygen dissolved in the liquid film, that is,

$$C_i^* = \frac{P_{O_2,i}}{H_c} = \frac{P_i}{H_c} Y_i \tag{3}$$

where P_i and Y_i are the total pressure and mole fraction of oxygen in the gas phase at stage i. The total pressure in each stage is represented by the sum of the atmospheric pressure and the liquid head. As one can see, C_i^* is proportional to P_i, and thus to the liquid head. For tall columns C_i^* near the bottom is larger than that in the head region. Substituting for C_i^* in Eqns. (1) and (2) leads to

$$n_{i-1}Y_{i-1} - n_iY_i - K_La_i \left(\frac{P_i}{H_c} Y_i - C_i\right)(1 - H_{di}) \frac{V_i}{m} = 0 \tag{4}$$

for the gas phase, and

$$QC_{i-1} - QC_i + K_La_i \left(\frac{P_i}{H_c} Y_i - C_i\right)(1 - H_{di}) V_i$$

$$- RX(1 - H_{di}) V_i = 0 \tag{5}$$

for the liquid phase.

The bubble movement in the annular region is more complicated than the upflow draft tube region, because larger bubbles form by coalescence and ascend to the top. Both cocurrent and countercurrent gas-liquid flows are present. To simulate both cocurrent and countercurrent gas liquid flows, two well-mixed balances are employed to separately characterize the effects of upflow and downward gas flow. A fraction, f, of the

volumetric gas flow to a well-mixed stage is assumed to reverse direction and flow upward due to coalescence. At each stage in the annular region, the same value of f is employed. Therefore, by assuming an inflow of n_o moles gas/sec to the airlift system and rn_o moles gas/sec as the entrained gas flow to the annular region, a mass flow sheet for the concentric airlift fermentor may be constructed as shown in Figure 2. Both gas bubbles which rise and those flowing downward are assumed to coexist in the same stage. When the liquid phase balance is made for the same stage, the mass transfer with both the upflow and downflow gas streams is considered. In the j-th stage in the annular region where the liquid, the upflow, and downflow gas phases coexist, three balances can be written. For the entrained gas phase which flows downward,

$$n_{j-1}Y_{j-1} - n_jY_j - n_j^T Y_j - K_La_j(\frac{P_j}{H_c}Y_j - C_j)(1 - H_{aj})\frac{V_j}{m} = 0 \qquad (6)$$

For the gas phase which flows upward,

$$n'_{j+1}Y'_{j+1} + n_j^T Y_j - n'_jY'_j - K_La'_j(\frac{P_j}{H_c}Y'_j - C_j)(1 - H_{aj})\frac{V_j}{m} = 0 \qquad (7)$$

For the liquid phase which flows downward,

$$QC_{j-1} - QC_j + K_La_j(\frac{P_j}{H_c}Y_j - C_j)(1 - H_{aj})V_j + K_La'_j(\frac{P_j}{H_c}Y'_j - C_j)$$

$$(1 - H_{aj})V_j - RX(1 - H_{aj})V_j = 0 \qquad (8)$$

In these equations, n_j^T is the molar gas flow rate of the gas bubbles which coalesce and reverse direction from downflow to upflow.

In the head region part of the gas bubbles pass upward into a continuous gas phase, and the rest are entrained downward by liquid circulation. The two-phase, gas-liquid flow in the head region is modeled by a well-mixed tank. Therefore, two mass balances are written for the head region.

These are

$$n_N Y_N + n'_{N+1} Y'_{N+1} - n_H Y_H - K_L a_H (\frac{P_H}{H_c} Y_H - C_H)(1 - H_H) \frac{V_H}{m} = 0 \qquad (9)$$

for the gas phase, and

$$QC_N - QC_H + K_L a_H (\frac{P_H}{H_c} Y_H - C_H)(1 - H_H) V_H$$

$$- RX(1 - H_H) V_H = 0 \qquad (10)$$

for the liquid phase, where the subscripts H, N, and N+1 represent the head region and the top stages in the draft tube and annular regions respectively. For the system of N stages in the draft tube, M stages in the annular region, and one stage for the head region, a *total of* 2N + 3M + 2 mass balances are employed in the model analysis. The system with 2N + 3M + 2 simultaneous alegraic equations comprises the model[17].

The dissolved oxygen concentration in an airlift is influenced significantly by the effect of liquid head on oxygen partial pressure. The total pressure changes vertically with position. The pressure term P_i in Eqn. (3) is defined as

$$P_i = P_{atm} + \alpha \{h_H(1 - H_H) + (h_d + h_{op})[1 - \frac{2i - 1}{2N}$$

$$(1 - H_{di})]\} \qquad (11)$$

for i-th stage in the draft tube region, and in a similar manner

$$P_j = P_{atm} + \alpha \{h_H(1 - H_H) + (h_d + h_{op})[\frac{2j - 1}{2M}(1 - H_{aj})]\} \qquad (12)$$

for j-th stage in the annular region, as well as

$$P_H = P_{atm} + \frac{1}{2}\alpha \cdot h_H(1 - H_H) \qquad (13)$$

for the head region, where P_{atm} = the atmospheric pressure, α = conversion factor (0.000968 atm/cm of water), h = height, and H = gas phase volume fraction.

Hatch[3] has determined the gas holdup in both the draft tube and annular regions from the vertical pressure gradients. The local static pressure was measured at 20 cm to 30 cm intervals by water manometers in both regions. The local gas holdup was given by the following equation:

$$H_G = \frac{\Delta h}{\Delta x} \tag{14}$$

where Δh = water level difference in the manometer, and Δx = axial distance between static pressure reading. Averaging the measured local gas holdup, as shown in Figure 3, the gas holdup and liquid volume distribution were presented with respect to the draft tube superficial gas velocity[3]. Plotting in a semi-log graph, one reaches the correlations as follows:

$$H_d = 0.277 \cdot \log v_s - 0.097 \tag{15}$$

for the draft tube region, and

$$H_a = 0.222 \cdot \log v_s - 0.09 \tag{16}$$

for the annular region, where v_s is the superficial gas velocity based on the draft tube cross-section. In this study, the gas holdup is assumed to be constant within the draft tube and also within the annular region. The value of gas holdup in the head region is difficult to measure due to the turbulent, wavy liquid surface; however, its value is assumed to be equal to that in the draft tube region.

For computer simulation, the numerical value of $K_L a_i$ is needed. Figure 3 shows the comparison of the oxygen transfer coefficients in the three regions of the airlift fermentor[3]. In the draft tube, $K_L a$ is assumed to be independent of stage number because cocurrent gas-liquid flow takes place. As gas bubbles rise in the draft tube, the pressure decreases and the bubbles expand in size. Some coalescence also occurs. Both holdup and gas bubble Sauter mean diameter increase with height. Since

$$a = \frac{6 \cdot H_G}{D_{SM}} \tag{17}$$

it seems reasonable to assume that the interfacial area is constant in the draft tube.

In the annular region, where cocurrent as well as countercurrent gas-liquid flow occurs, the interfacial area differs from stage to stage, and so does the volumetric oxygen transfer coefficient. In this study, the value of the oxygen transfer coefficient has been modified stage-by-stage. For the j-th stage in the annular region, the oxygen transfer coefficient for downward flow bubbles and upflow bubbles are given as

$$K_L a_j = \frac{M(1-f)^j \overline{K_L a}}{(1-f+f \cdot d_r)[\sum\limits_{K=0}^{M-1} (1-f)^K]} \tag{18}$$

and

$$K_L a_j' = \frac{Mfd_r(1-f)^{j-1} \overline{K_L a}}{(1-f+fd_r)[\sum\limits_{K=0}^{M-1} (1-f)^K]} \tag{19}$$

respectively, where $\overline{K_L a}$ is the average oxygen transfer coefficient in the annular region as shown in Figure 3, and d_r represents the ratio of the Sauter mean diameters of the bubbles flowing down to those flowing up in the annular region.

COMPUTER SIMULATION

In the previous section a model of multiphase flow in the airlift fermentor, as influenced by sparger air flow rate, has been presented. Sufficient information is available in Hatch's dissertation[3] to use this model to simulate the dissolved oxygen concentration distribution in airlift fermentors. The model shows that a concentric airlift fermentor of N stages in the draft tube, M stages in the annular region and one stage in the head reagion leads to a total of 2N + 3M + 2 simultaneous algebraic mass balances. Thus, a concentric airlift of five stages in the draft tube, five stages in the annular region, and one stage in the head region, comprises a system of 27 simultaneous algebraic equations. The computer subroutine SIMQ[18] was employed to solve these simultaneous equations.

A number of appropriate numerical values for use in simulation are available in Hatch's dissertation[3]. For example, values for n, Q and V are found in the dissertation. The values of gas holdup and oxygen transfer coefficient are modified as given in equations (15), (16), (18), and (19). The pressures at each stage in the draft tube and annular regions are given in equations (11) and (12). Since the fermentation proceeded at $30^{o}C$, the value of Henry's law constant is assumed to be 0.025 ℓ-atm./mg O_2 which is found from the literature. The value of r is assumed to be 0.3; that is, 30% of the sparged gas is entrained from the draft tube to the annular region. For the system of five stages in the annular region, for example, assuming half of the entrained gas would complete the circulation loop and enter the draft tube, the value of f is obtained from

$$rn_o (1-f)^5 = \frac{1}{2} rn_o$$

Therefore, $f = 0.1294$.

After specifically reading in appropriate values as shown in Table I, calling the subroutine SIMQ, the 27 simultaneous equations are solved to give the dissolved oxygen concentration and oxygen mole fraction in the gas phase at each stage.

In the simulation, the five stages in the draft tube are numbered 1 to 5 upwards, the five stages in the annular region are numbered 6 to 10 downwards, and the head region is labeled H. Airlift fermentors with draft tube heights of 300, 600 and 900 cm. are simulated. The height of the head region is selected to correspond to that found by Hatch[3] for the 300 cm. tall draft tube as shown in Table II. This same head region height is then used for the 600 and 900 cm. tall cases.

RESULTS AND DISCUSSION

Simulation results were obtained for concentric airlift fermentors, with draft tubes 300, 600 and 900 cm. high for cell respiration rates ranging from 0 to 1.0 mg. O_2/ℓ-sec. Gas flow rates to the sparger ranged from 300 to 600 liters/min. evaluated at standard conditions of temperature and pressure. Figure 4 shows the effect of gas flow rate on dissolved oxygen concentration for towers 300 and 900 cm. high. As illustrated in Figure 4, the shorter airlift tower has a more uniform dissolved oxygen concentration distribution than the taller column. At higher gas flow rates, the dissolved oxygen concentration is higher in the taller column because of the greater oxygen partial pressure which results because of the liquid head. In the taller column, the mean bubble residence time is longer and a larger fraction of the oxygen is absorbed by the liquid phase. Because of these factors the dissolved oxygen concentration at the bottom of the annular region is lower in the taller column.

Figures 5 to 10 show the variation of dissolved oxygen concentration for three different tower heights and two different sparger gas flow rates. The parameter is cell respiration rate in mg. O_2/ℓ-sec. In Figure 5, a sparger gas flow rate of 500 ℓ/min is used in an airlift tower in which the draft tube is 300 cm. high. The results show that a fairly uniform dissolved oxygen concentration is achieved throughout the tower.

In Figures 6 and 7, similar results are presented for airlift systems with draft tubes 600 and 900 cm. in height for a sparger gas flow rate of 500 ℓ/min. As the tower height increases, there is a greater variation in dissolved oxygen concentration with position because of the larger effect of pressure and the greater fraction of oxygen which is absorbed.

In Figures 8, 9, and 10 the sparger gas flow rate is 300 ℓ/min. and results are again presented for airlift towers with 300, 600 and 900 cm. draft tube height, respectively. Comparison of these results with those in Figures 5, 6, and 7 shows that the cell respiration rate is considerably lower at similar dissolved oxygen concentrations at the lower gas flow rate. This indicates that the amount of cell cultivation can be increased by increasing the sparger gas flow rate for the range of gas flow rates examined in this work. The transition from bubble flow to slug flow eventually limits the increase in oxygen transfer rate which results from increasing the sparger gas flow rate.

The maximum dissolved oxygen concentration is frequently observed at or near the middle of the draft tube as shown in Figures 5 to 10. The same observation has also been reported by Hatch[8]. This may be explained by the direction of oxygen transfer in the system with no cell respiration. In Figure 11, the dissolved oxygen concentration, C, and equilibrium oxygen concentration at the gas-liquid interface, C^*, is drawn stage by stage. In the lower half of the draft tube, C^* is greater than C, leading to an oxygen transfer from the gas phase into the surrounding liquid phase. However, when bubbles rise to near the middle of the draft tube, C^* becomes smaller than C, and the oxygen transfer process is from the liquid phase into the gas phase. This results in a decrease in the dissolved oxygen concentration in the upper half of the draft tube. In the annular region, it is reversed.

Figure 12 shows that oxygen mole fraction in the gas phase is greatly affected by position, tower height, and sparger gas flow rate. The bubble residence time significantly influences the gas phase oxygen content. The gas phase oxygen mole fraction decreases as bubble residence time increases.

Comparison of Figures 4 and 12 shows that both the dissolved oxygen concentration and the oxygen mole fraction in the gas phase show much greater variation with position for the taller columns. The oxygen mole fraction at the bottom of the annular region is much smaller than that which leaves the head region in the 900 cm. tall column.

An axial dissolved oxygen gradient was found in the upflow and downflow regions as shown in Figures 5 to 10. With cells cultivated in the medium, the lowest levels of dissolved oxygen occur at the fermentor base which is in agreement with Hatch's experimental observation[8]. For tall columns, the fraction of oxygen absorbed from the gas phase is significant and the low dissolved oxygen concentration in the annular region can be directly related to the low oxygen mole fraction in the gas phase. As illustrated in Figure 5 to 10, when the cell respiration rate exceeds 0.6 mg O_2/ℓ-sec., the dissolved oxygen concentration curve is often concave downwards and both the bottom stages in the draft tube and in the annular region exhibit low dissolved oxygen concentration.

Figures 4 to 12 should be helpful in designing tower fermentors in terms of tower height and operating parameters. Normally, for yeast, the growth limiting dissolved oxygen is of the order of 1 mg O_2/ℓ. The dissolved oxygen content in the medium should always exceed this value in all parts of the column.

The simulation results from the mathematical model which treats the head region as a well-mixed stage, and the draft tube and annular regions as tanks-in-series reactors are in good qualitative agreement with the experimental results of Hatch[8]. The model is simple enough to use in design studies and to gain a better appreciation of oxygen transfer in various airlift systems with different configurations.

NOMENCLATURE

a = interfacial area between phases per unit volume of the liquid medium, cm^2/cm^3

C = dissolved oxygen concentration in liquid phase, mg O_2/ℓ

D = column diameter, cm

d_r = ratio of Sauter mean diameters of the downward flow bubbles to the upflow bubbles, dimensionless

f = for the gas phase which flows downward into a stage, f is the fraction of that flow which reverses direction due to coalescence, $0 \leq f \leq 1$, dimensionless

h = height, cm

H_c = Henry's law constant, ℓ-atm/mg O_2

H = gas holdup, dimensionless

K_L = mass transfer coefficient in liquid film, cm/sec

M = total number of stages in the annular region, dimensionless

m = molecular weight of oxygen, mg O_2/mole

N = total number of stages in the draft tube, dimensionless

n_o = initial molar air flow rate, moles/sec

P = pressure head as defined in equations (11), (12), and (13), atm

Q = volumetric liquid flow rate, ℓ/sec

r = the fraction of gas which entrains from the draft tube to annular region, dimensionless

RX = respiration consumption rate of microorganisms, mg O_2/ℓ-sec

V = volume, ℓ

Y = mole fraction of oxygen in gas phase, mole O_2/mole gas

α = conversion factor, = 0.000968 atm/cm of water

Superscripts

* = at equilibrium

' = of the reversed upflow gas phase

Subscripts

a   =   annular region

d   =   draft tube region

H   =   head region

i   =   i-th stage in the draft tube

j   =   j-th stage in the annular region

M   =   bottom stage in the annular region

N   =   top stage in the draft tube

op   =   the opening between the draft tube and tower bottom

1   =   inner column of the annular region

2   =   outer column of the annular region

References

1. Wang, D. I. C., "Protein from Petroleum", Chem. Engg., 75, No. 18, 99, August 26 (1968).

2. Lefrancois, L., C. G. Mariller, and J. V. Mejane, "Effectionnements aux procedes de Cultures forgiques et de Fermentations Industrielles", Brevet D'Invention, France #1,102,200, Delivree le 4 Mai (1955).

3. Hatch, R. T., "Experimental and Theoretical Studies of Oxygen Transfer in the Airlift Fermentor", Ph.D. Thesis, Massachusetts Institute of Technology (1973).

4. Hatch, R. T., "Fermentor Design", Single-Cell Protein II, (ed.) Tannenbaum, S. R., and D. I. C. Wang, p. 46, The MIT Press, Cambridge, Massachusetts (1975).

5. Hatch, R. T., and D. I. C. Wang, "Oxygen Transfer in the Airlift Fermentor", Presented at 1st Chemical Congress of the North American Continent, Mexico City, December, (1975).

6. Huang, S. Y., "Performance of Mixing and Oxygen Transfer in Air Lift Fermentor", Proc. National Science Council, Part 3, Engineering and Applied Science, 8, 297 (1974).

7. Chakravarty, M., S. Begum, H. D. Singh, J. N. Baruah, and M. S. Iyengar, "Gas Hold-Up Distribution in a Gas-Lift Column", Biotechnol. Bioeng. Symp., No. 4, 363 (1973).

8. Cooper, P. G., R. S. Silver, and J. P. Boyle, "Semi-Commercial Studies of a Petroprotein Process Based on N-Paraffins", Single-Cell Protein II, (ed.) Tannenbaum, S. R., and D. I. C. Wang, p. 454, The MIT Press, Cambridge, Massachusetts (1975).

9. Lefrancois, L., "Problems of Aeration and Circulation in Aerobic Fermentation Vats", Presented at the Proceedings of the 34th International Conference of Industrial Chemistry, Section 14, Fermentation Industries, Belgrade, Sept. 22-29 (1963).

10. Gasner, L. L., "Development and Application of the Thin Channel Rectangular Air Lift Mass Transfer Reactor to Fermentation and Waste-Water Treatment Systems", Biotechnol. Bioeng., 16, 1179 (1974).

11. Belfield, A. R., Jr., "Experimental Studies of Oxygen Transfer in a Split Cylinder Airlift", M.S. Thesis, University of Maryland (1976).

12. Kanazawa, M., "The Production of Yeast from n-Paraffins", Single-Cell Protein II (ed.) Tannenbaum, S. R., and D. I. C. Wang, p. 438, The MIT Press, Cambridge, Massachusetts (1975).

13. Moo-Young, M., "Microbial Reactor Design for Synthetic Protein Production", Can. J. Chem. Eng., 53, 113 (1975).

14. Gow, P. G., J. D. Littlehailes, S. R. L. Smith, and R. B. Walter, "SCP Production from Methanol: Bacteria", Single-Cell Protein II, (ed.) Tannenbaum, S. R., and D. I. C. Wang, p. 370, The MIT Press, Cambridge, Massachusetts (1975).

15. Mimura, A., I. Takeda, and R. Wakasa, "Some Characteristic Phenomena of Oxygen Transfer in Hydrocarbon Fermentation", Biotechnol. Bioeng. Symp., No. 4, 467 (1973).

16. Levenspiel, O., Chemical Reaction Engineering, John Wiley & Sons, Inc., New York, N.Y. (1962).

17. Ho, C. S., "Mathematical Model of Oxygen Transfer in Airlift Fermentor", Proceedings of the Sixth Biochemical Engineering Symposium, Published by Iowa State University, (1976).

18. Subroutine SIMQ, Version III, Programmer's Manual, System/360 Scientific Subroutine Package, IBM Application Program.

TABLE 1. Numerical values used for computer simulation.

$$d_r \quad = \quad 0.25 \quad [-]$$

$$D_d \quad = \quad 20.6 \quad [cm]$$

$$D_1 \quad = \quad 21.0 \quad [cm]$$

$$D_2 \quad = \quad 30.0 \quad [cm]$$

$$f \quad = \quad 0.1294 \quad [-]$$

$$H_c \quad = \quad 0.025 \quad [\ell\text{-atm/mg } O_2]$$

$$M \quad = \quad 5 \quad [-]$$

$$N \quad = \quad 5 \quad [-]$$

$$op \quad = \quad 10.0 \quad [cm]$$

$$r \quad = \quad 0.3 \quad [-]$$

TABLE II. Data for the head region height.

$$h_H = \frac{\frac{4 \times 200{,}000}{\pi} - D_d^{\,2}(h_d + h_{op})(1-H_d) - (D_2^{\,2} - D_1^{\,2})(h_d + h_{op})(1-H_a)}{D_2^{\,2} \times (1-H_H)}$$

Sparger gas flow rate (Std. ℓ/min)	Head region height (cm.)
200	71.98
300	91.56
400	107.04
500	118.13
600	131.48

a. Air Pressure Regulator
b. Rotameter
c. Glass Wool Air Filter
d. Millipore Air Filter
e. Check Valve
f. Air Sparger
g. Heating & Cooling Coil
h. pH electrode
i. Oxygen Probe
j. Centrifugal Pump
k. Thermistor Probe
m. Silica Gel Bed
n. Diaphram Pump
o. Paramagnetic Oxygen Analyzer
p. Recorder

sample port

water out
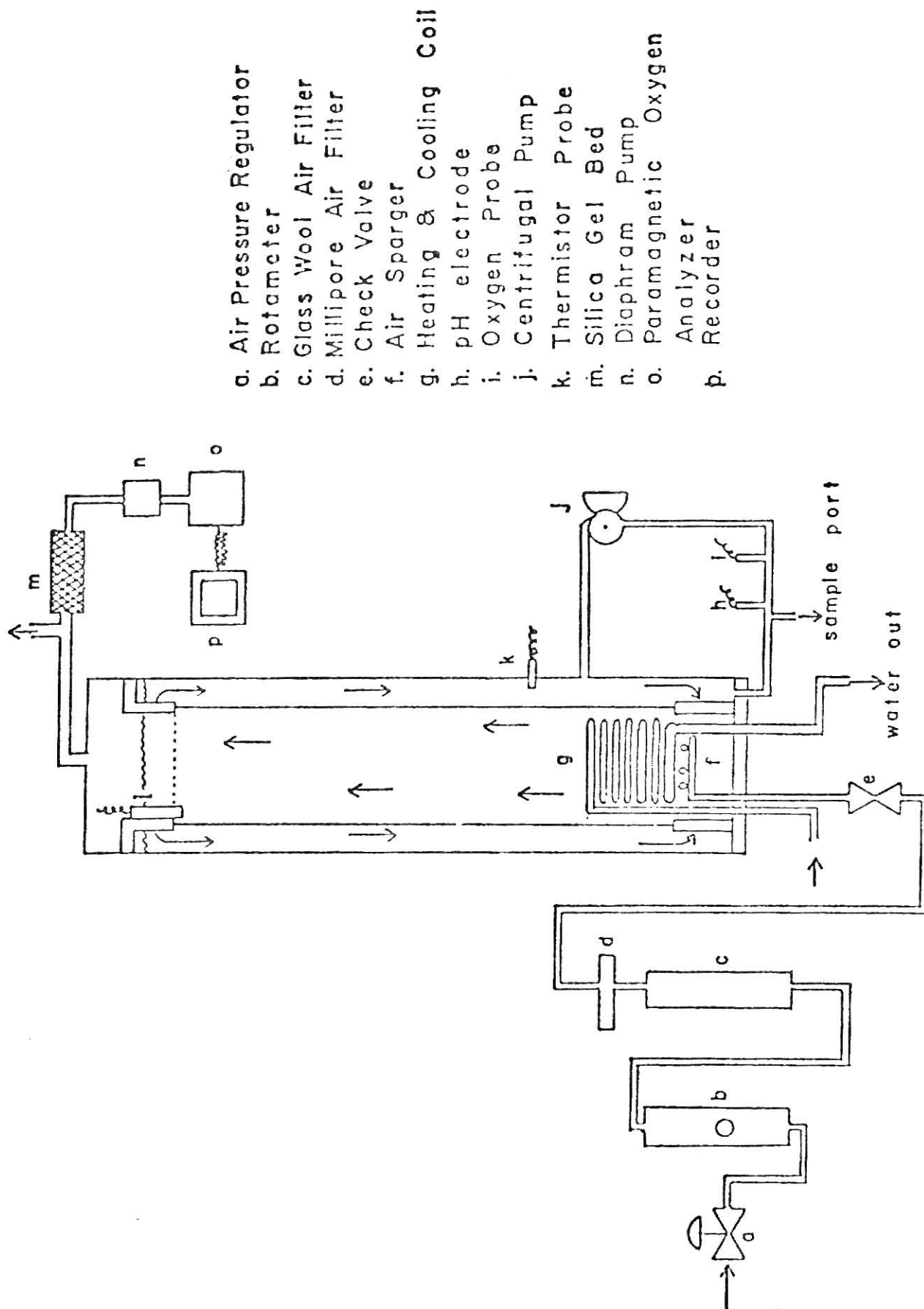
Fig. 1. Schematic of the concentric airlift fermentor used by Hatch (From Hatch[3])
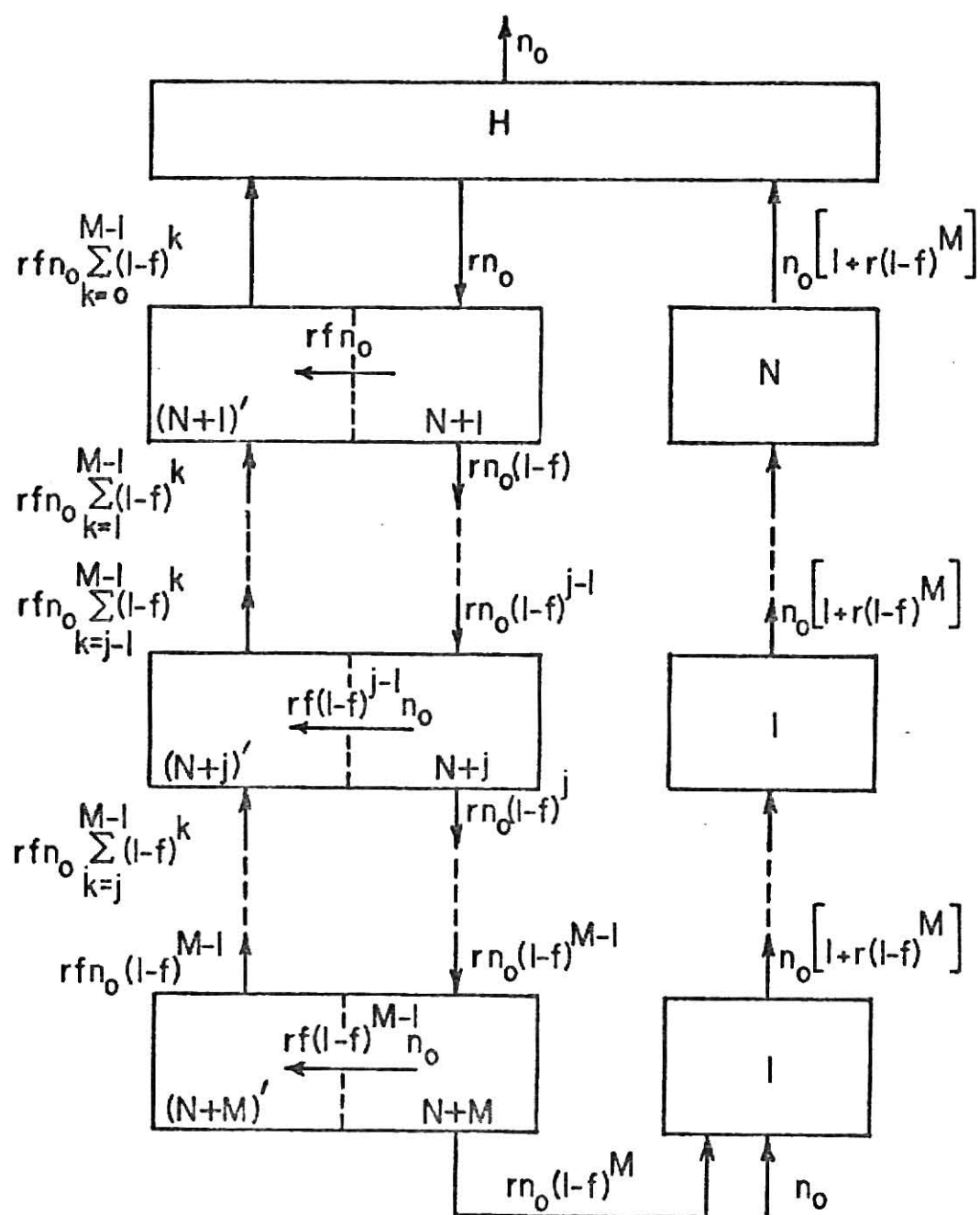
Fig. 2. Model for gas flow in the airlift fermenter
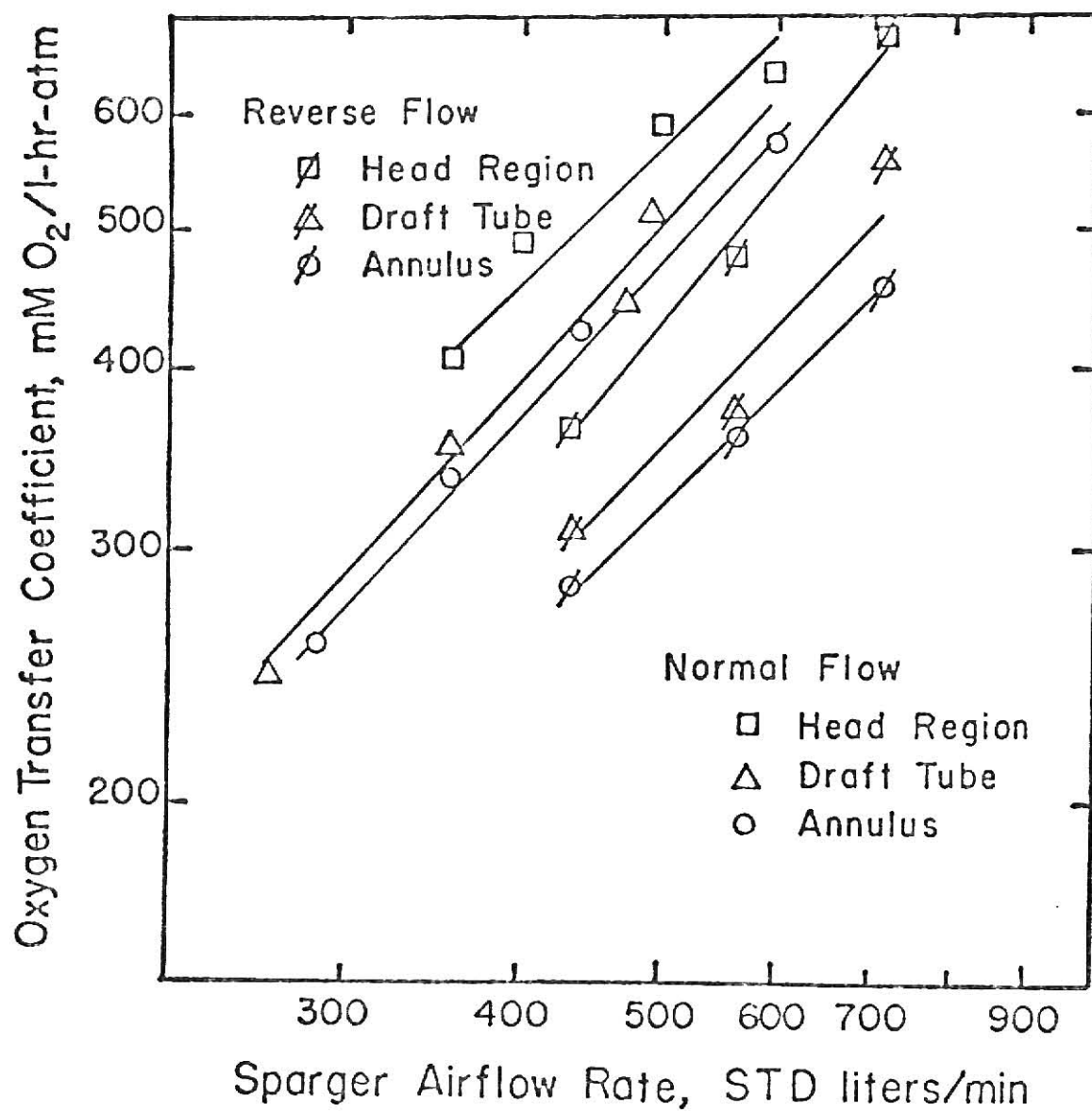
Fig. 3. Comparison of the oxygen transfer coefficients in the three regions of the airlift fermentor (From Hatch[3])
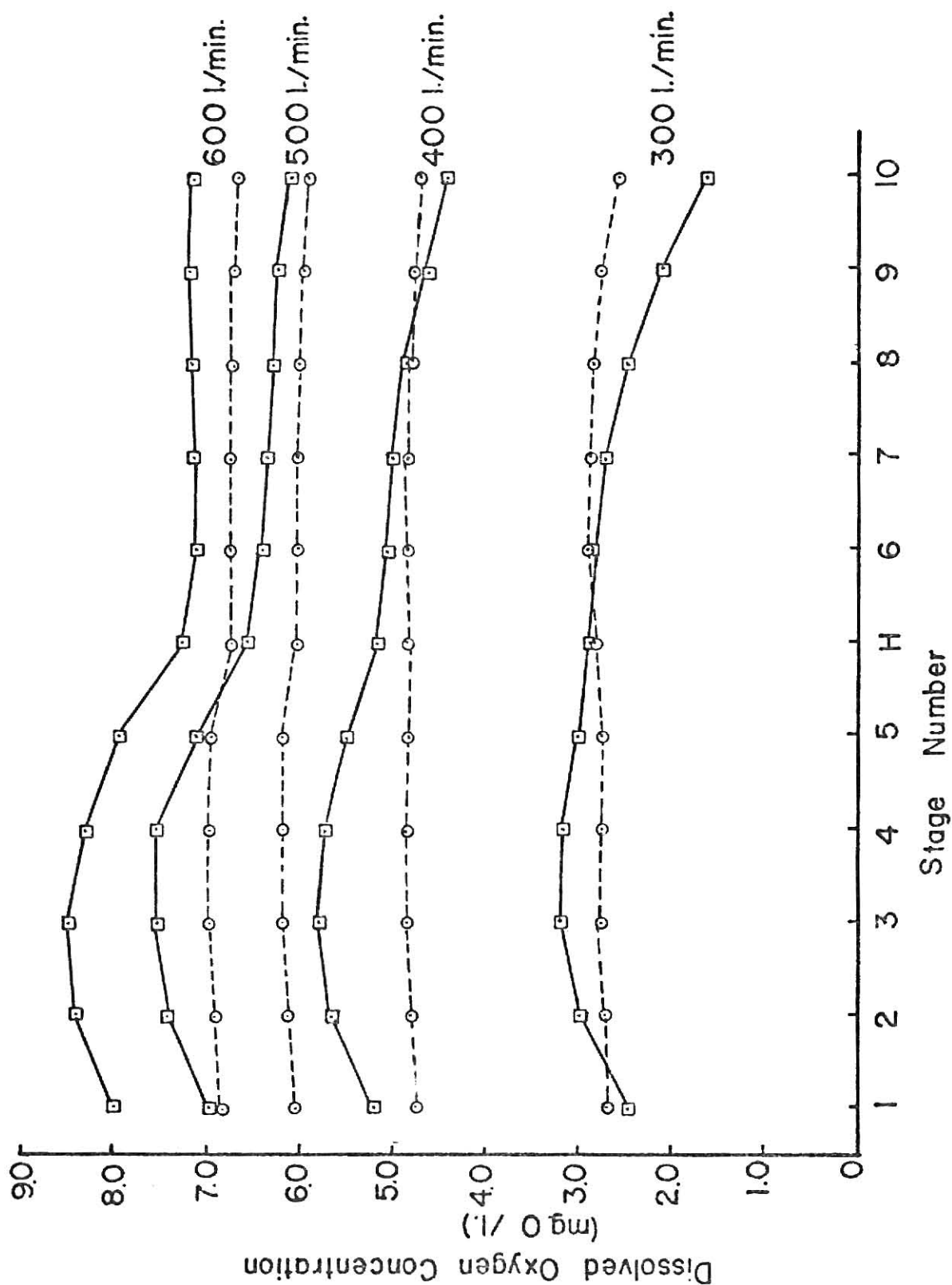
Fig. 4. Dissolved oxygen concentration distributions for towers of 300 cm. ⊙
and 900 cm. ⊡ height with cell respiration rate of 0.5 mg O_2/l-sec.
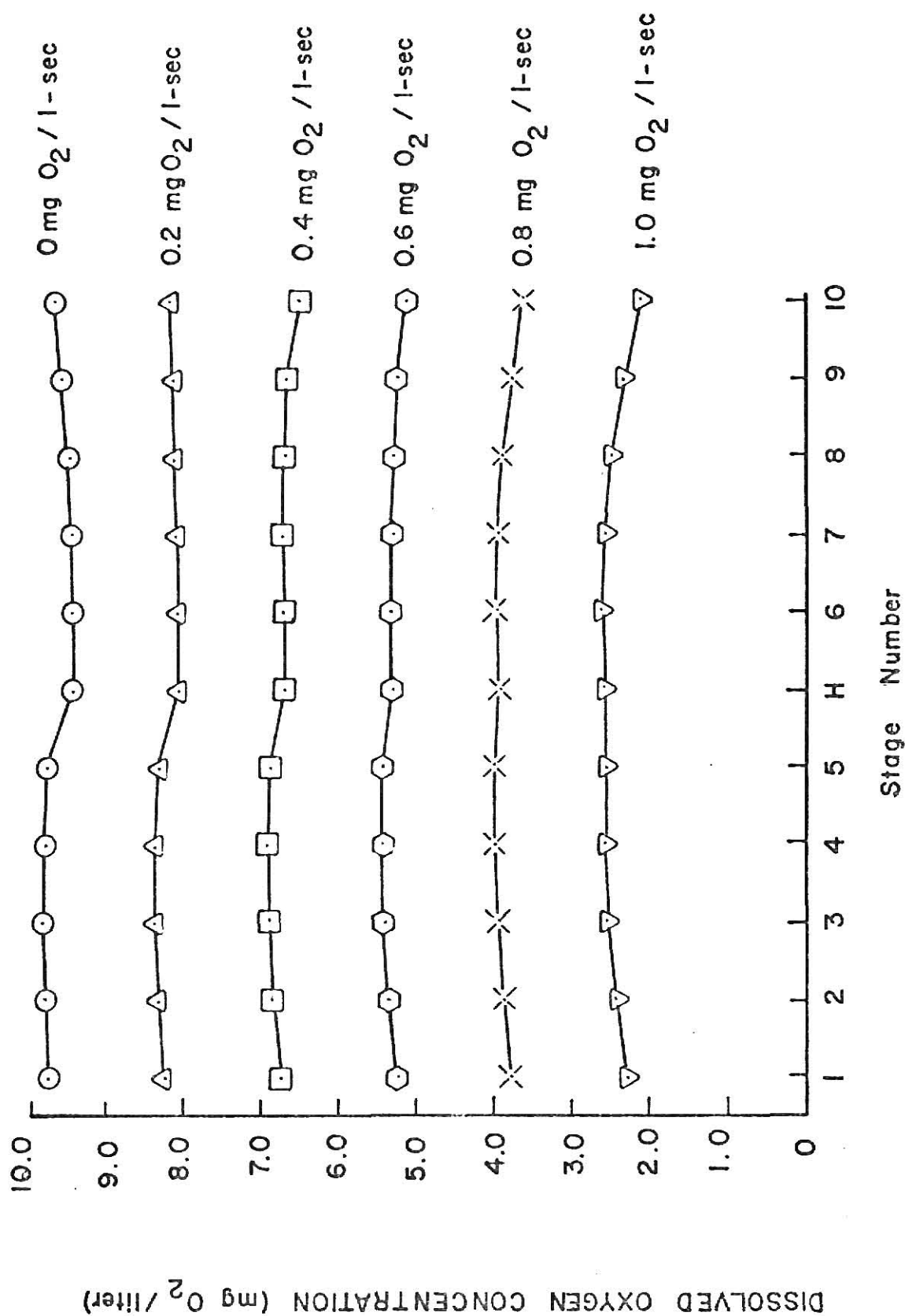
Fig. 5. Variation of dissolved oxygen concentration with position in towers of 300 cm height for a sparger gas flow rate of 500 l/min. Parameter is cell respiration rate.

129
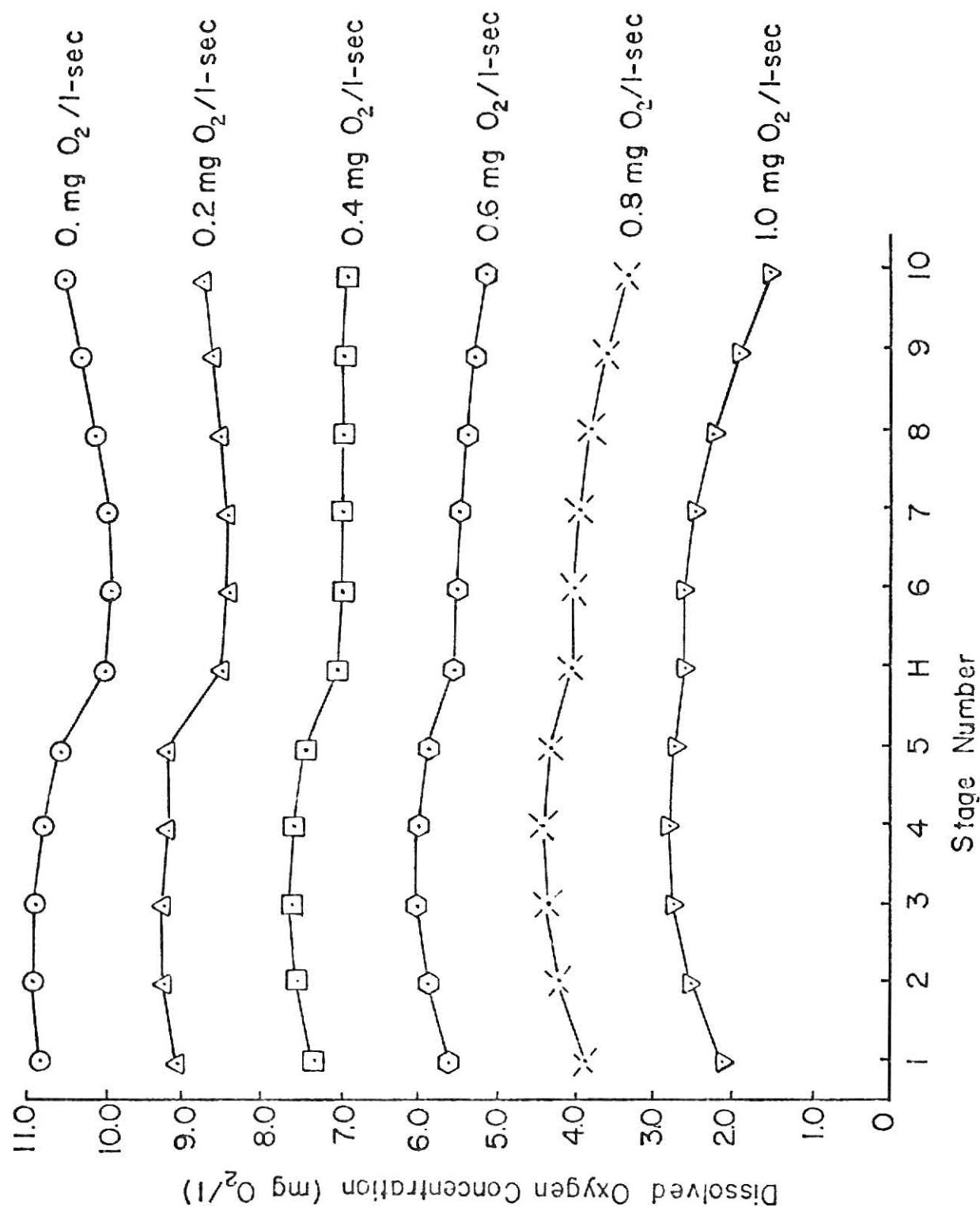
Fig. 6. Variation of dissolved oxygen concentration with position in towers of 600 cm height for a sparger gas flow rate of 500 l/min. Parameter is cell respiration rate.
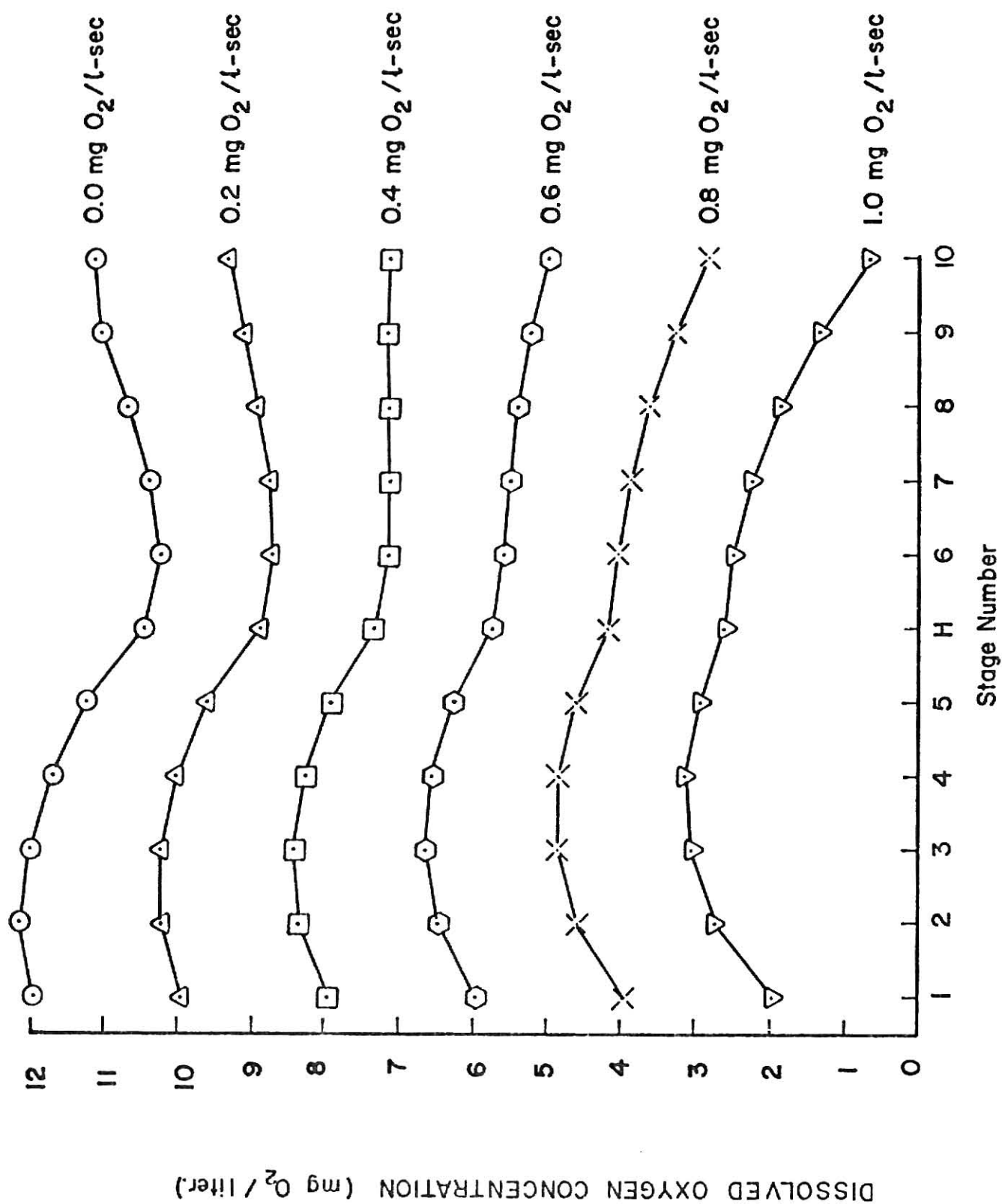
Fig. 7. Variation of dissolved oxygen concentration with position in towers of 900 cm height for a sparger gas flow rate of 500 1/min. Parameter is cell respiration rate.
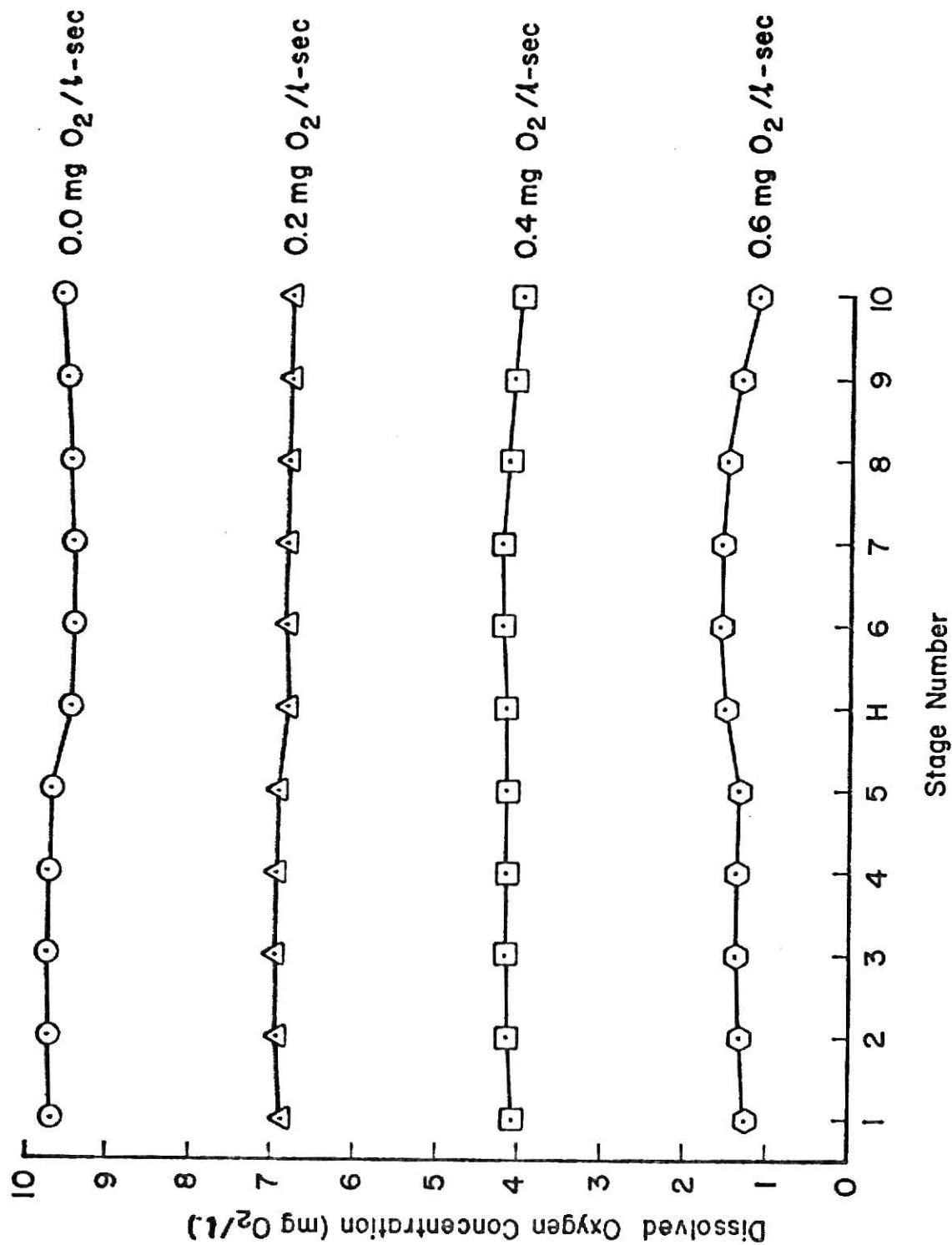
Fig. 8.   Variation of dissolved oxygen concentration with position in towers of 300 cm height for a sparger gas flow rate of 300 l/min.   Parameter is cell respiration rate.
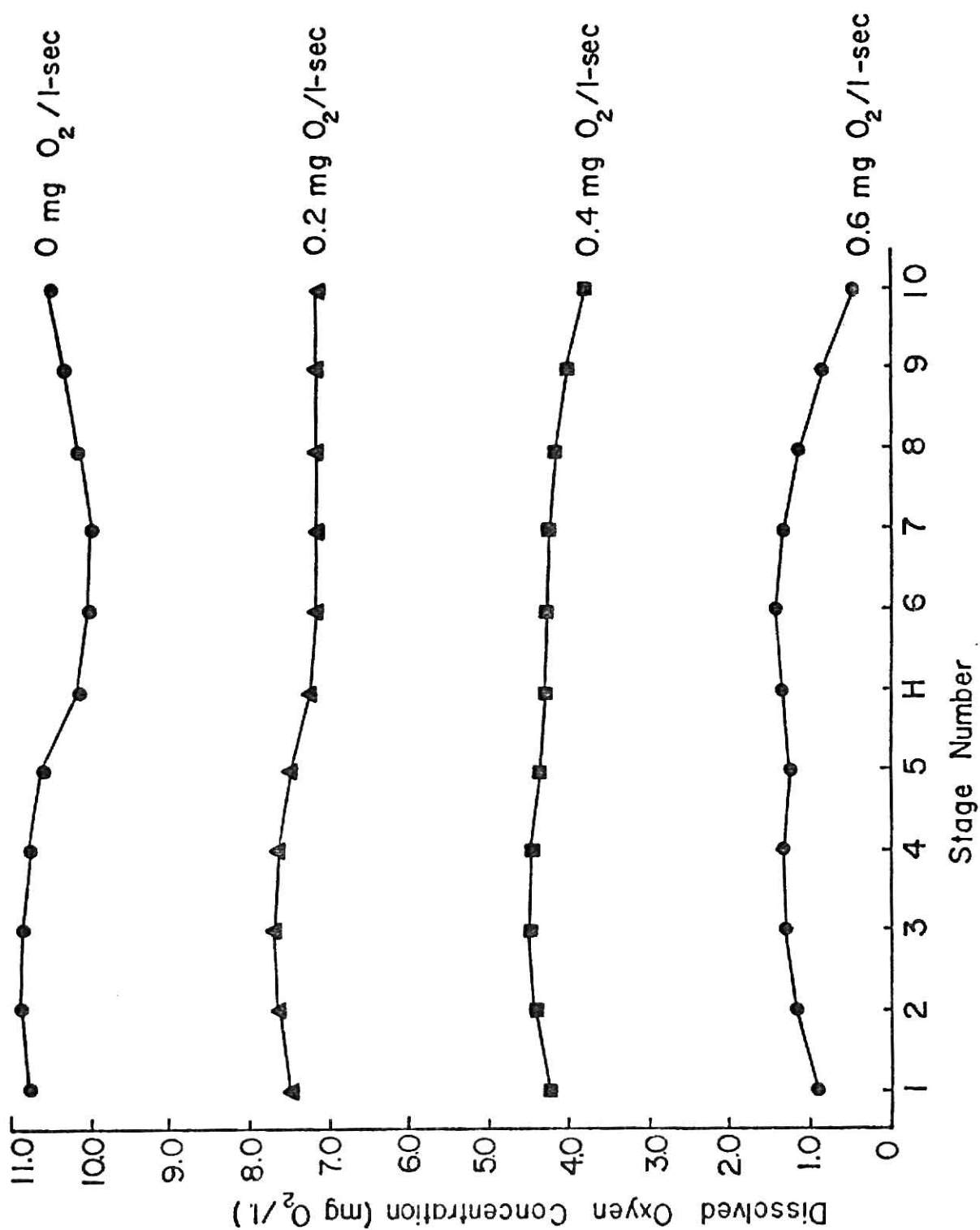
Fig. 9. Variation of dissolved oxygen concentration with position in towers of 600 cm height for a sparger gas flow rate of 300 l/min. Parameter is cell respiration rate.
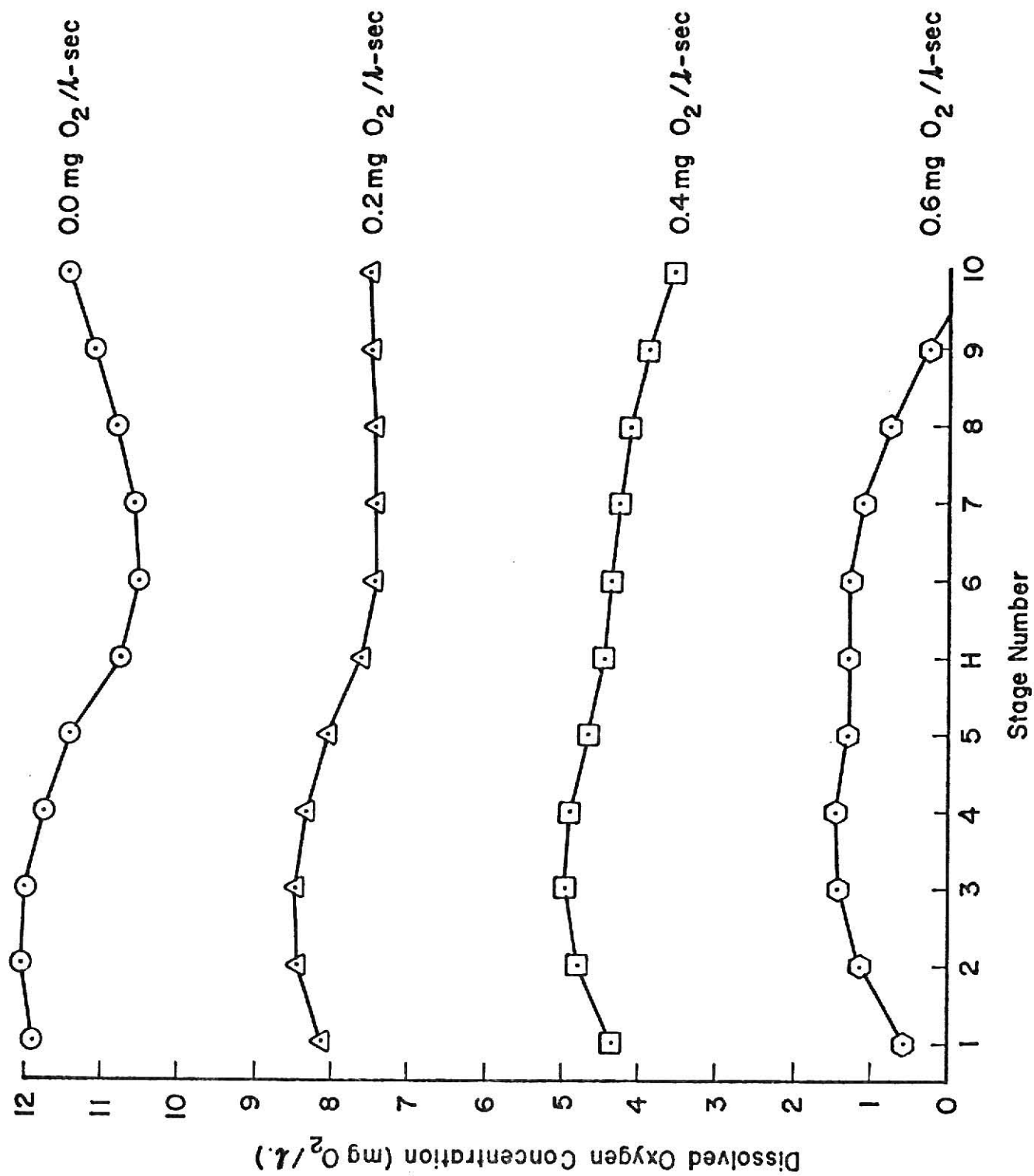
Fig. 10. Variation of dissolved oxygen concentration with position in towers of 900 cm height for a sparger gas flow rate of 300 1/min. Parameter is cell respiration rate.
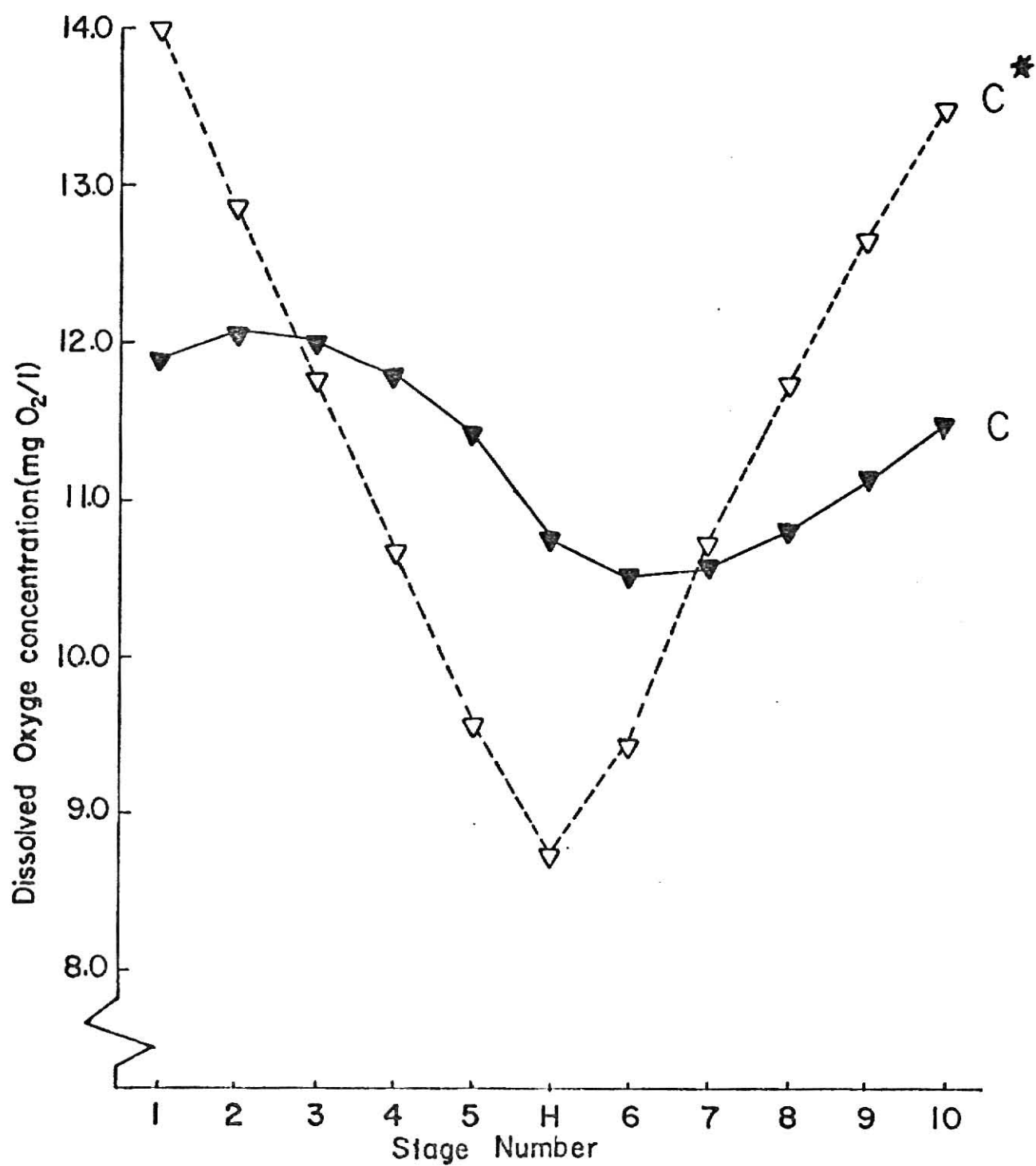
Fig. 11. Variation of C^* and C with position in a 900 cm tall airlift
fermentor for a sparger gas flow rate of 300 1/min and no
cell respiration.
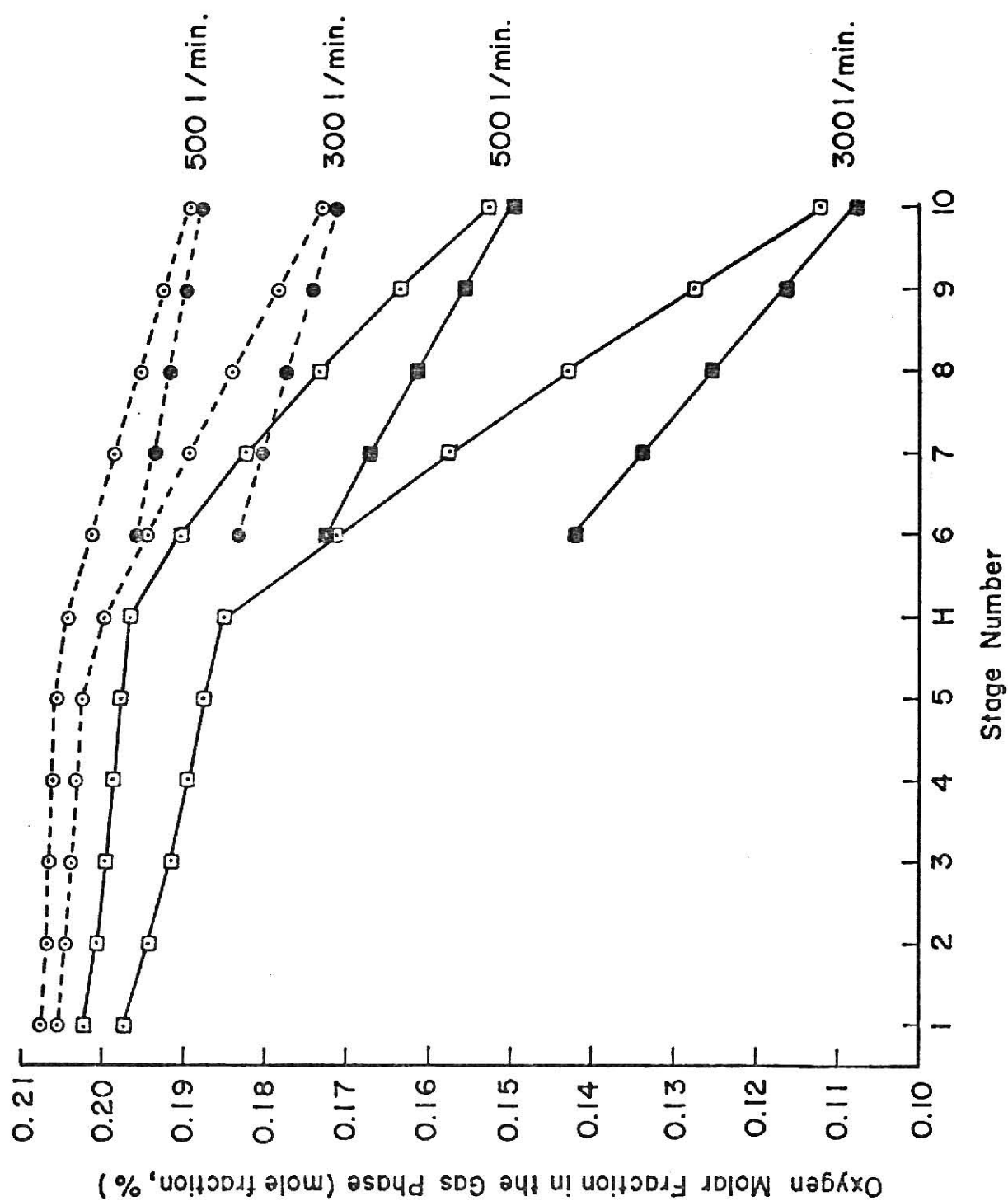
Fig. 12. Oxygen mole fraction in the gas phase for towers of 300 cm. ⊙ and 900 cm. ⊡ height with cell respiration rate of 0.5 mg O_2/l-sec (● and ■ represent the upflow bubble flow in the annular region). Parameter is sparger gas flow rate in std. l/min.

CHAPTER V

DISTRIBUTION OF DISPERSED OIL PHASE IN HYDROCARBON FERMENTATION

INTRODUCTION

Much has been said and written about mass transfer in biological
growth systems containing hydrocarbon as the carbon source[1,2] but, because
of its complexity, the behavior of the hydrocarbon phase during the course
of fermentation is not yet fully understood. In this study the behavior
of the hydrocarbon phase in airlift tower fermentors is examined. The
location and distribution of the relatively insoluble hydrocarbon substrate
is investigated. The effect of the gas phase on the movement and distri-
bution of the hydrocarbon is examined under the assumption that the spreading
coefficient is positive and the oil spreads at the gas-liquid interface.

The thermodynamic criterion for the hydrocarbon phase (o) to displace
the water film (ℓ) originally surrounding the gas bubble (a) is given by
the spreading coefficient, $S_{o/\ell a}$, as follows[3]:

$$S_{o/\ell a} = \gamma_{\ell/a} - \gamma_{o/a} - \gamma_{o/\ell} \tag{1}$$

where the 's are the appropriate interfacial tensions. Spreading of oil
at the air-water interface occurs when the spreading coefficient is numer-
ically zero or greater. The velocity of the spreading is directly propor-
tional to the value of $S_{o/\ a}$ and inversely proportional to the sum of the
viscosities of the liquids. Experimental results show that the interfacial
tension decreases during the course of hydrocarbon fermentation[4,5,6].
Figure 1 shows the change of interfacial tensions during a hydrocarbon
fermentation in which the initial hexadecane volume fraction was 14%.
According to eqn. (1), the spreading coefficient increased to positive
values as shown in Figure 2. This indicates that oil spreads at the air-
water interface under fermentation conditions, although pure hexadecane

does not spread on water[4].

Erickson et al.[4,7] observed that the oil concentration measured in a tower fermentor with external forced circulation varied with position in the tower and return flow as shown in Figure 3. The top sampling point was located 9 cm below the overflow to the circulation arm; therefore, samples from it might not be representative of the liquid surface. Larger concentrations of oil and cells have frequently been observed in the return flow and upper portion of the tower. This observation may be directly related to the spreading of the oil phase at the air-water interface because many gas bubbles with an oil film will break at the liquid surface. The liquid in the upper portion of the tower and external circulation arm are two possible harbors for the suspended oil droplets resulting from bubble breakage.

Hattori et al.[8] examined the performance of a draft tube fermentor which has a conventional agitator as shown in Figure 4. They found that the oil volume fraction varied with position in the fermentor. For example, with agitation at 150 rpm, the maximum oil concentration was detected at or near the middle of the draft tube; however, with agitation at 250 rpm, good mixing of the hydrocarbon phase was attained and a slightly higher oil volume fraction was observed in the head region rather than in the draft tube as shown in Figure 5. This may again be attributed to the breakup of oil film-carrying bubbles at the liquid surface.

Prokop and Sobotka[2] have also discussed the spreading coefficient and suggested that it may go positive on account of the decrease of inter-facial tension and cell presence at the interface. They have detected the presence of an oil film on gas bubbles microphotographically in the gas oil fermentation[2].

Increasing evidence has favored the spreading of the hydrocarbon phase at air-liquid interfaces; however, only recently[7] has the hydrocarbon film been considered as a mechanism for the upward flow of oil. In this work, balances for the hydrocarbon phase in the airlift fermentor are presented and simulation is used to examine the effect of the oil film at gas bubble surfaces on the distribution of oil within the fermentor.

THEORY

As discussed above, in airlift fermentors hydrocarbons are carried in the form of oil droplets by the aqueous phase and as oil films by the gas phase. A tanks-in-series model has been used[10] to account for the degree of axial dispersion in the gas and liquid phases in the draft tube and annular regions of the airlift fermentor. In this work, the tanks-in-series model shown in Figure 6 will be used with the following assumptions:

(1) Hydrocarbon dissolution in the aqueous phase can be neglected,

(2) All bubbles are covered by the oil film,

(3) The oil film thickness is thin compared to the bubble diameter. The ratio of oil droplets in the aqueous phase to overall oil content in stage j is defined as the oil droplet fraction, Z_j. Balancing the oil content in stage j leads to

$$V_{\ell j} \frac{d\phi_j}{dt} = QZ_{j-1}\phi_{j-1} - QZ_j\phi_j + (n_b A_b \delta)_{j-1} - (n_b A_b \delta)_j \qquad (2)$$

where $V_{\ell j}$ = volume of the liquid dispersion, Q = volumetric liquid flow rate, n_b = number of gas bubbles which enter or leave the stage per unit time, A_b = average surface area of a single bubble, ϕ = oil volume fraction, and δ = oil film thickness. The number of bubbles entering a stage is equal to the overall gas volume divided by the mean bubble volume; that is,

$$n_b = \frac{v_S A}{V_b} = \frac{q}{V_b} \qquad (3)$$

For spherical gas bubbles, Equation (3) may be used to obtain

$$n_b A_b \delta = 6(v_S A)\left(\frac{\delta}{D_b}\right) = 6 \cdot q\left(\frac{\delta}{D_b}\right) \qquad (4)$$

where v_S = superficial gas velocity, A = cross-sectional area of the stage, q = volumetric gas flow rate, and D_b = bubble diameter. Under steady state conditions, Eqation (1) becomes

$$QZ_{j-1}\phi_{j-1} - QZ_j\phi_j + 6\cdot q_{j-1}(\frac{\delta}{D_b})_{j-1} - 6\cdot q_j(\frac{\delta}{D_b})_j = 0 \qquad (5)$$

By assuming an inflow of q_o liters gas/sec to the airlift system, and rq_o liters gas/sec as the entrained gas flow from the head to annular region, the mass flow sheet for the concentric airlift fermentor may be depicted as shown in Figure 6. The oil balance in the draft tube becomes

$$QZ_M\phi_M - QZ_D\phi_D + 6\cdot q_M(\frac{\delta}{D_b})_M - 6\cdot q_D(\frac{\delta}{D_b})_D = 0 \qquad (6)$$

where the subscripts D and M represent the draft tube and bottom stage in the annular region respectively.

In the draft tube, only one stage is needed under steady state conditions. The important phenomena of fresh air bubbles being surrounded by an oil film is assumed to occur as soon as the air bubbles enter the draft tube through the sparger. The use of additional stages in modeling the draft tube would have no effect on the steady state simulation results as long as the oil film thickness, and the gas-liquid interfacial area per unit volume are assumed to remain constant from stage to stage.

In the head region, gas bubbles which are surrounded by oil films reach the liquid surface. The gas leaves the fermentor and the oil forms into oil droplets. The turbulent gas-liquid motion disperses oil droplets in such a way that the well-mixed model can be employed to represent the dispersed oil phase. For the head region, the oil balance is thus

$$QZ_D\phi_D - QZ_H\phi_H + 6\cdot q_D(\frac{\delta}{D_b})_D + 6\cdot q_1'(\frac{\delta}{D_b})_1' - 6\cdot(rq_o)(\frac{\delta}{D_b})_H = 0 \qquad (7)$$

where subscript H represents the head region and q_1' represents the

volumetric flow of gas from the top stage in the annular region to the head region.

Oil balances can also be written for the annular region in a similar manner. However, bubble movement in the annular region is more complicated than the upflow region, because larger bubbles which are formed by coalescence and covered by the oil film frequently acend to the top. As shown in Figure 6, a fraction, f, of the downward volumetric gas flow to a well-mixed stage reverses direction and flows upward due to coalescence. At each stage in the annular region, the same value of f is employed. Obviously, both cocurrent and countercurrent flow are present and should be considered in the oil balances. In the downflow annular region, a *tanks-in-series* reactor is employed to model the dispersed oil phase. The appropriate number of stages depends on the amount of axial dispersion. At steady state, the oil balance over the j-th completely mixed stage in the annular region becomes

$$QZ_{j-1}\phi_{j-1} - QZ_j\phi_j + 6 \cdot q_{j-1}(\frac{\delta}{D_b})_{j-1} - 6 \cdot q_j(\frac{\delta}{D_b})_j$$
$$+ 6 \cdot q'_{j+1}(\frac{\delta}{D_b})'_{j+1} - 6 \cdot q'_j (\frac{\delta}{D_b})'_j = 0 \tag{8}$$

The value of gas holdup in the concentric airlift fermentor is given in Hatch's dissertation[9]. As shown in Figure 7, the gas holdup can be correlated with draft tube superficial gas velocity as follows:

$$H_D = 0.277 \log v_S - 0.097 \tag{9}$$

for the draft tube, and

$$H_A = 0.222 \log v_S - 0.09 \tag{10}$$

for the annular region. No measurement of gas holdup in the head region is available. In this study, the same correlation is assigned for the draft tube and head regions.

Based on the definition of the oil droplet fraction, that is, fraction of the oil in droplet form to the overall oil content in the draft tube, the following balance is obtained

$$(1 - H_D)Z_D\phi_D + a\delta = (1 - H_D)\phi_D$$

where $a\delta$ represents the total amount of oil that surrounds gas bubbles. Substituting the interfacial area, $a = \dfrac{6 \cdot H_D}{D_b}$, into the preceding equation leads to

$$(1 - H_D)Z_D\phi_D + 6 \cdot H_D(\frac{\delta}{D_b})_D = (1 - H_D)\phi_D \tag{11}$$

for the draft tube region. Similarly, for the head region,

$$(1 - H_H)Z_H\phi_H + 6 \cdot H_H(\frac{\delta}{D_b})_H = (1 - H_H)\phi_H \tag{12}$$

and for the j-th stage in the annular region,

$$(1 - H_j - H_j')Z_j\phi_j + 6 \cdot H_j(\frac{\delta}{D_b})_j + 6 \cdot H_j'(\frac{\delta}{D_b})_j'$$

$$= (1 - H_j - H_j')\phi_j \tag{13}$$

where H_j and H_j' are the gas holdups associated with the downward and upward gas flows, respectively, in the annular region. In the annular region, the downward and reversed upward bubble flows coexist in the same stage. The bubble size for downward gas flow is assumed to be constant and that for the reversed upward gas flow is also assumed constant. In this study, the ratio among bubble diameters in the draft tube, in the upward flow in the annular region and in the downward flow in the annular region is assumed to be 4:5:2. Therefore, for example, if the bubbles in the draft tube are 2mm in diameter, then those flowing upward in the annular region are 2.5mm and those flowing downward are 1mm in diameter, respectively.

Numerical values of the gas holdup in the draft tube and head regions were given in Equation (9). But, to specify the value of gas holdup at each stage in the annular region requires more deliberation because gas bubbles coalesce with each other giving rise to a distribution of gas holdups. Both the upflow and downflow bubbles contribute to the gas holdup distribution. From the definition of superficial gas velocity in the annular region, that is

$$v_S \cdot A = v_{act} \cdot H_A \cdot A = q_{vol.} \quad , \tag{14}$$

one obtains the following relation between the upflow and downflow gas phases at stage j,

$$\frac{q_j}{v_{act} \cdot H_j} = \frac{q'_j}{v'_{act} \cdot H'_j} \tag{15}$$

An expression for the holdup associated with the upward bubbles can be obtained by rearranging Equation (15)

$$H'_j = \frac{q'_j}{q_j} \cdot \frac{v_{act}}{v'_{act}} \cdot H_j = \frac{q'_j}{q_j} \cdot V_{du} \cdot H_j \tag{16}$$

where V_{du} is ratio of the downflow bubble velocity to the reversed up-flow bubble velocity. Substituting in Equation (16) for q_j and q'_j as shown in Figure 6, the gas holdup becomes

$$H'_j = \frac{rf \, q_o \sum\limits_{K=j-1}^{M-1} (1-f)^K}{rq_o(1-f)^j} \cdot V_{du} \cdot H_j$$

which reduces to

$$H'_j = [\frac{1}{1-f} - (1-f)^{M-j}] \cdot V_{du} \cdot H_j \tag{17}$$

In the annular region considering both the downward and reversed upward

bubble flows, the total volumetric gas flow at stage j is

$$q_j + q_j' = H_j v_{act} A + H_j' v_{act}' A = (V_{du} \cdot H_j + H_j') \cdot v_{act} A$$

This can be rearranged to give

$$\frac{V_{du} H_j + H_j'}{q_j + q_j'} = \frac{1}{v_{act} A} \tag{18}$$

The value of v_{act} is assumed to be constant throughout the annular region because the bubble size for the downward gas flow has been assumed invariable. Therefore, the following general expression is obtained

$$\frac{V_{du} \cdot H_M + H_M'}{rq_o (1-f)^{M-1}} = - - - - = \frac{V_{du} \cdot H_j + H_j'}{rq_o (1-f)^{j-1}[1 + (1-f) - (1-f)^{M-j+1}]}$$

$$= - - - - = \frac{V_{du} \cdot H_1 + H_1'}{rq_o [1 + (1-f) - (1-f)^M]} \tag{19}$$

Combining eqns. (17) and (19) leads to

$$H_j = \frac{[1 + (1-f) - (1-f)^{M-j+1}]}{(1-f)^{M-j+1} \cdot [1 + \frac{1}{1-f} - (1-f)^{M-j}]} \cdot H_M \tag{20}$$

where H_M is the gas holdup of the bottom stage. In a system of five stages in the annular region, ten equations are required to solve for the ten gas holdups. In addition to the above-mentioned nine equations, there is the overall gas volume balance

$$\sum_j V_j (H_j + H_j') = H_A \cdot \sum_j V_j \tag{21}$$

where V_j represents the volume of stage j. Combining eqns. (17), (20), and (21), the ten gas holdups in the annular region are expressed in Table 1. The gas holdup distribution in the annular region is shown in Figure 8 for a

draft tube superficial gas velocity of 20 cm/sec which is at or near the middle of the range that Hatch has tested.[9] From Figure 8, one should realize that the averaged overall gas holdup deviates from the actual gas holdup distribution significantly. In this study, a variable gas holdup from stage to stage in the annular region is employed.

RESULTS

Substituting the gas holdups as expressed in equations (9) and (10), and Table 1 into equations (6), (7), (8), (11), (12), and (13), a system of fourteen simultaneous oil balances are tabulated. The numerical values of volumetric liquid flow rate, Q, sparger gas flow rate, q_o, and average gas holdups as expressed in Eqns. (9) and (10), are based on Hatch's work[9]. In this study, f is set equal to 0.1294. Half of the gas which enters the annular region reverses direction and half passes into the upflow draft tube region. The numerical vlaue of f is derived from

$$rq_o \ (1-f)^M = rq_o \ (1-f)^5 = \frac{1}{2} \ rq_o.$$

The entrainment of the sparged gas from the draft tube into the annular region is assumed to be 30% or r = 0.3.

The holdup of gas bubbles in the annular region is influenced by the ratio of actual mean velocities of the downflow to upflow bubbles, V_{du}. In the early part of this study, V_{du} is set equal to 1.0 by assuming that the actual velocities of the upflow and downflow bubbles are equal. In a later part of this study, different values of V_{du} (0.5, 1.0, and 1.5) are assigned in order to find out the influence of V_{du} on the gas holdup and the distribution of oil in the annular region. The mean bubble size of the upflow and downflow bubbles in the annular region are visually estimated to be 2.5 and 1.0 mm, respectively; in the draft tube and head regions, the mean bubble size is assumed to be 2.0 mm. After assigning appropriate values for V_{du} and $(\frac{\delta}{D})_{b \ j}$'s; the oil volume fraction ϕ_j's, and oil droplet fraction, z_j's, are obtained.

Figures 9, 10, and 11 show the effect of oil film thickness and oil volume fraction on the fraction of oil in droplet form as a function of position. At each stage, the fraction of oil which is not in droplet form is

assumed to be present in film form at air bubble surfaces. The fraction of oil in droplet form decreases as holdup increases, as oil film thickness increases, and as oil volume fraction decreases. Comparison of these figures shows that the oil film thickness and oil volume fraction should be considered together because when the value of $\frac{\delta}{\phi}$ is constant, similar vlaues are obtained for the fraction of oil in droplet form in Figures 9, 10, and 11. For example, the curve for 5μ film thickness and 10% oil volume fraction in Fig. 9 is similar to that for 2.5μ film thickness and 5% oil volume fraction shown in Fig. 10. Thus, as the volume fraction of oil in the fermentor decreases, a larger fraction of it is in film form provided the film thickness remains constant.

Figures 12 and 13 show that changing the ratio of downflow to upflow bubble velocity in the annular region, V_{du}, has only a small effect on the fraction of oil in droplet form. When V_{du} is larger, the fraction of oil in droplet form is also larger.

Figure 14 shows the variation of oil volume fraction with position for the case where the draft tube oil volume fraction is 5% and the film thickness is 2.5μ and 5.0μ. There is considerable variation in oil volume fraction with position. The oil volume fraction in the draft tube is smallest because the gas phase rapidly carries oil upward in film form in the draft tube.

Experimental observations of the oil concentration in the liquid phase should not be expected to give an accurate estimate of the total oil fraction in the fermentor. In general samples taken from the liquid phase will include only the fraction of oil in droplet form. In Fig. 14, the lower two curves show the results one would expect to find from liquid phase samples, while the upper two curves show the actual oil volume fraction.

The experimental results in Fig. 3 are qualitatively in agreement with those shown in Figure 14. At the bottom of the draft tube, one would expect to find the lowest oil concentration. The concentration at the bottom of the recirculation arm is expected to be larger than that in the draft tube because in the lower two curves of Fig. 14, the results at point 5 are higher than those at point D.

CONCLUSIONS

The effect of oil spreading at the surface of air bubbles in airlift fermentors on the distribution of oil with position has been examined. Oil films on air bubbles affect the distribution of oil in the fermentor and the results of experimental measurements in which the liquid phase is sampled. Differences in oil phase concentration with position which have been observed experimentally in tower systems may be due to oil films on air bubble surfaces, and the movement of oil by the bubbles.

NOMENCLATURE

A = cross-section of the draft tube, cm^2

D_b = bubble diameter, cm

f = for the gas phase which flows downward into a stage, f is the fraction of that flow which reverses direction due to coalescence, $0 \leq f < 1$, dimensionless

H = gas holdup, dimensionless

j = j-th stage in the annular region, dimensionless

M = total number of stages in the annular region, dimensionless

n_b = the number of bubbles, dimensionless

Q = volumetric liquid flow rate, ℓ/sec

q_o = initial volumetric gas flow rate, ℓ/sec

r = fraction of gas volume which is entrained downward from the head region to the annular region, dimensionless

$S_{o/\ell a}$ = spreading coefficient, defined in eqn. (1), dyne/cm

t = time, sec

V = volume, ℓ

V_{du} = $(\dfrac{v_{act}}{v_{act}})$, ratio of the actual velocity of downflow bubbles to that of the reversed upflow bubbles, dimensionless

V_ℓ = liquid volume, ℓ

v_s = draft tube superficial gas velocity, cm/sec

Z = oil droplet fraction, i.e., the fraction of oil droplets in the aqueous phase to overall oil content in the stage, dimensionless

γ = surface or interfacial tension, dyne/cm

δ = oil film thickness surrounding bubbles, μ

ϕ = oil volume fraction, dimensionless

Superscript

' = of the reversed upward bubble flow in the annular region

Subscripts

A = of the annular region

a = of the gas phase

b = of the gas bubble

D = of the draft tube region

H = of the head region

j = of the j-th stage in the annular region

ℓ = of the aqueous phase

M = of the bottom stage in the annular region

o = of the hydrocarbon phase

REFERENCES

1. Erickson, L. E., T. Nakahara, and A. Prokop, "Growth in Cultures
    with Two Liquid Phases: Hydrocarbon Uptake and Transport", Process
    Biochem., 10, No. 5, 9 (1975).

2. Prokop, A., and M. Sobotka, "Insoluble Substrate and Oxygen Trans-
    port in Hydrocarbon Fermentation", Single-Cell Protein II, (ed.)
    Tannenbaum, S. R., and D. I. C. Wang, p. 127, The MIT Press, Cambridge,
    Mass. (1975).

3. Davies, J. T., and E. K. Rideal, Interfacial Phenomena, Academic Press,
    New York, N.Y. (1961).

4. Erickson, L. E., J. R. Gutierrez, and T. Nakahara, "Growth of Cultures
    with Two Liquid Phases in Tower Systems", Fifth International
    Fermentation Symposium, p. 132, Berlin (1976).

5. Prokop, A., M. Ludvik, and L. E. Erickson, "Growth Models of Cultures
    with Two Liquid Phases. VIII. Experimental Observations on Droplet
    Size and Interfacial Area", Biotechnol. Bioeng., 14, 587 (1972).

6. Velankar, S. K., S. M. Barnett, C. W. Houston, and A. R. Thompson,
    "Microbial Growth on Hydrocarbons--Some Experimental Results",
    Biotechnol. Bioeng., 17, 241 (1975).

7. Erickson, L. E., T. Nakahara, J. R. Gutierrez, G. T. MacLean, and
    L. T. Fan, "Modelling and Characterization of Hydrocarbon Fermenta-
    tions", Presented at the Joint US/USSR Conference on Data Acquisition
    and Processing for Laboratory and Industrial Measurements in Fermen-
    tation Process, Univ. of Pennsylvania, Philadelphia, August 12-15,
    (1975).

8. Hattori, K., S. Yokoo, and O. Imada, "Performance of Draft Tube
    Fermentor for Hydrocarbon Fermentation", J. Ferment. Technol.,
    52, 583 (1974).

9. Hatch, R. T., "Experimental and Theoretical Studies of Oxygen
    Transfer in the Airlift Fermentor", PhD Thesis, Massachusetts
    Institute of Technology (1973).

10. Ho, C. S., "Mathematical Model of Oxygen Transfer in Airlift
    Fermentors", Proceedings of the Sixth Biochemical Engineering
    Symposium, Published by Iowa State University (1976).

Table 1. Expression for the gas holdup in each stage
of the annular region.

$$H_5 = 5 \cdot H_A / \{ [1+(\frac{1}{1-f} - 1)V_{du}] + \frac{[1+(1-f)-(1-f)^2] \cdot [1+(\frac{1}{1-f} - (1-f))V_{du}}{(1-f)^2 \cdot [1+\frac{1}{1-f} - (1-f)]} +$$

$$\frac{[1+(1-f)-(1-f)^3] \cdot [1+(\frac{1}{1-f} - (1-f)^2)V_{du}]}{(1-f)^3 \cdot [1+\frac{1}{1-f} - (1-f)^2]} + \frac{[1+(1-f)-(1-f)^4] \cdot}{(1-f)^4 \cdot}$$

$$\frac{[1+(\frac{1}{1-f} - (1-f)^3)V_{du}]}{[1+\frac{1}{1-f} - (1-f)^3]} + \frac{[1+(1-f)-(1-f)^5] \cdot [1+(\frac{1}{1-f} - (1-f)^4)V_{du}]}{(1-f)^5 \cdot [1+\frac{1}{1-f} - (1-f)^4]} \}$$

$$H_5^{'} = [\frac{1}{1-f} - (1-f)^0] \cdot V_{du} \cdot H_5$$

$$H_4 = \frac{[1+(1-f)-(1-f)^2]}{(1-f)^2 \cdot [1+\frac{1}{1-f} - (1-f)]} \cdot H_5$$

$$H_4^{'} = \frac{[1+(1-f)-(1-f)^2] \cdot [\frac{1}{1-f} - (1-f)]}{(1-f)^2 \cdot [1+\frac{1}{1-f} - (1-f)]} \cdot V_{du} \cdot H_5$$

$$H_3 = \frac{[1+(1-f)-(1-f)^3]}{(1-f)^3 \cdot [1+\frac{1}{1-f} - (1-f)^2]} \cdot H_5$$

$$H_3^{'} = \frac{[1+(1-f)-(1-f)^3] \cdot [\frac{1}{1-f} - (1-f)^2]}{(1-f)^3 \cdot [1+\frac{1}{1-f} - (1-f)^2]} \cdot V_{du} \cdot H_5$$

$$H_2 = \frac{[1+(1-f)-(1-f^4]}{(1-f)^4 \cdot [1+\frac{1}{1-f} - (1-f)^3]} \cdot H_5$$

$$H_2' = \frac{[1+(1-f)-(1-f)^4] \cdot [\frac{1}{1-f} - (1-f)^3]}{(1-f)^4 \cdot [1+\frac{1}{1-f} - (1-f)^3]} \cdot V_{du} \cdot H_5$$

$$H_1 = \frac{[1+(1-f)-(1-f)^5]}{(1-f)^5 \cdot [1+\frac{1}{1-f} - (1-f)^4]} \cdot H_5$$

$$H_1' = \frac{[1+(1-f)-(1-f)^5] \cdot [\frac{1}{1-f} - (1-f)^4]}{(1-f)^5 \cdot [1+\frac{1}{1-f} - (1-f)^4]} \cdot V_{du} \cdot H_5$$

Table 2.   Simultaneous equations used to find oil distribution.

$$QZ_5\phi_5 - QZ_D\phi_D + r(1-f)^5 \cdot q_o \cdot 6\left(\frac{\delta}{D_b}\right)_A - [1+r(1-f)^5]q_o \cdot 6\left(\frac{\delta}{D_b}\right)_D = 0$$

$$QZ_D\phi_D - QZ_H\phi_H + [1+r(1-f)^5]q_o \cdot 6\left(\frac{\delta}{D_b}\right)_D + r[1-(1-f)^5]q_o \cdot 6\left(\frac{\delta}{D_b}\right)_A' - rq_0 \cdot 6\left(\frac{\delta}{D_b}\right)_H = 0$$

$$QZ_H\phi_H - QZ_1\phi_1 + rq_o \cdot 6\left(\frac{\delta}{D_b}\right)_H - r(1-f)q_o \cdot 6\left(\frac{\delta}{D_b}\right)_A - rfq_o \cdot 6\left(\frac{\delta}{D_b}\right)_A' = 0$$

$$QZ_1\phi_1 - QZ_2\phi_2 + rf(1-f)q_o \cdot 6\left(\frac{\delta}{D_b}\right)_A - rf(1-f)q_o \cdot 6\left(\frac{\delta}{D_b}\right)_A' = 0$$

$$QZ_2\phi_2 - QZ_3\phi_3 + rf(1-f)^2 q_o \cdot 6\left(\frac{\delta}{D_b}\right)_A - rf(1-f)^2 q_o \cdot 6\left(\frac{\delta}{D_b}\right)_A' = 0$$

$$QZ_3\phi_3 - QZ_4\phi_4 + rf(1-f)^3 q_o \cdot 6\left(\frac{\delta}{D_b}\right)_A - rf(1-f)^3 q_o \cdot 6\left(\frac{\delta}{D_b}\right)_A' = 0$$

$$QZ_4\phi_4 - QZ_5\phi_5 + rf(10f)^4 q_o \cdot 6\left(\frac{\delta}{D_b}\right)_A - rf(1-f)^4 q_o \cdot 6\left(\frac{\delta}{D_b}\right)_A' = 0$$

$$(1-H_D)Z_b\phi_b + H_b \cdot 6\left(\frac{\delta}{D_b}\right)_D = (1-H_D)\phi_D$$

$$(1-H_H)Z_H\phi_H + H_H \cdot 6\left(\frac{\delta}{D_b}\right)_H = (1-H_H)\phi_H$$

$$(1-H_1-H_1')Z_1\phi_1 + H_1 \cdot 6\left(\frac{\delta}{D_b}\right)_A + H_1' \cdot 6\left(\frac{\delta}{D_b}\right)_A' = (1-H_1-H_1')\phi_1$$

$$(1-H_2-H_2')Z_2\phi_2+H_2\cdot 6\left(\frac{\delta}{D_b}\right)_A+H_2'\cdot 6\left(\frac{\delta}{D_b}\right)_A' \quad = \quad (1-H_2-H_2')\phi_2$$

$$(1-H_3-H_3')Z_3\phi_3+H_3\cdot 6\left(\frac{\delta}{D_b}\right)_A+H_3'\cdot 6\left(\frac{\delta}{D_b}\right)_A' \quad = \quad (1-H_3-H_3')\phi_3$$

$$(1-H_4-H_4')Z_4\phi_4+H_4\cdot 6\left(\frac{\delta}{D_b}\right)_A+H_4'\cdot 6\left(\frac{\delta}{D_b}\right)_A' \quad = \quad (1-H_4-H_4')\phi_4$$

$$(1-H_5-H_5')Z_5\phi_5+H_5\cdot 6\left(\frac{\delta}{D_b}\right)_A+H_5'\cdot 6\left(\frac{\delta}{D_b}\right)_A' \quad = \quad (1-H_5-H_5')\phi_5$$

Table 3. Values of volumetric liquid flow rate
used for simulation.

Sparger gas flow rate (ℓ/min)	Volumetric liquid flow rate (ℓ/min)
200	122.38
300	237.90
400	347.63
500	429.49
600	499.40
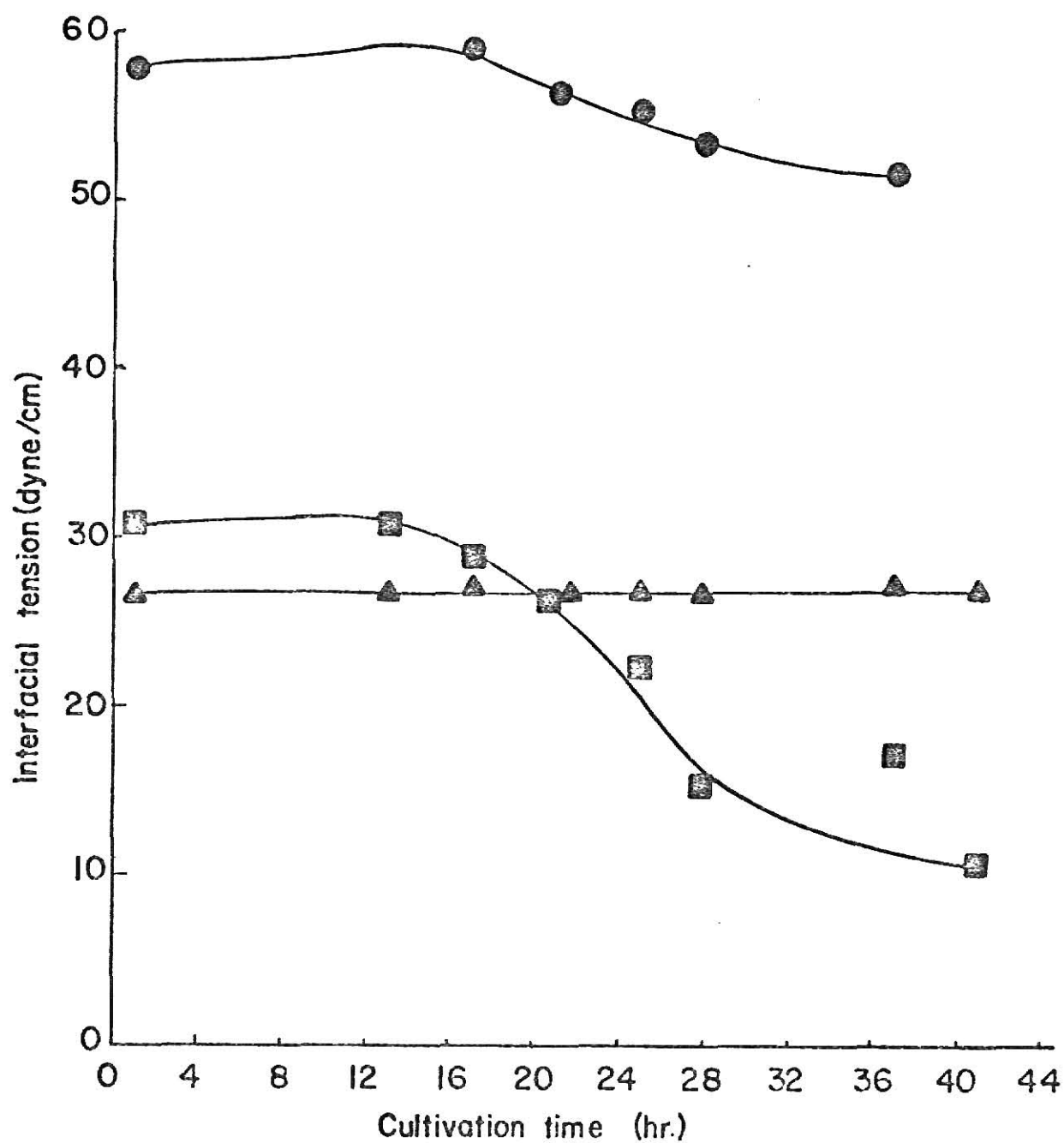
Fig. 1. Effect of cultivation on surface and interfacial tensions during
fermentation (From Erickson et al.[4])

● Interfacial tension between water and oil

▦ Interfacial tension between oil and air

▲ Interfacial tension between water and air.
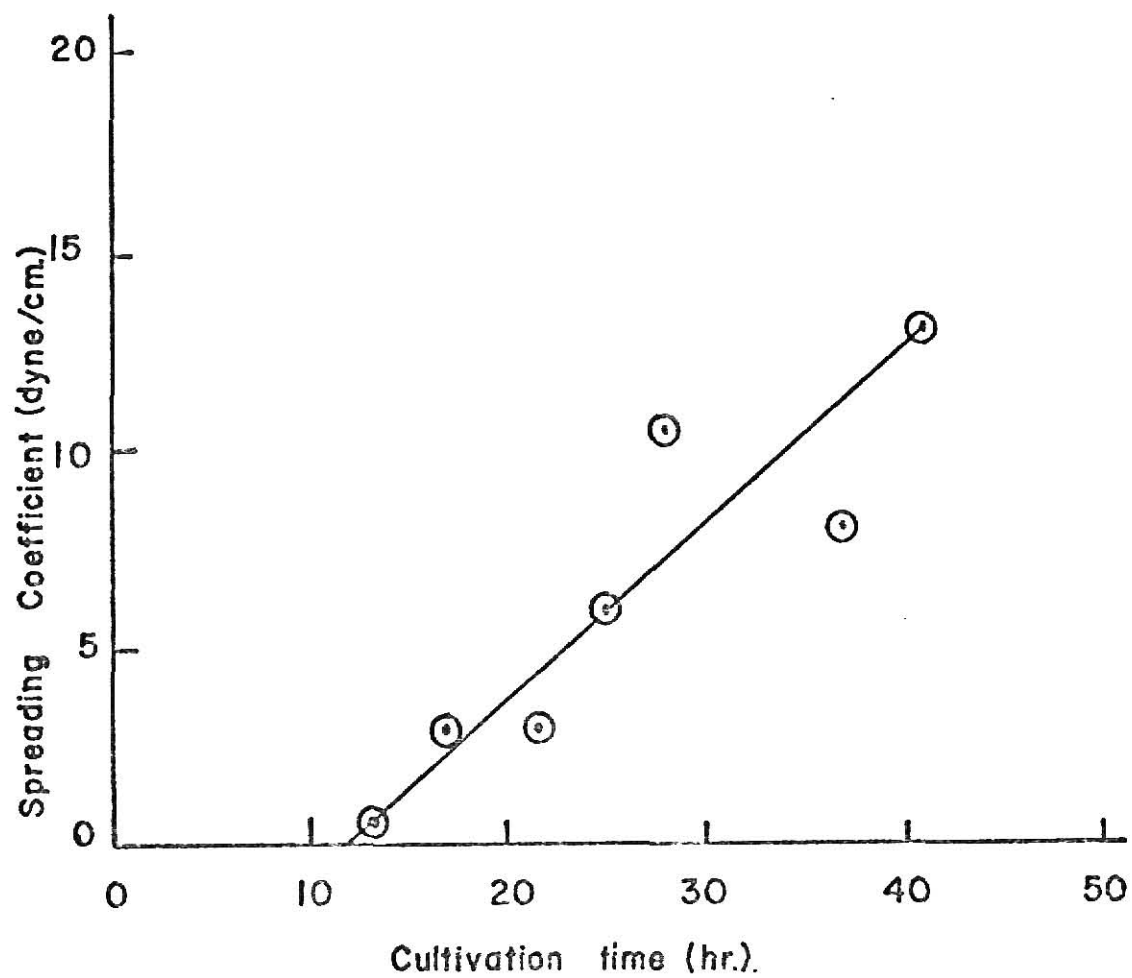
Fig. 2. Effect of cultivation on spreading coefficient during
batch fermentation (From Erickson et al.[4])
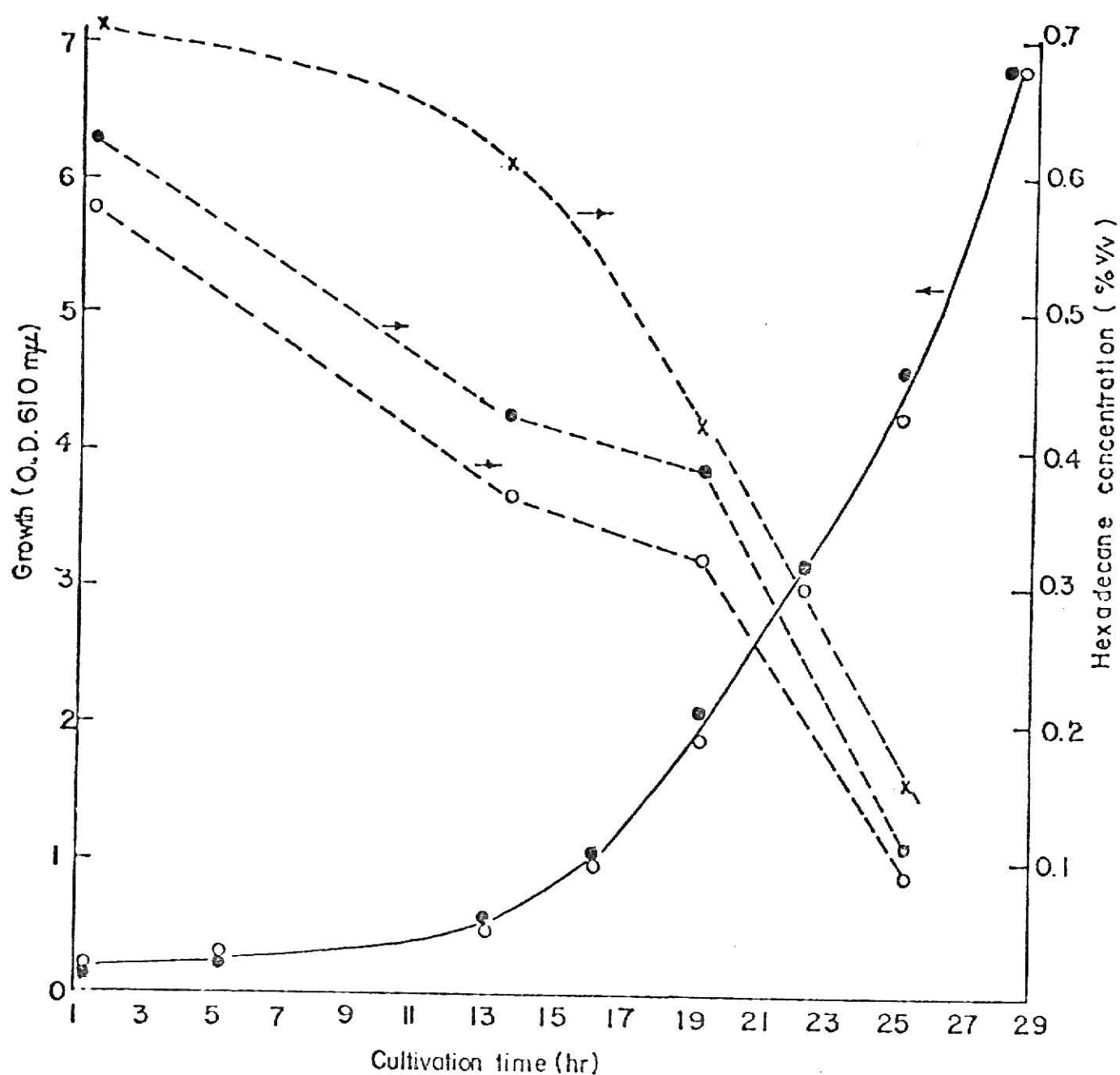
Fig. 3. Effect of cultivation on hexadecane concentration distribution

Koch mixers. (From Erickson et al.[4,7])

● Concentration at top

O Concentration at bottom

X Concentration at bottom of circulation arm.
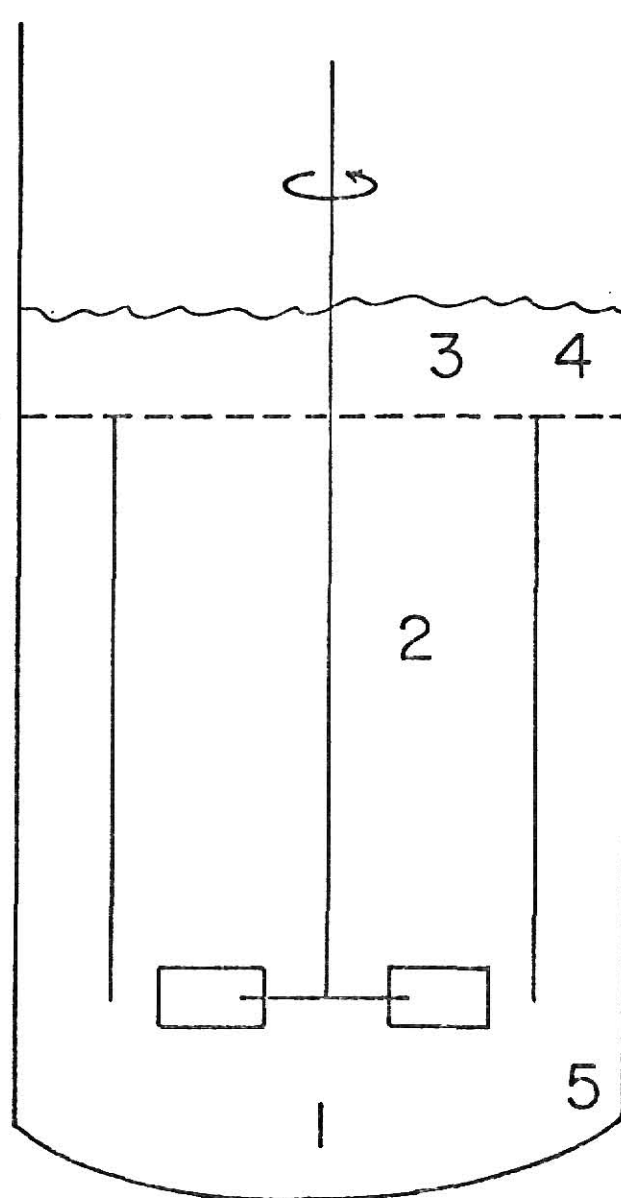
Fig. 4. Configuration of fermentor used by
Hattori et al.[6] (From Hattori et al.[6])
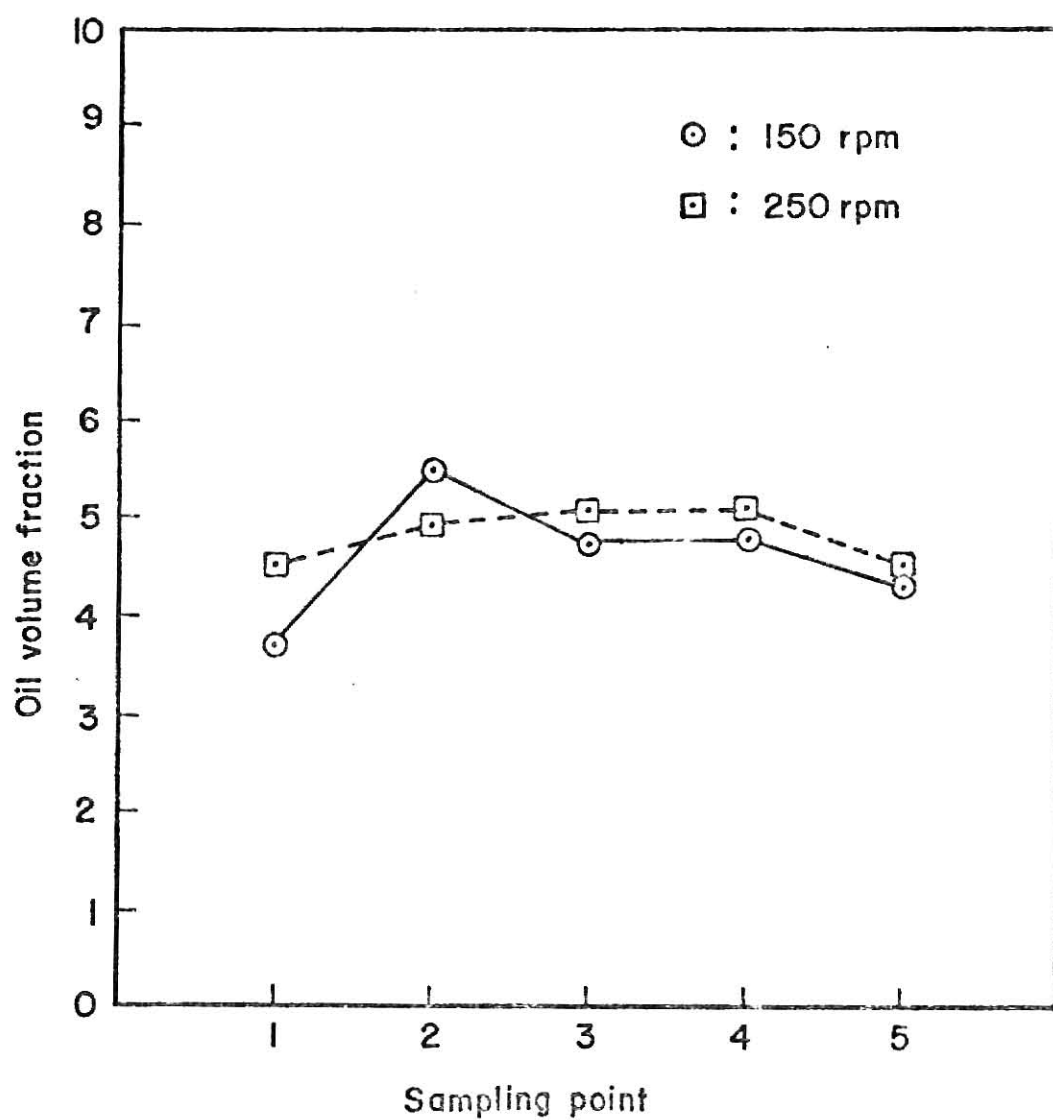
Fig. 5. Variation of oil fraction with position in fermentor
used by Hattori et al.[6] (From Hattori et al.[6])
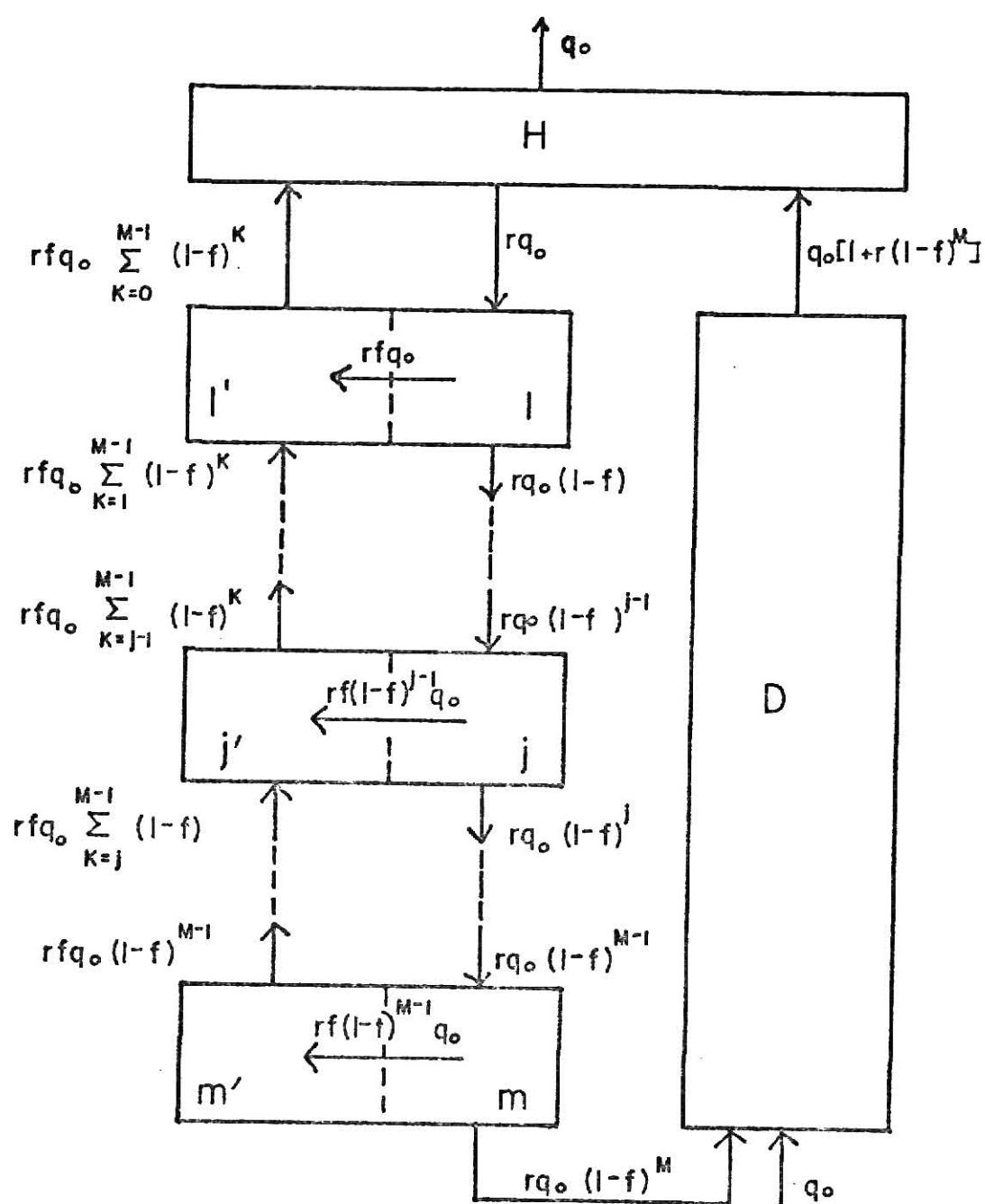
Fig. 6. Flow model for oil phase balances in the airlift fermentor
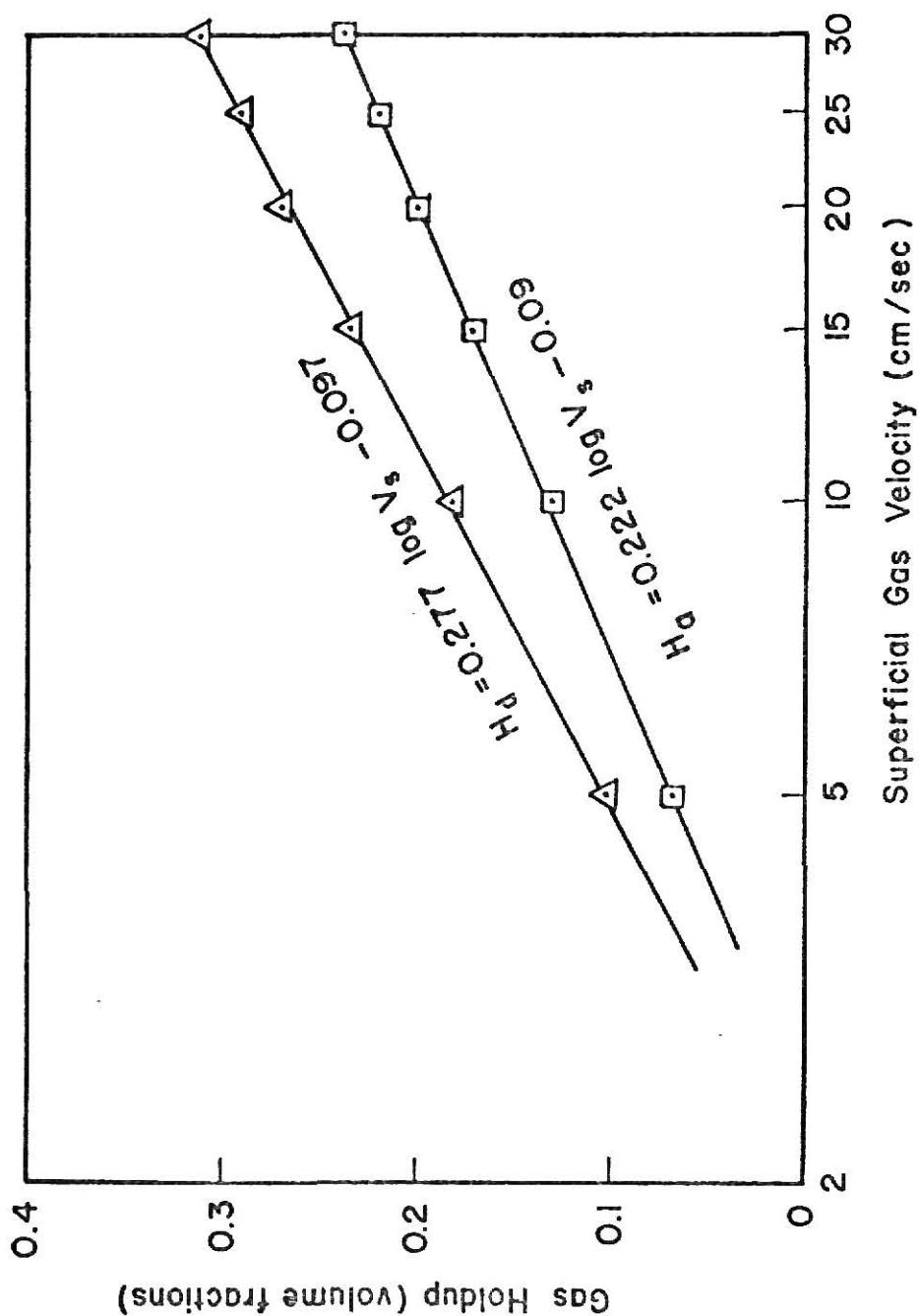
Fig. 7. Correlation of gas holdup with draft tube superficial gas velocity
in the concentric airlift fermentor. (Data from Hatch[9])

△ draft tube, ⊡ annular region.
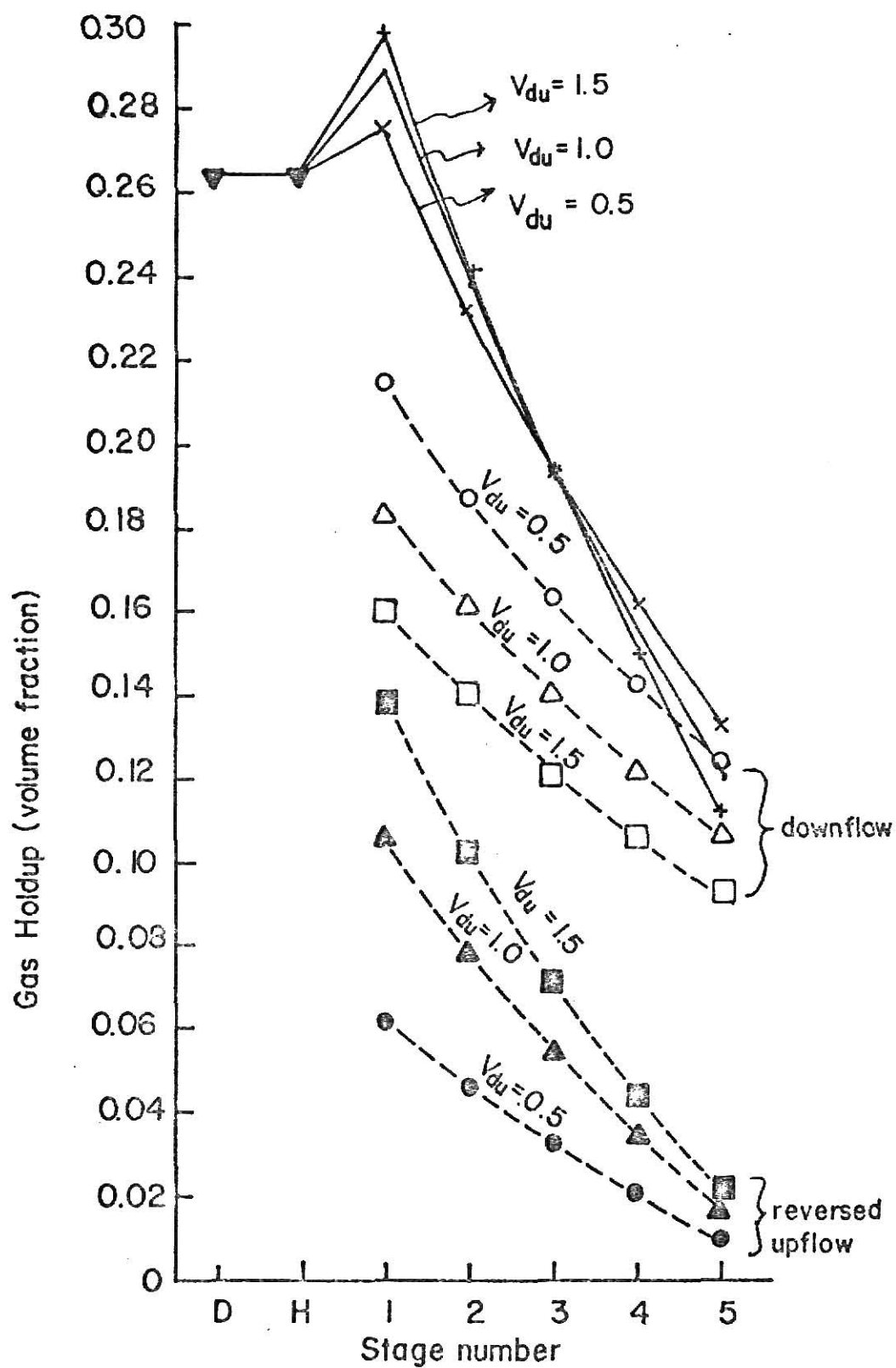
Fig. 8. Effect of position and relative gas velocity on gas
holdup. Solid lines give the total holdup in each
stage. Average holdup in annular region is 0.2.
Draft tube superficial gas velocity is 20 cm/sec.
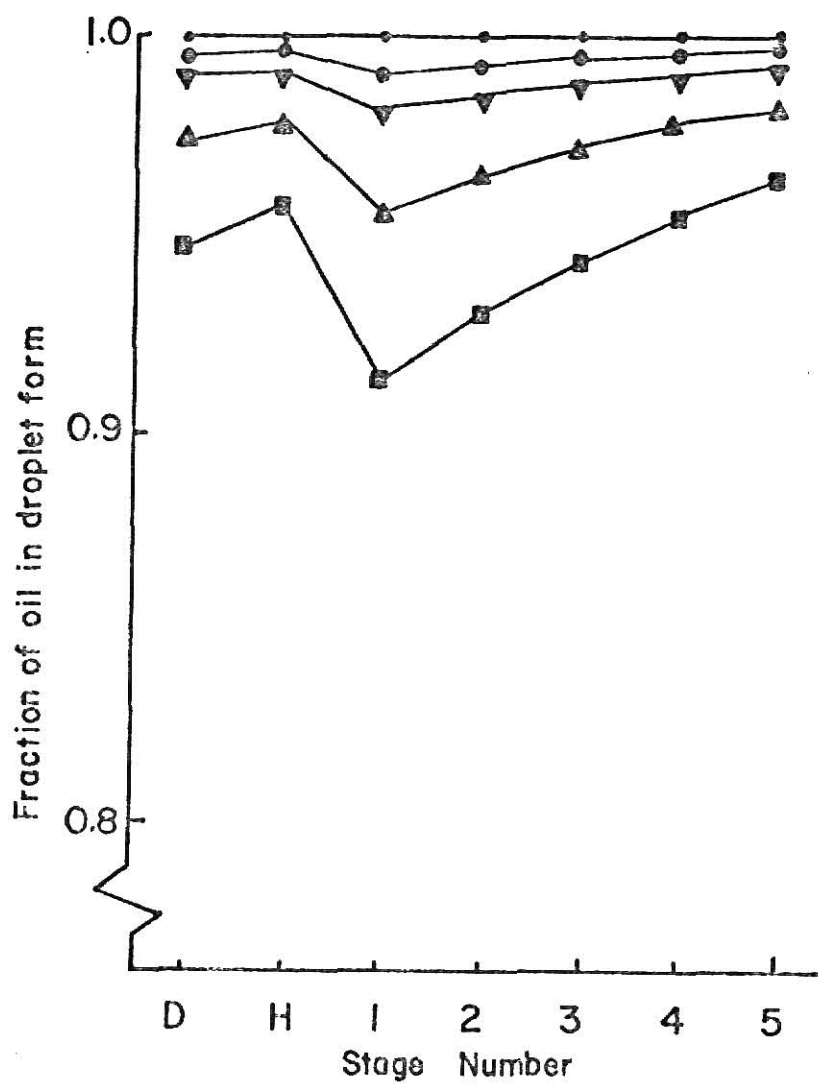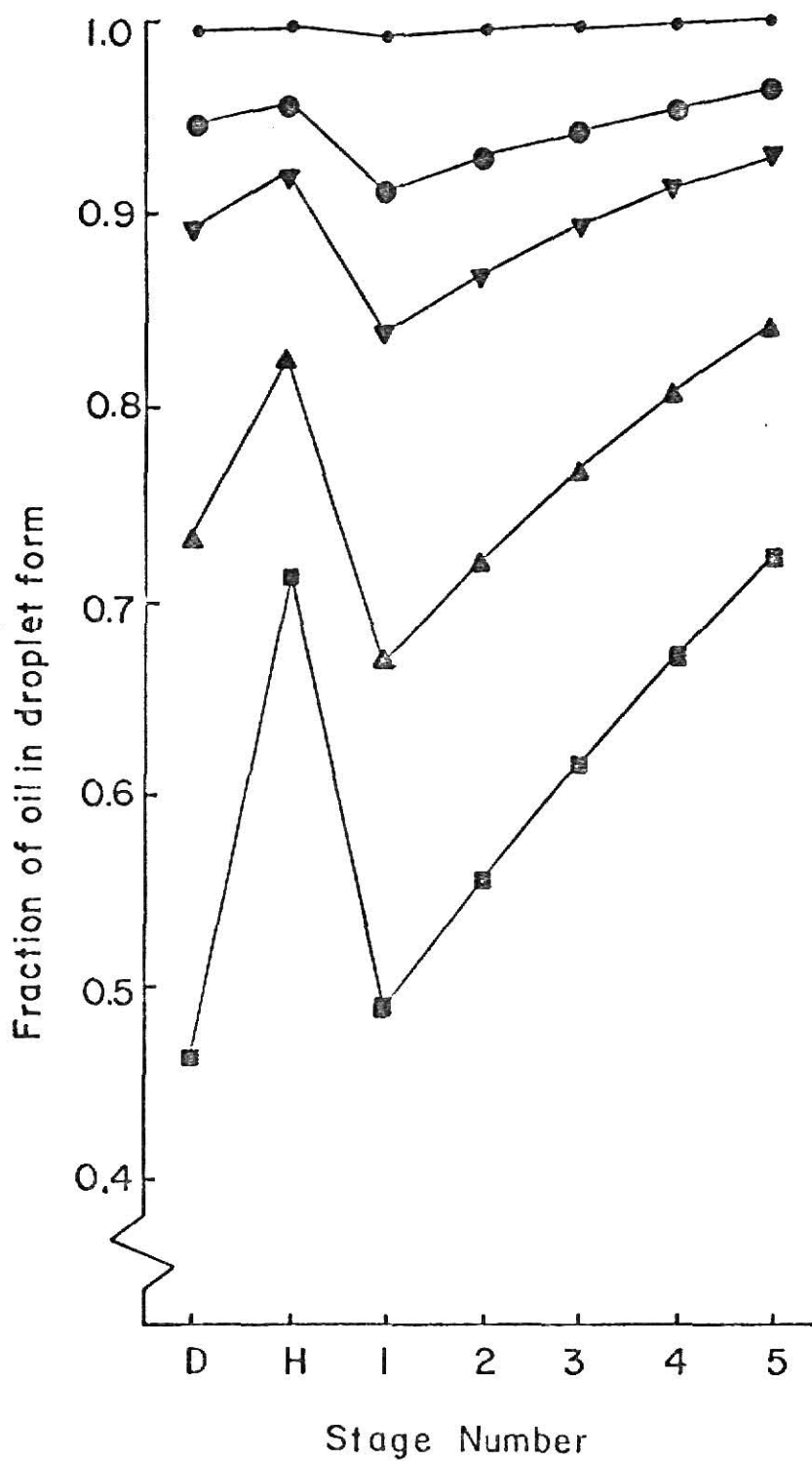
Fig. 9. Fraction of oil in droplet form vs. position
with oil film thickness as parameter for 10%
oil volume fraction. • =0.05 μ, ● = 0.5 μ,
▼= 1 μ, ▲= 2.5 μ, and ▥= 5 μ.
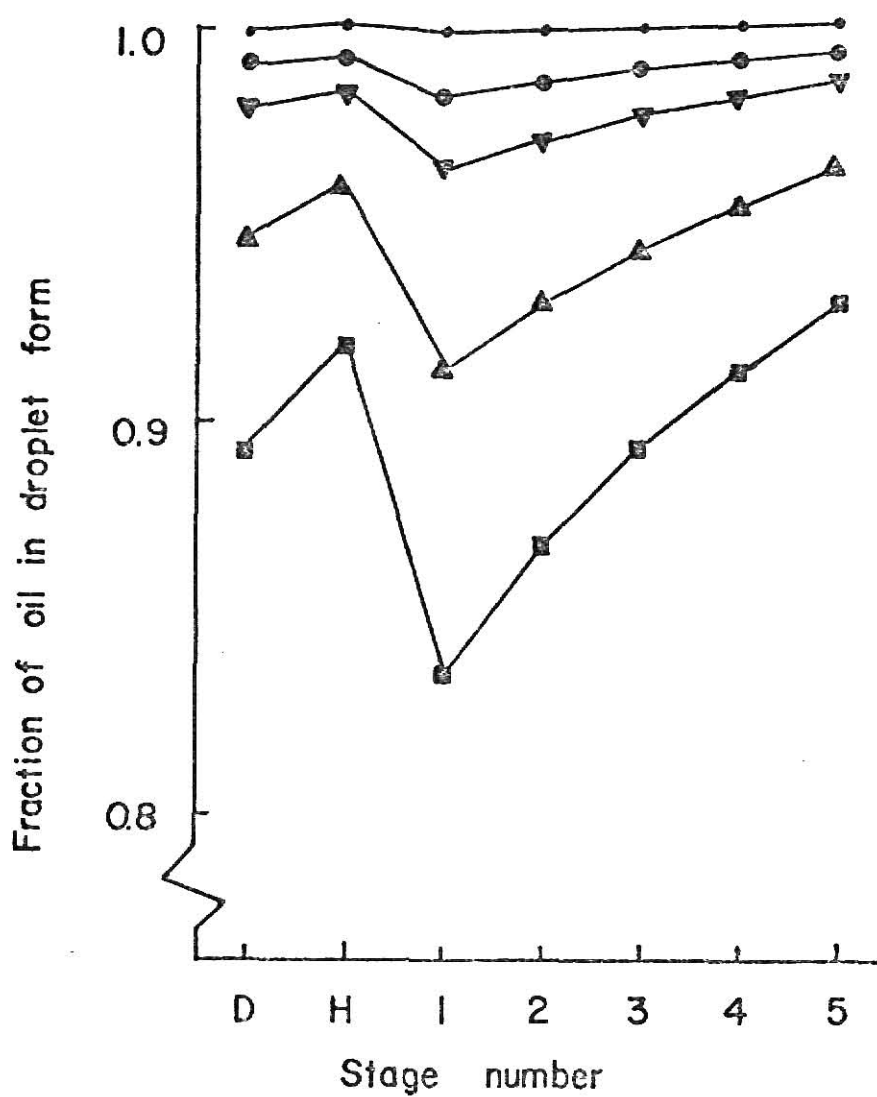
Fig. 10. Fraction of oil in droplet form vs. position
with oil film thickness as parameter for 5%
oil volume fraction. • = 0.05 μ, ● = 0.5 μ,
▼ = 1 μ, ▲ = 2.5 μ, and ▦ = 5 μ.

Fig. 11. Fraction of oil in droplet form vs. position with oil film thickness as parameter for 1% oil volume fraction. • = 0.05μ , ◉ = 0.5μ , ▼= 1μ , ▲ = 2.5μ , and ▩ = 5μ .
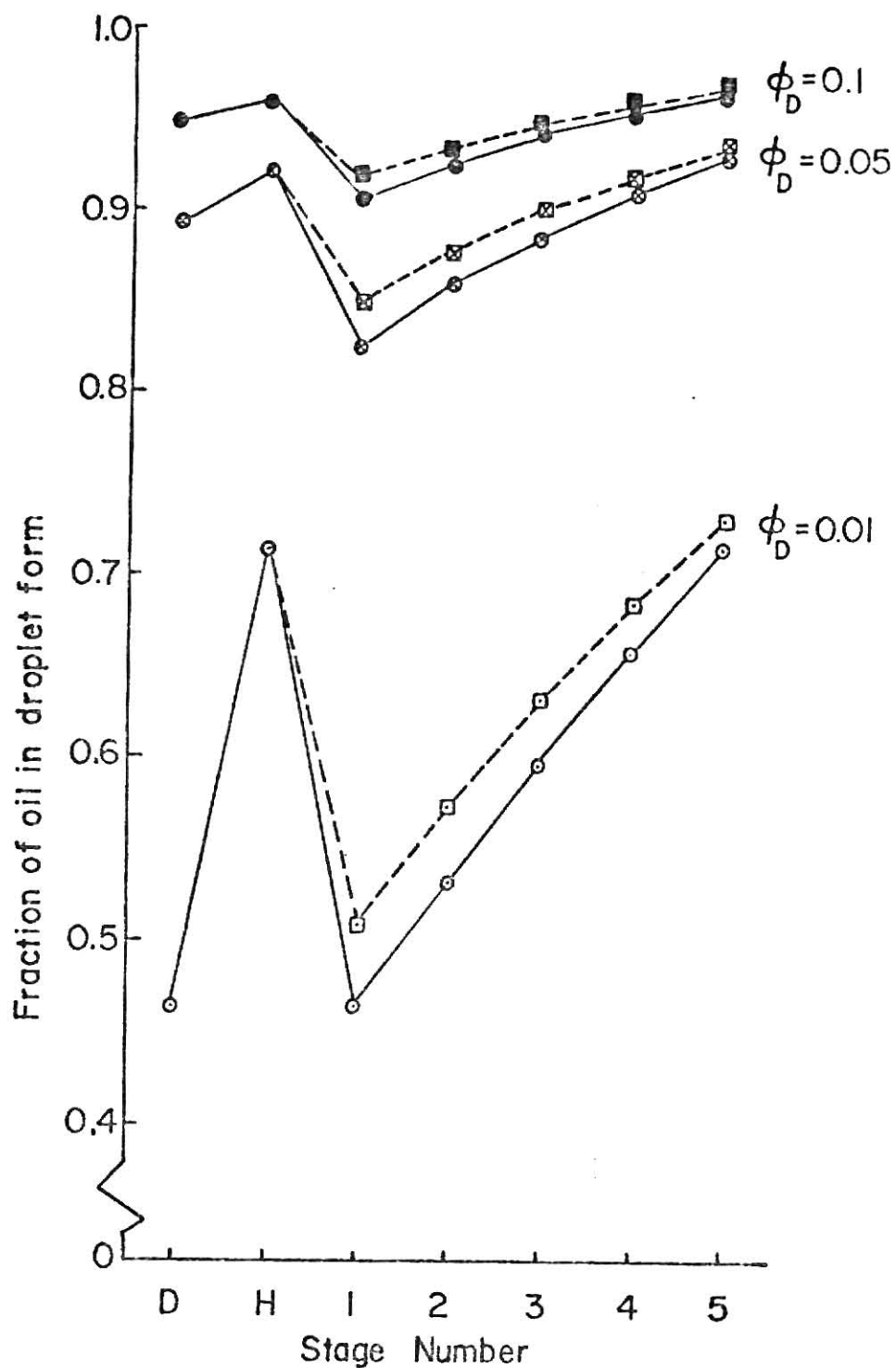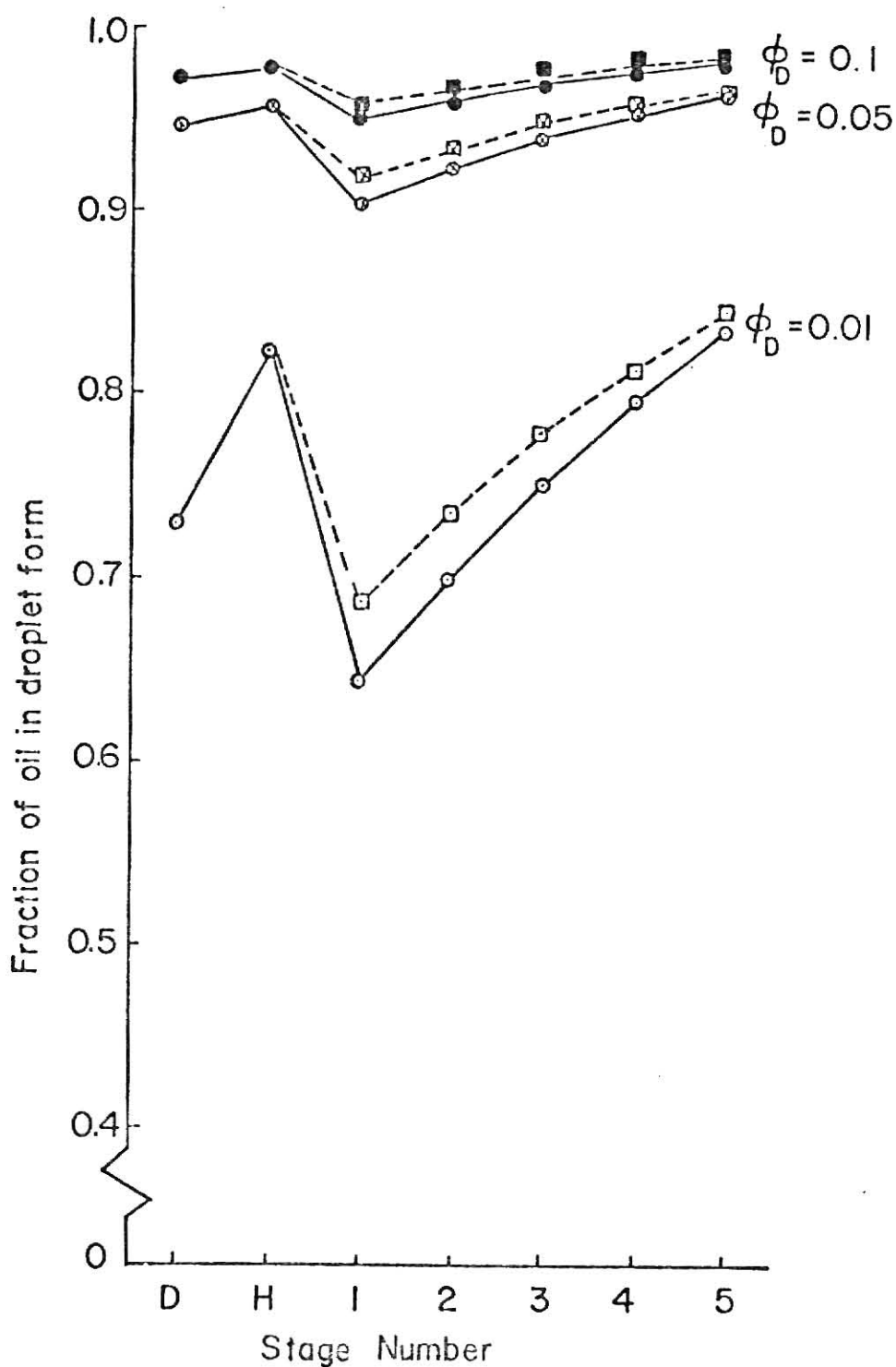
Fig. 12. Effect of position, oil phase volume fraction, and
relative gas velocity on fraction of oil in droplet
form when oil film thickness is 5_μ .

—O— V_{du} = 0.5

‐‐‐☐‐‐‐ V_{du} = 1.5

Fig. 13. Effect of position, oil phase volume fraction, and
relative gas velocity on fraction of oil in droplet
form when oil film thickness is 2.5_μ .
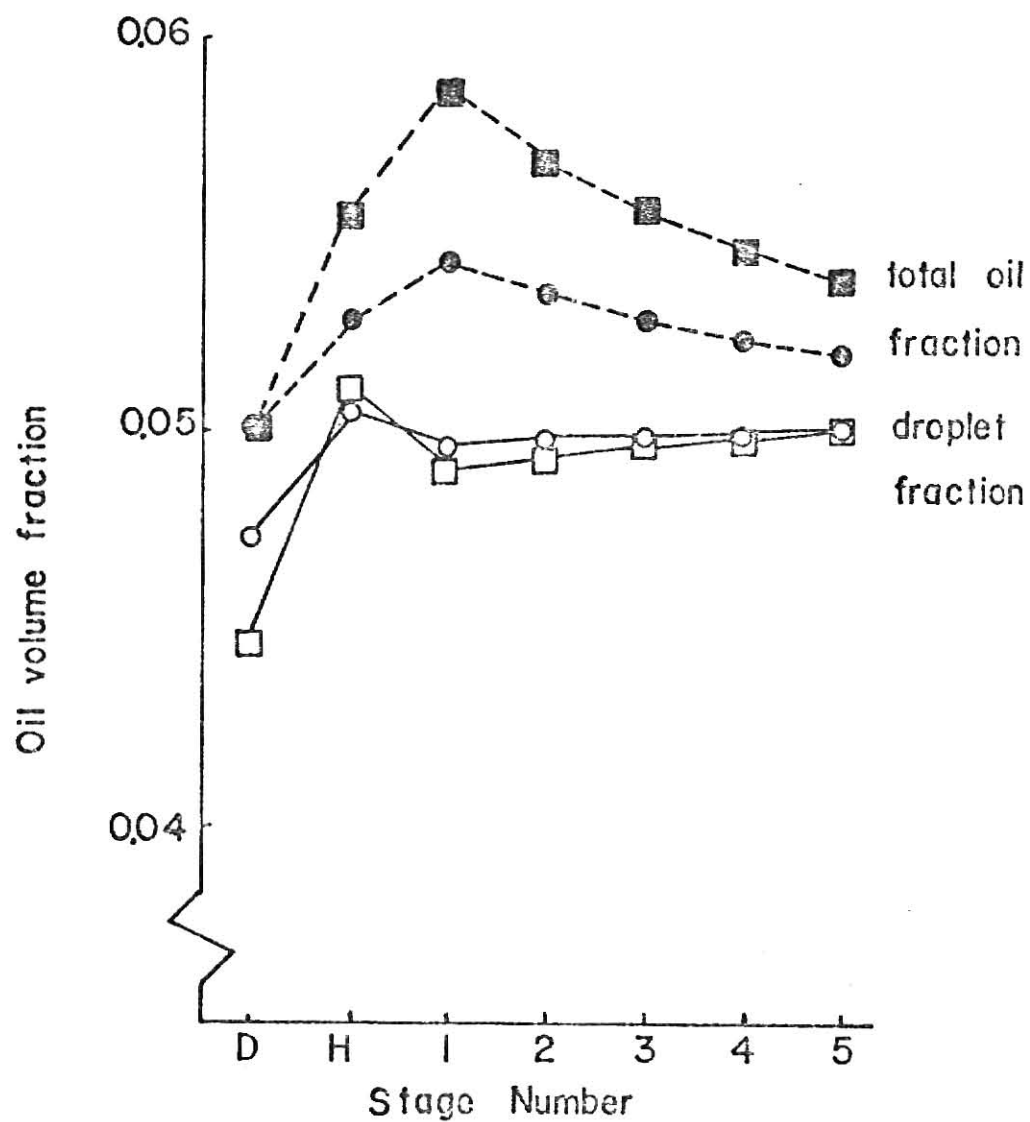
—O— V_{du} = 0.5

··□·· V_{du} = 1.5

Fig. 14. Distribution of oil volume fraction in airlift
fermentor when draft tube oil volume fraction is
is 0.05 for oil films with 2.5 μ thickness O ,
● , and 5.0 μ thickness □ , ▨ .

CHAPTER VI

CONCLUDING REMARKS

CONCLUSIONS

The major results of this study are summarized in this section.

(1) The liquid flow in the airlift fermentor approaches plug flow behavior in the upflow and downflow regions, and well-mixedness in the head region.

(2) The effect of hydrostatic pressure is significant when a large scale airlift fermentor is under consideration.

(3) The shorter airlift tower reaches a more uniform dissolved oxygen concentration distribution than the taller column.

(4) Because of the larger effect of hydrostatic pressure and the greater fraction of oxygen which is absorbed, a greater variation in dissolved oxygen concentration with position is reached as the tower height increases.

(5) For similar dissolved oxygen concentrations, the cell respiration rate is considerably lower at lower gas flow rates. The rate of oxygen transfer and the cell productivity can be increased by increasing the sparger gas flow rate for the range of gas flow rates examined in this study.

(6) The maximum dissolved oxygen concentration is frequently observed at or near the middle of the draft tube. The same observation has been reported by Hatch.

(7) The spreading coefficient frequently becomes positive when _Candida_ _lipolytica_ are cultivated on n-hexadecane, indicating the spreading of the hydrocarbon phase at air-liquid interfaces.

(8) The fraction of oil in droplet form decreases as gas holdup increases, as oil film thickness increases, and as oil volume fraction decreases.

(9) Changing the ratio of downflow to upflow bubble velocity in the annular region, V_{du}, has only a small effect on the fraction of oil in

droplet form. When V_{du} is larger, the fraction of oil in droplet form is also larger.

(10) The oxygen mole fraction in the gas phase is frequently affected by position, tower height, and sparger gas flow rate. The gas phase oxygen mole fraction decreases as bubble residence time increases.

(11) The models presented in this thesis are simple enough to be used in design studies and they can easily be adapted to other airlift system configurations.

RECOMMENDATIONS

Recommendations for further research are summarized in this section.

(1) Airlift fermentors can be stacked up one above another to form a multi-stage airlift fermentor. Since, in the multistage airlift system, the oxygen input for a stage is the exhaust of the stage right beneath, this setup achieves better utilization of oxygen. Cultivating yeasts in tall single stage airlift fermentors has a larger chance in forming dead space, where dissolved oxygen is insufficient, than in shorter airlift systems. Several shorter airlift fermentors forming a multistage airlift reduces the opportunity for dead space.

(2) In Chapter IV, the gas holdup distribution in the annular region was assumed constant; whereas, in Chaper V, a position–dependent gas holdup in the annular region was presented. It is recommended that the model with variable gas holup in the annular region also be employed for the study of oxygen transfer in airlift fermentors.

ACKNOWLEDGMENTS

At various stages of the research I have profited from my major professor, Dr. L. E. Erickson, whose excellent advice, constructive criticism, and constant encouragement have greatly enhanced the quality of my research. The helpful suggestions and valuable comments from Dr. L. T. Fan are also deeply appreciated. I have always been greatly inspired by his enthusiastic attitude towards his profession. They both deserve my respect.

I am extremely fortunate to have had the constant emotional support and understanding of my loving wife, Fong-Chu. I am sincerely grateful to her. I wish to express my utmost thanks to my beloved parents, Mr. and Mrs. Kuan-Wen Ho. Without their support, I would have not been able to study abroad. It is to Fong-Chu and my parents that I dedicate it in gratitude and affection.

MODELING AND SIMULATION OF MASS TRANSFER IN AIRLIFT FERMENTORS

by

CHESTER SHOU-TIE HO

B.S.,Chung-Yuan College of Science and Engineering, 1972

_____

AN ABSTRACT OF A MASTER'S THESIS

submitted in partial fulfillment of the

requirements for the degree

MASTER OF SCIENCE

Department of Chemical Engineering

KANSAS STATE UNIVERSITY

Manhattan, Kansas

1977

ABSTRACT

The airlift fermentor has recently received a great deal of attention because it provides a high mass transfer rate with low power consumption in the hydrocarbon fermentation. Several problems related to the modeling, simulation, and analysis of mass transfer in airlift fermentors with two liquid phases have been investigated. A comprehensive review of recent research which is important to the oxygen transfer and hydrocarbon transfer in tower fermentors with two liquid phases has also been carried out.

A mathematical model for simulation of oxygen transfer in airlift fermentors is presented. The airlift fermentor is represented by a number of interconnected compartments, each of which is assumed to be well mixed. In the annular region, the model includes both upflow and downflow for the gas phase. The effect of hydrostatic pressure is also included in the model. The model is simple enough to be used in design studies and it can be easily adapted to other airlift system configurations.

The distribution of the dispersed oil phase in an airlift fermentor with two liquid phases has been studied. Since recent experimental results show that the spreading coefficient frequently becomes positive when Candida lipolytica is cultivated on n-hexadecane, the effects of oil spreading at the surface of air bubbles in an airlift fermentor are examined using a mathematical model. The distribution of the oil phase with position and among the phases is determined using computer simulation. The simulation results qualitatively explain some of the experimental observations which have been previously reported.